For Earth, For Life
Kubota

KUBOTA TECHNICAL REPORT

JANUARY 2025

57

ISSN 0916-8249

KUBOTA TECHNICAL REPORT

No.57 JANUARY 2025

CONTENTS

Our Efforts to Address the SDGs

- Kubota Supports the Earth and People in the Fields of Food, Water and Environment -

The Kubota Group works on the SDGs, which are the common development goals for the international community, and is taking on the challenges to solve global issues through its business activities.

What are the SDGs?

These are 17 goals set jointly by the nations around the world as issues to be tackled cooperatively.

The goals were adopted at the United Nations Summit in 2015 with 2030 set as the target for their achievement.

"Sustainable Development Goals" is abbreviated as SDGs, which is translated as “Jizokukanona Kaihatsu Mokuhyo” in Japanese.

Association between the published articles and SDGs

Primarily related field		Closely related: ★ Related: ●
Food	Water Environment	Published article
■		Development of the Compact Tractor ST Series for the Domestic Market
■		Development of the Method for Durability Improvement by Using Drive Simulation
■		Development of the Combine Harvester DC-120X for Thailand
■		Development of the Unmanned Autonomous Combine Harvester “DRH1200A-A”
■		Development of the Riding Type Rice Transplanter KA Series for China
■	■	Development of the Gasoline Engine GZ850H
■	■	Development of the Diesel Engine for Industrial Use “V5009”
■	■	Development of SCR Catalyst Performance Degradation Prediction Technology
■	■	Establishment of Design Guidelines of Casting Plans for Large Engine Castings
	■	Development of the Expanding Working Range Technique for Mini Excavators
	■	Development of the Compact Track Loader SVL75-3 for North America
	■	Development of a Feeder Controller with a Focus on DX at Manufacturing Sites
■		Development of an Automatic Watering Control System Based on Wilt Detection
	■	Development of Inspection Technology for the Outer Surface of Pipes
	■	Development of a Large Diameter Electro Fusion Socket
	■	Development of an Automatic High-pressure Cleaning System for the Gravity Belt Thickener
	■	Development of Inspection Rationalization Technology Using MR Devices
	■	Development of the MBR Operating System with a TMP Prediction Model
■	■	Introduction of Kubota Research and Development Europe (KRDE)

For more information on SDGs (Sustainable Development Goals),
please visit the website of the United Nations Information Center.
https://www.unic.or.jp/activities/economic_social_development/sustainable_development/2030agenda/

	SDG goals																
	1	2	3	4	5	6	7	8	9	10	11	12	13	14	15	16	17
		★						★	★							●	●
	★	★										★				●	●
		★						★	★							●	●
		★						★	★							●	●
		★						★	●							●	●
							★	★								●	●
							★		★		●					●	●
							★		★		●					●	●
							★		★			★				●	●
								★	★		●					●	●
									★		★					●	●
							★		★			★				●	●
		★						★	★							●	●
						★			★							●	●
						●		★	★		●					●	●
						★		★	★							●	●
				★				★	★							●	●
						★	★		★							●	●
								★	★		●					●	★

Embodying “On Your Side” in Research and Development

President and
Representative Director
Yuichi Kitao

At the start of 2024, the lives of many people in the Noto Peninsula were affected by the earthquake. In recent years, the frequency and intensity of natural disasters, including earthquakes and torrential rains, are increasing worldwide. Extreme weather events such as insufficient sunlight and record-breaking heatwaves often disrupt the stability of agricultural supply, posing significant impact on people’s livelihoods. Meanwhile, the continued deterioration of water infrastructure due to aging is becoming more and more serious. For example, drainage pump stations used for more than 40 years lose their ability to prevent flooding, posing heightened risks to the people’s daily life. Globally, it’s estimated that 2.2 billion people lack access to safe water due to inadequate sanitation and the effects of climate change.

In this world of growing instability, Kubota envisions itself as an “Essentials Innovator for Supporting Life,” committed to a prosperous society and cycle of nature. We will go beyond the conventional sales model focusing on selling products only and instead, aim at delivering integrated solutions combining products and services. By doing so, Kubota aims to address customer challenges and societal issues across various countries and regions in the field of food, water, and environment.

This year, the 2024 Nobel Prizes in Physics and Chemistry were both awarded for advancements in the field of artificial intelligence. At Kubota as well, we have set 2024 as the beginning year of our journey to advance AI integration, not just in research and development, but throughout the company, including manufacturing and sales.

Our company was a global pioneer in achieving automation of key agricultural machinery, including tractors, combine harvesters, and rice transplanters. We believe this was achieved because Kubota started engaging in GNSS and accumulating our expertise of the technology from when it first emerged in the 1980s despite its high cost. By identifying and continuously mastering the new technologies essential for the future, we aim to continually deliver new added value.

At the same time, we must never lose sight of the core of Kubota’s technology: our commitment to working closely with the actual users. In 2006, I visited India to introduce tractors, confident that lightweight, compact tractors would be well-received. However, I constantly struggled with the sales due to the differences in how the tractors were used and the significantly high requirements for durability. This event made me deeply understand the importance to actually experience the local culture to develop products tailored to local needs.

Our “On Your Side” philosophy is embodied by providing products, technologies, and services that exceed customer expectations at an incomparable speed. It is crucial to embrace the actual needs at the field and continually consider how to bring maximum satisfaction to our customers. By honing our research and development to balance innovation with a field-based approach, Kubota strives to become the most trusted company, contributing to society on a global scale.

This 57th issue of the Kubota Technical Report highlights innovations developed using AI technology such as the industry’s first autonomous combine harvester and the withering detection-based automated irrigation control system. It also covers the technology for detecting defects on ductile iron pipe surfaces using AI image analysis. From the food sector, we feature developments such as a compact tractor equipped with an electronically controlled HST and a riding rice transplanter for the Chinese market, designed to improve wet field maneuverability and planting accuracy. From the water and environment sectors, we showcase a compact track loader for the North American market designed for ease of operation, large-diameter plastic fittings resistant to corrosion, and development of technologies for streamlining inspections of drainage pump stations critical for flood prevention. We invite you to explore this issue in full.

Kubota will remain committed to advancing research and development for the betterment of society. We deeply appreciate your continued support.

Development of the Compact Tractor ST Series for the Domestic Market

Core Platform Engineering Dept. ／ Tractor Engineering Dept. Ⅰ
Farm and Industrial Machinery R&D Dept. Ⅲ

The total domestic demand for tractors is on a declining trend, but tractors with 20 to 40 horsepower still represent a significant volume zone, accounting for more than half of the total demand. Many users of small tractors in this horsepower range are part-time, small-scale farmers, and a high percentage of them are elderly. Therefore, there is a demand for affordable and easy-to-use products. In response, Kubota has developed the ST series, a fully redesigned model, to achieve even greater operability at a low price. This paper discusses the development technology of the electronically controlled HST, which is being introduced in this class for the first time by Kubota.

【Key Word】
Tractor, Electric Control, Hydro Static Transmission

Related SDGs

1. Introduction

Although the overall demand for tractors in Japan has been declining due to a decrease in the number of farming households that are potential customers, tractors between 20 and 40 horsepower (hp) continue to be an important volume segment, accounting for the majority of the total demand. In this horsepower range, Kubota has been marketing FT series tractors (22–30 hp) since 2012. The models in this series are basic tractors designed for ease of operation, compactness of body, and low cost, and are aimed primarily at small-scale rice farmers. Since such tractors are typically used only 20 to 50 hours per year, and nearly 40% of users are elderly and over 70 years old, affordable and easy-to-use features are especially important.

Kubota has newly developed the ST series tractors (Fig. 1) , which are models that have been completely redesigned from the FT series. The ST series models are the first in Kubota's lineup in the same horsepower range to feature an electronically controlled hydrostatic transmission (HST) in response to market demand for even better driving operability. The HST, which consists of a hydraulic pump and a hydraulic motor, is a continuously variable transmission that changes speed by changing the angle of the swash plate of the hydraulic pump (hereinafter referred to as the "HST swash plate"). The electronically controlled HST is an HST that uses an electronic control unit (ECU) to perform this speed change operation. It eliminates the need for cumbersome human operation because it controls not only speed change but also back and forth switching and stopping operations. This paper introduces the newly developed electronically controlled HST technology.

Fig. 1 Compact Tractor “ST Series”

2. Development concept and target values

2-1 Development concept

The development concept of the ST series was to improve basic functions such as driving operability and driver comfort while retaining the affordable and easy-to-use features of the FT series. Therefore, it was necessary to develop an affordable electronically controlled HST, which is a component that has a major impact on driving operability.

2-2 Development goals

The electronically controlled HST used in the high-end models of Kubota’s compact tractors changes speeds by controlling the angle of the HST swash plate with an electromagnetic proportional valve via a hydraulic servo piston. If a similar mechanism were to be used in the ST series, it would require investment in new molds for HST housings, resulting in high costs, contrary to the development concept. To avoid this issue, the ST series adopted a method of attaching an electric motor and electronically controlled gearbox externally to the existing HST, electronically controlling the HST without investing in a new HST housing. For the existing HST, the HST for the LX series tractors (35–40 hp) for Europe and North America was adopted. In the LX series, the HST swash plate is operated by a mechanical link mechanism connected to a pedal. In the ST series, on the other hand, the pedal and mechanical link mechanism are replaced by an electronically controlled gearbox (a gearbox equipped with components necessary for electronic control) driven by an electric motor (Fig. 2). The electronically controlled gearbox includes reduction gears to amplify the torque of the motor and an angle sensor to detect the angle of the HST swash plate for improved control accuracy.

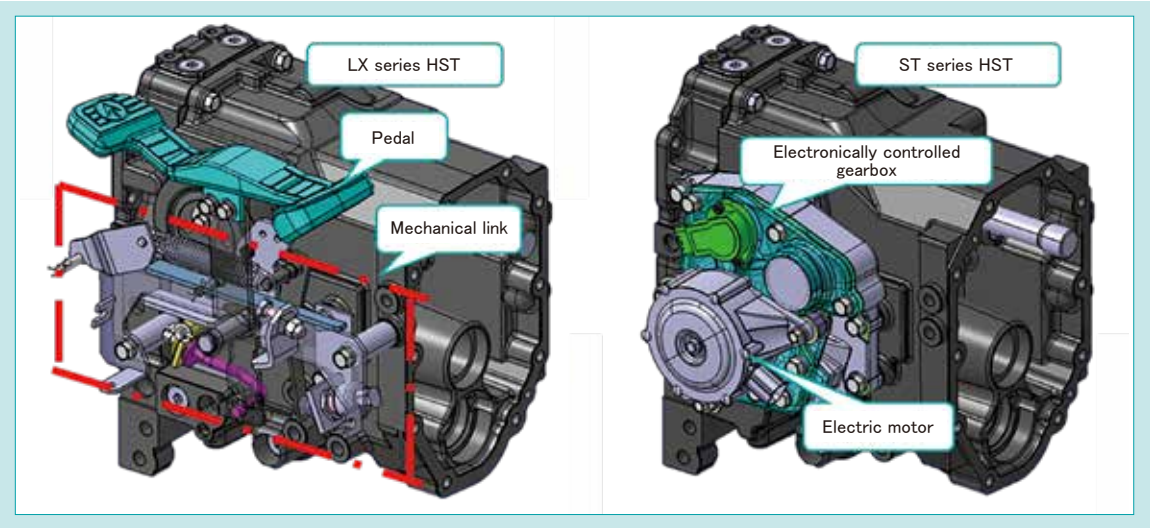

Fig. 2 Comparison of the LX Series HST and ST Series HST

Since agricultural work in Japan is often performed by maintaining a constant tractor speed, it should be easy to reproduce the working speed of the vehicle. For this reason, speeds are changed using a shift lever rather than a pedal, unlike in the European and North American markets. In the existing FT series models, the HST swash plate is operated by a main shift lever.

The main shift lever is connected to the HST swash plate via the mechanical link, and the lever operation allows the driver to set the vehicle speed, switch back and forth, and start and stop the vehicle.

The electronically controlled HST mounted on the newly developed ST series allows the HST swash plate to be operated by two different levers: (1) the main shift lever, which sets the vehicle speed (Fig. 3); and (2) the shuttle lever, which switches back and forth and starts and stops the vehicle (Fig. 4).

The driver often moves the tractor back and forth when working in the field, and the shuttle lever allows the driver to switch back and forth with a finger while holding the steering wheel and looking around. This mechanism eliminates the need to operate the main shift lever when switching back and forth, starting, or stopping, thereby greatly reducing the number of times the speed needs to be reset once the appropriate speed for the job is set. In addition, the use of the electronically controlled HST has enabled the implementation of the Easy Brake function, which allows the driver to adjust the vehicle speed or stop the vehicle by simply operating the brake pedal, without using the clutch pedal, and the Easy Turn function, which automatically decelerates the vehicle when turning to allow for a more relaxed turning operation.

This newly developed technology enables much less labor in the field. The goal was to allow the driver to concentrate on the job without looking at the controls.

Fig. 3 Main Shift Lever

Fig. 4 Shuttle Lever

3. Technical issues to be solved

3-1 Ensuring neutral-recovery capability

The HST can stop the vehicle by controlling the angle of the HST swash plate within a certain range. This range of angles is called "neutral." For product safety, when a neutral command is given with the shuttle lever in the neutral position, the vehicle must stop. Therefore, the challenge was to ensure neutral-recovery capability.

3-2 Reduction of vibration and noise caused by hydraulic pressure

In the electronically controlled HST of the ST series, the HST swash plate angle is controlled by the electric motor through gears. As the swash plate vibrates significantly due to hydraulic pulsation, this vibration is transmitted to the gears and the motor. Therefore, there is a risk of collision between the gear teeth due to gear vibration, resulting in abnormal noise or damage due to the large vibrations transmitted to the motor. For these reasons, the challenge was how to reduce the vibration transmitted to the gears and the motor.

3-3 Improvement of operability

As mentioned above, in the ST series designed for the domestic market, it is desirable to use a stepwise main shift lever for setting the vehicle speed because of the importance of reproducing the working speed of the vehicle. However, installing a stepless main shift lever also benefits the user, who can take advantage of the smooth shifting action and flexible speed setting of the continuously variable HST. Therefore, the challenge was to develop a main shift lever that could combine the advantages of both stepwise and stepless shifting.

4. Developed technology

4-1 Development of a neutral-recovery assist structure

The electronically controlled HST of the ST series uses an external electric motor to tilt the HST swash plate. Since the swash plate always generates torque due to the hydraulic reaction force inside the HST while the vehicle is running, an external torque is always applied to the electric motor via gears. Since the tractor cannot maintain a constant speed if the motor is rotated by the torque, the motor is equipped with a locking function that prevents it from being rotated by external torque. In a pedal-link type HST, the pedal and the HST swash plate automatically return to neutral by spring force when the foot pedal is released, but the electric motor cannot return them to neutral by spring force alone because of the locking function. Therefore, in the ST series, when neutral is commanded by lever operation, the motor rotates to return the HST swash plate to the neutral position. However, due to the presence of chatter and gear backlash between the motor and the HST swash plate, the swash plate cannot be held within the neutral range even if the motor is precisely controlled (Fig. 5). Therefore, a neutral-recovery assist structure was developed and installed inside the electronically controlled gearbox. This structure is designed to guide the gears to the position where the bearing fits into the cam by pressing the bearing against the cam portion of the gears connected to the HST swash plate by the force of a torsion spring (Fig. 6). This design allows the motor to bring the HST swash plate close to neutral, ensuring that the gears are guided to the neutral position within the chatter and backlash range.

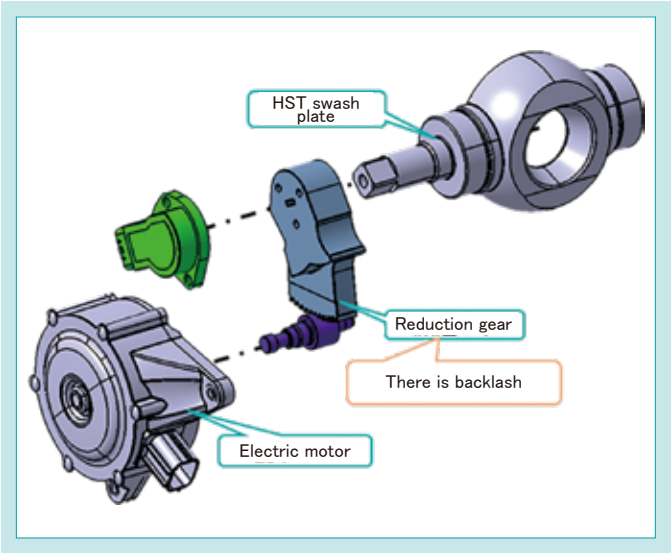

Fig. 5 Structure of the Motor Power Transmission Unit

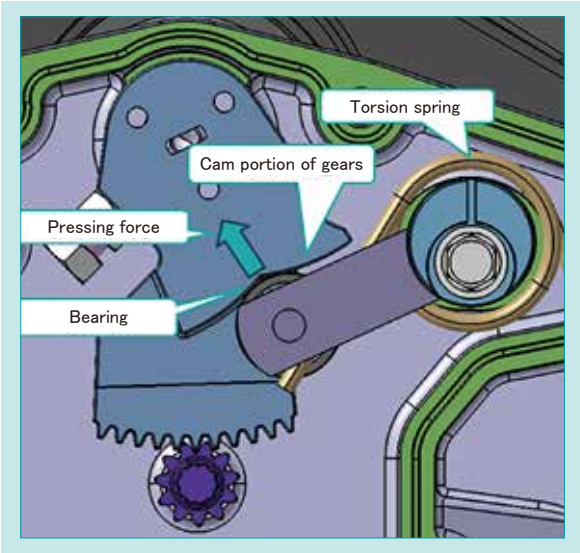

Fig. 6 Neutral-Recovery Assist Structure

4-2 Reduction of vibration noise by the electronically controlled gearbox

From the results of acoustic analysis and acceleration measurements, it was estimated that the vibration noise was caused by the oscillation of the gears in the gearbox due to the vibration transmitted from the HST, resulting in collision of the teeth of the mating gears. Therefore, the following three vibration countermeasures were implemented to solve the problem.

4.2.1 Reduction of gear tooth impact shock

The gearbox was lubricated for the damping effect of the oil film between the gear teeth when they collide with each other[1)] and for the viscous damping effect of the oscillating gears moving in the oil. In addition, the neutral-recovery assist structure described in section 4-1 keeps the torque acting on the gears in one direction at all times, thereby preventing the teeth of the gears from separating and colliding with each other. In addition, rubber was added to each axis that oscillates when vibration occurs in order to create a sliding resistance that dampens vibration (Fig. 7).

4.2.2 Reduction of gearbox vibration

Noise is thought to be generated by vibrations transmitted to the gearbox, where the sound is amplified in the housing and becomes louder. Therefore, the vibration of the gearbox was reduced to reduce noise amplification. Specifically, the rigidity of the gearbox was increased by increasing the number of gearbox fastening points and using cast iron as a damping effect material.

4.2.3 Reduction of vibration transmitted to the motor

To prevent damage to the motor from vibration, vibration-damping rubber was added to the motor mounting area to create a rubber mounting structure that reduces vibration transmitted to the motor (Fig. 8).

The above measures have significantly reduced noise from the gearbox and vibration transmitted to the motor.

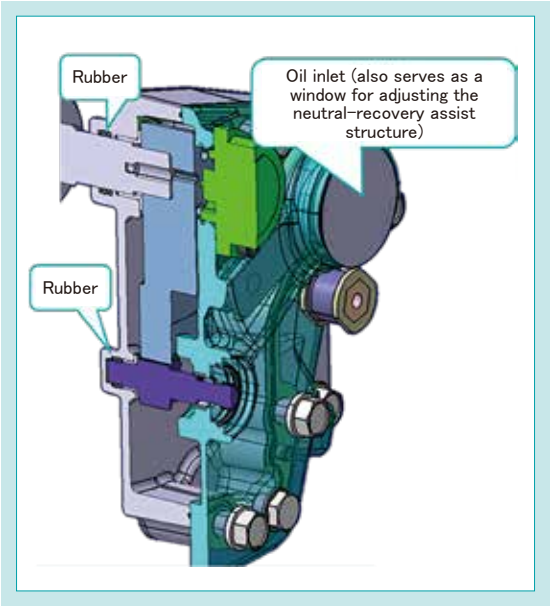

Fig. 7 Structure for Collision Mitigation

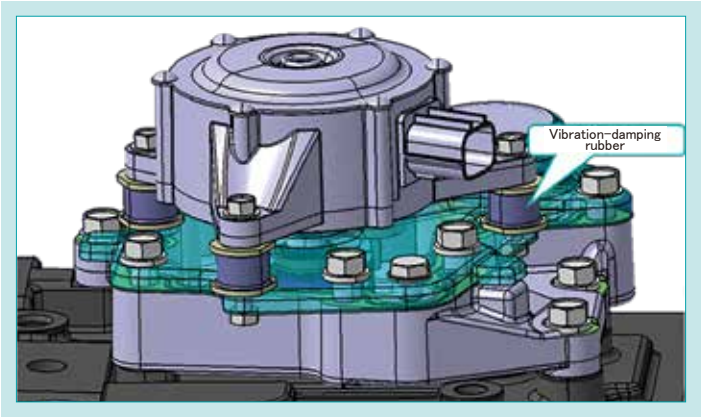

Fig. 8 Vibration-damping Rubber for the Motor

4-3 Stepwise/stepless shifting function

In order to provide smooth shifting and flexible speed setting by taking advantage of the characteristics of the HST, while ensuring the vehicle speed reproducibility required in the domestic market, a stepwise/stepless shift function was added to the main shift lever of the ST series (Fig. 9). This allows the operator to switch between stepwise and stepless modes by twisting the grip of the main shift lever. In stepwise mode, a roller is stuck in a detent as shown in the figure, and when the operator's hand is released from the lever, the lever stops in a position where the roller is stuck in one of 10 detents, creating a 10-step variable speed lever. This allows the lever position to be changed with high reproducibility, and the click felt in the hand when overcoming the bumps between the detents allows the vehicle speed to be adjusted by the desired number of steps without looking at the hand. In stepless mode, on the other hand, turning the grip moves the link and pulls the cable, lifting the roller out of contact with the detents. This allows the driver to freely set the vehicle speed without being restricted by the lever positions defined by the detents, and also allows the driver to intuitively increase or decrease the speed with a light hand movement, thus providing driving comfort. The main shift lever is held by the friction plate even when the hand is released in stepless mode. Depending on the user's preference, either stepwise or stepless mode can always be used, and when the user wants to switch between modes, it can be done instantly with a simple twist of the grip. This feature is available in the ST series under the name Easy Select.

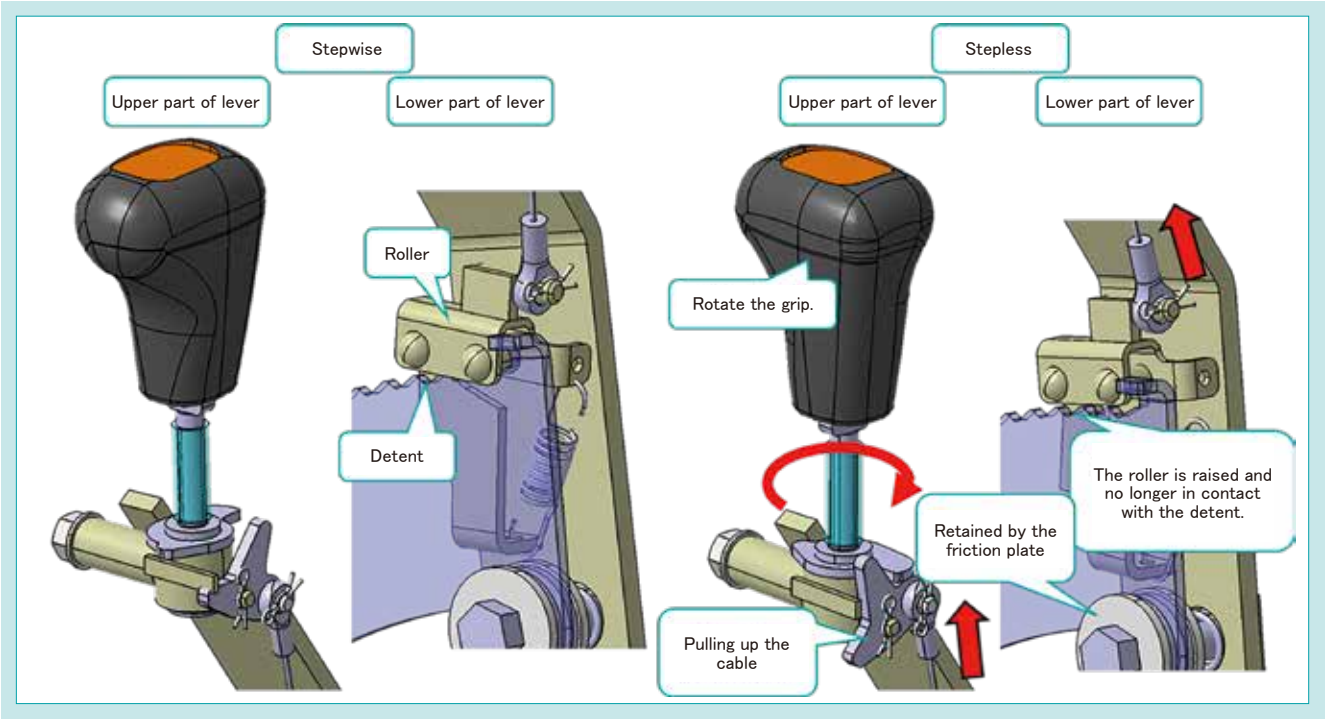

Fig. 9 Overview of "Easy Select"

5. Conclusion

The newly developed ST series of compact tractors for the Japanese market inherit the affordable and easy-to-use features of the existing FT series, while further improving driving operability with the introduction of an electronically controlled HST, the first in its class. We believe this technology can reduce complicated operations and help reduce operator fatigue. This technology can lead to automated driving operations and is versatile enough to be implemented in other existing HSTs. In the future, this technology will be extended to tractors for other regional markets to further reduce the workload of users.

Contribution to SDG targets

2.4 Achieving sustainable and robust agriculture
Electronic control of driving operations to reduce and simplify tillage operations

8.2 Improved productivity through innovation
First in its class to have an electronically controlled HST mounted to reduce unnecessary operations

9.5 Promotion of scientific research and innovation
Contributing to the spread of advanced agriculture through the development of new technologies

Reference

1) Kazuhide Ohta, Koichiro Ikeda, Toshiki Yamanoi, Rei Enokizono, and Xie Xiaoyu: "Analysis of Vibration and Noise of Internal Combustion Engine Considering Gear Impact" Dynamics & Design Conference, 2016, Vol. 2016, Session ID 333, p. 333-.

Development of the Method for Durability Improvement by Using Drive Simulation

Analysis Center

In recent years, the farm and industrial machinery consolidated department has aimed to expand our product lineup for farming tractors in Europe and the high-speed utility vehicle (UV) market in North America. It is difficult to ensure the durability of the body. Because the tractors can be used for various high-load operations in farming, the load of the UV is unclear when driving on rough roads. In the past, products were developed by repeating a design based on experience and durability tests on actual machines, but this experience may not apply for new markets. Additionally, our previous analysis method needs the load condition, calculated by using actual measurement, so its measurement needs a lot of time and we cannot determine the optimal design. Therefore, we have developed an analysis method that can calculate the load which is applied to the vehicle, and consider the improvement of durability by performing virtual work on a simulation.

【Key Word】
Drive Simulation, Fatigue Analysis, Tractor, Utility Vehicle

Related SDGs

1. Introduction

In the European market, tractors are getting bigger for more efficient farming, and heavy work is being done with implements weighing more than 2 tons. In the North American utility vehicle (UV) market, high durability is required, such as for driving over rough terrain with heavy loads (Fig. 1) . Since Kubota had no experience in developing products for such workloads, it was difficult to assume all workloads in the design phase to ensure durability. If a prototype is damaged in an endurance test, it must be redesigned and retested, prolonging development time and preventing adequate consideration of appropriate shapes.[1)]

For future business expansion and continuity, design process innovation (DPI) is needed to ensure the strength of the entire vehicle in the product design phase and to enable the development of highly reliable products in a short time.

Fig. 1 Work of the Tractor and UV

2.Development concept and target values

In the conventional strength analysis of driving tests on rough roads and uneven terrain, the load applied to the vehicle body is unknown, so a prototype machine is first built to measure the loads in actual machine testing to determine the analysis conditions, and then a machine with improved durability is rebuilt. This approach requires at least two prototypes to be built for passing endurance testing, which lengthens development time and makes it impossible to fully study the optimal shape. Therefore, in order to realize DPI, we developed a new analysis technology to predict the loads applied to a tractor or UV at the design phase and to evaluate the damage to the vehicle body to ensure durability at an early phase before prototyping, with the goal of passing endurance testing with a single prototype (Fig. 2) .

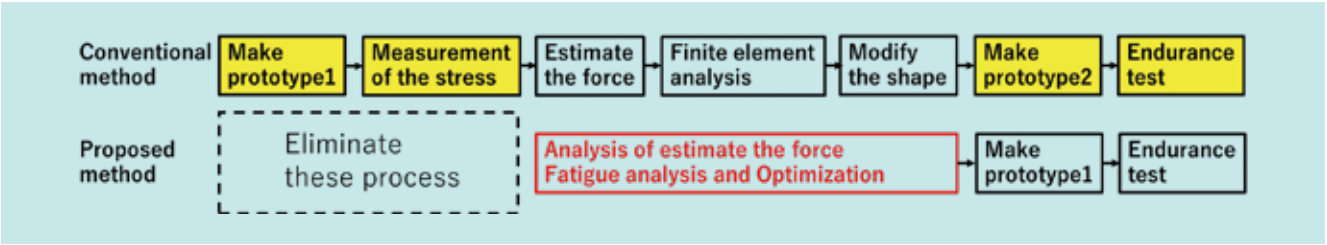

Fig. 2 Previous Development Process and Proposed Development Process

3. Technical issues to be solved

By virtually simulating the work and driving of tractors and UVs, durability is improved in the design phase without using a real machine. There are three challenges to this end:

(1) Driving analysis technology

In the analysis, the working and running conditions of actual machines in endurance testing are described to enable the prediction of time variations in ground input loads, vehicle posture, and the inertial forces of heavy objects, which are required for strength analysis.

(2) Fatigue life analysis technology

A method is to be developed to evaluate fatigue accumulated in vehicle bodies by accurately calculating the stress distribution that continuously changes with time-varying loads, so that durability can be evaluated by considering the entire process.[2)]

(3) Optimal design technology

Optimal design without repetitive prototyping is enabled, for example, by suggesting the lightest shape while ensuring target durability.

4. Developed technology

4-1 Driving analysis technology

4.1.1 Solution 1: Creation of a tire property measurement and analysis model

A vehicle body's input load and behavior when driving over bumps on an rough road vary greatly depending on the tire type and size, and have a significant impact on durability. Therefore, it is necessary to accurately measure and model the tire stiffness and damping characteristics in driving analysis.[3] However, due to the large size of tractor tires, it is not possible to measure all the characteristics with automobile test equipment. In addition, because tractor tires have a high flat ratio and large lugs, high-frequency load variations caused by large tire deformation and lugs when driving over bumps at high speeds cannot be represented by tire analysis models for automobiles.

Therefore, in cooperation with tire manufacturers, we obtained the dynamic characteristics of tires at different step heights and vehicle speeds, which could not be obtained from test equipment, through simulation using a tire analysis model that incorporates the properties and internal structure of rubber. However, the tire analysis model used in the characteristic measurement is not applicable to a simulation in which tires are mounted on tractors to run on the road surface for long periods because of the large volume of analysis data. Therefore, tires were represented by spring and damper elements, and parameters were identified that would make the characteristics of dozens of patterns match between the aforementioned simulation and actual measurements. This resulted in a tractor tire model that accurately represents tire deformation and can represent the transfer of the high-frequency loads that occur when driving on rough roads (Fig. 3).

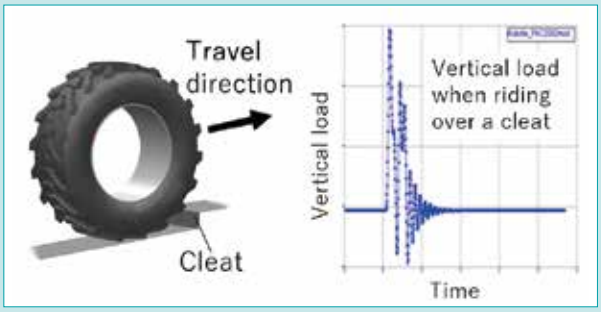

Fig. 3 Tire Simulation Model and Vertical Load

4.1.2 Solution 2: Measurement technology for 3D profiling of uneven road surfaces for UV endurance testing

An accurate 3D road surface model is necessary for high-precision driving analysis. For roads with concrete or similar surfaces, the 3D shape of the roadway can be created from drawing data. However, when analyzing the results of endurance tests on uneven terrain or on external travel path surfaces without drawings, it was necessary to capture the geometry of the entire travel path with an accuracy finer than the tire surface irregularities. A lightweight, simple scanning device that could be mounted on a hand-held scanner or drone could not capture the slope of the entire travel path surface, and the target accuracy could not be achieved. Therefore, we collaborated with a company that possesses technology to measure the shape of desert roads (Fig. 4).

The principle of measurement is that a crawler vehicle is equipped with a laser capable of capturing 360° shape data, and the vehicle's position and posture are determined from high-precision GPS data. This technology makes it possible to scan small

Fig. 4 Road Surface Measurement Vehicle

irregularities in the road surface while keeping track of a large area.

In the case of UVs, uneven road surfaces are often sharply undulating, unlike desert dunes, so repeated measurements were taken from all directions and the results were superimposed to create a shape. To further improve the accuracy of the road surface shape, filter processing was performed to remove grass and fine pebbles not needed for driving analysis, resulting in the conversion of data from complex, uneven road surfaces over a large area into a 3D shape within a target error (Fig. 5).

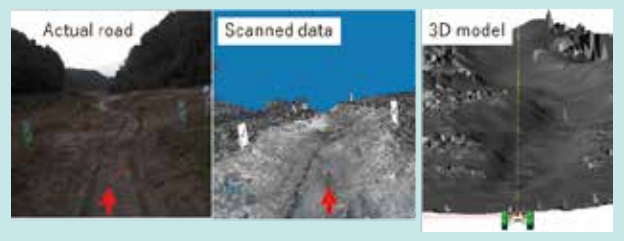

Fig. 5 3D Modeling of a Rough Road

4.1.3 Solution 3: Advanced vehicle driving model

(1) Implement and cabin-mount modeling method

The plough (a type of implement) mounted on a tractor tends to flex, and the tractor cabin has a cabin mount, so they behave differently than the vehicle body when driving on rough roads. Therefore, we modeled the implement as an elastic body and the cabin mount as a spring-damper element. This makes it possible to account for the behavior of heavy objects, as well as phase differences and structural damping when loads are transferred to the vehicle body.

(2) Drive-train modeling

By modeling drivetrains, including differentials for driving analysis, and expressing the distribution of driving torque and tire turning angle according to the throttle opening and steering angle, we enabled the analysis of vehicle behavior with high accuracy.

4-2 Fatigue life analysis technology

4.2.1 Solution 1 for fatigue life analysis technology: Analysis technology for evaluating stress in a time series

(1) Analysis modeling method

UV tires are connected to the vehicle by A-arm and suspension linkage, and tractor implements are connected to the vehicle by 3P linkage. For such linkages, the conventional analysis method of directly connecting the load points and the vehicle body with rigid elements results in low stress accuracy at the root of the connection. Considering that this was due to the fact that the actual load distribution of the linkage could not be represented in the analysis, we included the suspension mechanism and the 3P linkage in the analysis to develop a model that provides joint conditions according to the actual movement. This allowed the loads on the vehicle body to be distributed with an error of less than 3%, achieving a stress prediction accuracy exceeding the target (Fig. 6).

(2) Stress evaluation method

With conventional methods, it took several hours to calculate the stress distribution throughout a vehicle at a given time, and several months to perform a stress analysis for an entire long endurance test. Considering that the stress generated in each part of the frame is mainly the static stress generated by finding balance with input loads, we applied a method that can evaluate the stress state sequentially by linearly superposing stresses against time-series loads. This method has saved several months of analysis time because the stress history is determined by the stress obtained by the unit load multiplied by the input load history (red frame in Fig. 7).

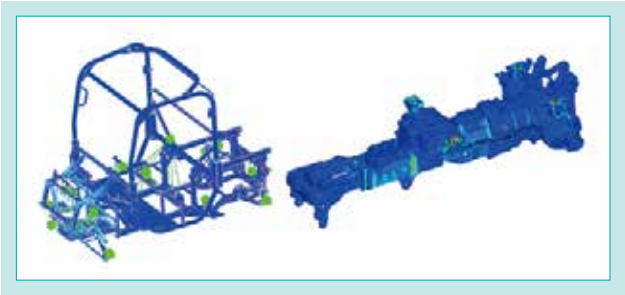

Fig. 6 Analysis Models

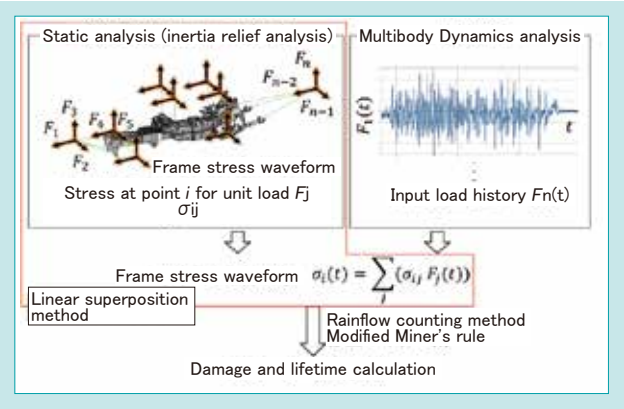

Fig. 7 Process of Estimating the Fatigue

4-3 Optimal design technology

(1) Sheet metal frame optimization method

There are tens of thousands of combinations of sheet metal frame component thicknesses, and the designer's experience and intuition alone were insufficient to determine the optimal combination of thicknesses within the development time, making it difficult to reduce weight. Therefore, we applied a method to automatically optimize the sheet thickness of each component, using the thicknesses available on the market as candidates, and made it possible to quickly determine the lightest sheet thickness while maintaining durability.

(2) Cast parts optimization method

Previously, weight reduction depended on the designer's experience based on stress analysis results for multiple conditions, which prevented adequate investigation of weight reduction. Therefore, we used a shape optimization method that varies the surface shape of the casing as a design variable to clarify the areas that contribute significantly to stiffness, allowing us to add the necessary ribs and fillets. To ensure endurance performance for multiple load conditions, we developed a method that uses a stress threshold based on the number of endurance cycles as a constraint and a method that allows optimization to account for the rigidity of the implement, which varies with each operation. This made it possible to create the lightest shape while maintaining durability under all load conditions.

4-4 Verification of effectiveness

To verify the accuracy of the developed technology, an endurance test was conducted on a circular rough road using Kubota's first 170-hp M7 tractor. Wheel force transducer capable of measuring the loads applied to the tractor axle was used (Fig. 8). The six-axis transducer and measuring jigs were designed to match the weight conditions of an actual machine's endurance test by using aluminum alloys in some parts to reduce weight while ensuring strength to withstand the high load of the M7. In addition, acceleration sensors were installed in a total of eight locations on the four wheels, cabin, vehicle body, front weight, and implement, and gyro sensors were installed on the vehicle body to measure the load on the tractor and the behavior of the vehicle body during the test. At the same time, the stresses generated in the vehicle body were measured.

As a result of the verification, it was confirmed that the load input from the ground to the axle through the tires can be calculated with an accuracy of 10% or less in peak value error from the comparison between the driving analysis and the actual measurement (Fig. 9).

We also confirmed that the error between the measured and analyzed stresses was 15% or less at the time when high stresses occurred in the vehicle body (Fig. 10). Finally, the fatigue life which was analyzed was compared with the fatigue life calculated from the measured stress data, and it was confirmed that the fatigue life could be predicted within an order of magnitude error even in areas of high fatigue, indicating that fatigue life can be evaluated with high accuracy (Fig. 11).

Fig. 8 Verification Test Using an Actual Machine

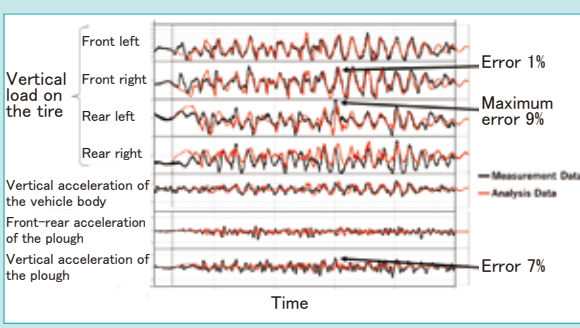

Fig. 9 Validation of the Running Analysis

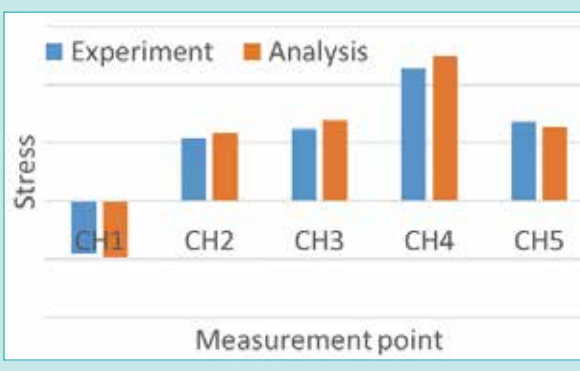

Fig. 10 Validation of the Stress

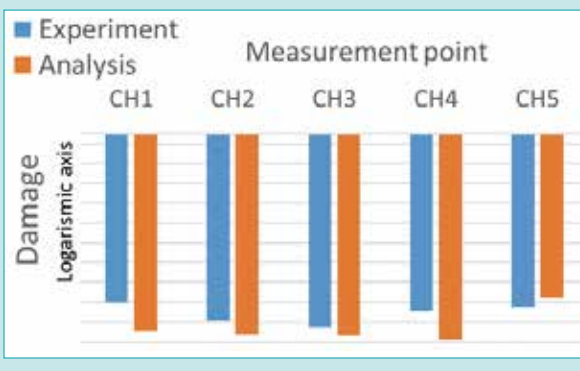

Fig. 11 Validation of the Fatigue Life

5. Conclusion

The technology described here enables Kubota to ensure durability in a short time at the design phase for products with which the Kubota has no previous development experience.

In the future, we will apply the developed technology to other agricultural and construction machines.

Contribution to SDG targets

1.a Strengthening cooperation in the development of emerging countries
Applying technology and contributing to the mechanization of agriculture in emerging countries

2.4 Achieving sustainable and resilient agriculture
Ensuring necessary product durability at an early stage

12.2 Sustainable management and efficient use of natural resources
Contributing to resource conservation by reducing prototype creation

Reference

1) Masato Abe: “Automotive Vehicle Dynamics” Tokyo Denki University Press, 2008, p. 181-194.
2) Koji Koibuchi: “Introduction to Material Mechanics and Fatigue Design” Nikkan Kogyo Shimbun, 2009, p. 108-123.
3) Yohei Kubota: “Rough Road Fatigue Life Estimation by Flex-body Full Vehicle Simulation” Transactions of the Society of Automotive Engineers of Japan, Inc., Vol. 41, No. 2, 2010, p. 183-188.

Development of the Combine Harvester DC-120X for Thailand

Combine Harvester Engineering Dept. ／ Analysis Center

Kubota has acquired the top share in the Thailand combine harvester market in terms of sales volume. However, the market share remains relatively low in the harvesting area in the main north-eastern region. This is due to the strong popularity of machines manufactured by other companies in Thailand, which have high work efficiency in spite of the adverse conditions of the long-culm lodging rice and deep wet fields that are prevalent in the north-eastern region. Therefore, we developed a new model to improve "long-culm lodging performance" and "wet field performance" with a 2-pump 2-motor transmission, aiming to improve work efficiency under adverse conditions.

【Key Word】
Combine Harvester, Long-culm Lodging Rice, Wet Field, 2P2M T/M

Related SDGs

1. Introduction

The mechanization rate of rice farming in Thailand has reached almost 100%, and Kubota has the leading share of the country's combine harvester market in terms of sales volume. However, in the northeastern part of the country, which is the main rice-growing region, the company's share remains relatively low in terms of the area harvested. This is because local machines with high horsepower in the 200 hp range (compared with Kubota's current machines of around 100 hp) and high work efficiency remain popular in the northeastern region, where adverse conditions of long-culm lodging rice and deep wet fields (Fig. 1) , i.e., highly viscous deep muddy wet paddies, are common. The local machines have 2P2M transmissions, which means that two hydraulic motors drive the left and right crawler tracks, respectively. This provides excellent turning performance in deep wet fields through soft-turns, i.e., gentle turning with both wheels driven.

On the other hand, the heavy weight of the local machines is a disadvantage. While Kubota's existing machines weigh about 4.6 tons, the local machines are very heavy at about 8 tons because they are equipped with a high-horsepower engine and two hydraulic motors. Machines that are too heavy can easily disturb fields and cause problems such as damage to roads and the ridges between fields. Kubota's existing machines have earned a reputation in the market for not disturbing fields due to their light weight, and there is a growing demand for products that can handle the aforementioned adverse conditions while being lightweight.

Based on the above, we worked to develop a combine harvester that would improve work efficiency by improving long-culm lodging performance and wet field performance, while maintaining the light weight that is a strength of Kubota machines.

Fig. 1 Wet Field

2. Development concept and target values

2-1 Development concept

The concept of the newly developed DC-120X (Fig. 2) is as follows: a combine harvester that achieves high efficiency, extended operating hours, and improved adaptability to conditions, while maintaining the high durability of the existing machines' driving function, which is highly regarded in the market. In this paper, we describe our efforts to realize this concept in terms of improving long-culm lodging performance and wet field performance.

[Improvement of long-culm lodging performance]

- Reduce the frequency of long-culm rice windings and jams by improving the rice passage performance from the feeder to the thresher.

[Improvement of wet field performance]

- Improve operability and turning performance by mounting 2P2M transmissions.
- Avoid the vehicle bottom getting stuck in the mud by increasing the minimum ground clearance.
- Improve the front-rear balance by adopting rear-wheel drive.
- Improve wet field driving performance by designing a front/rear boat-shaped crawler track profile.

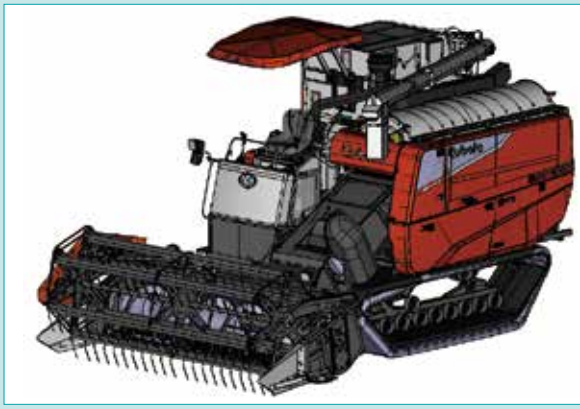

Fig. 2 Combine Harvester DC-120X

2-2 Target values

The local machine mentioned in the previous sections has a throughput, expressed as the product of the harvesting width and the maximum vehicle speed during operation (i.e., the theoretical harvesting area per second for a standard standing crop), which is approximately 1.45 times that of Kubota's existing DC-105X machine. On the other hand, the throughput of the developed DC-120X machine is 1.32 times greater than that of the DC-105X machine. Since it is difficult to actually measure the work efficiency of the local machine in the field, we assume that the work efficiency of the local machine is 1.45 times higher than that of the DC-105X even in long-culm lodging rice. Assuming that the long-culm lodging rate is 50%, based on past data, the DC-120X must have 1.58 times higher work efficiency for long-culm lodging rice than the DC-105X in order to have an average work efficiency 1.46 times that of the DC-105X. Therefore, the target value of work efficiency is given as at least 1.60 times the work efficiency of the existing DC-105X in harvesting long-culm lodging rice (Table 1).

In terms of wet field performance, while the DC-105X can work in a field with a foot sinkage of 30 cm, the goal is to be able to work in a field with a foot sinkage of 40 cm or more (approximately 1.33 times greater than the existing machine), where the local machine has been proven to work.

Table 1 Comparison of Throughput and Target Values

Item	Existing model DC-105X	Local model	Developed model DC-105X	
Work efficiency for a standard standing crop (based on throughput)	1	1.45 times	1.32 times	
Work efficiency for long-culm lodging rice	1	1.45 times	1.60 times or more	
Average work efficiency	1	1.45 times	1.46 times or more	← Target value
Wet field performance (workable foot sinkage)	30 cm	40 cm or more (1.33 times or more)	40 cm or more (1.33 times or more)	

3. Technical issues to be solved

3-1 Long-culm lodging performance

While the total height of Japanese rice plants ranges from 70 to 115 cm, the long-culm rice plants common in northeastern Thailand grow to 170 to 200 cm (Fig. 3), with some varieties reaching over 300 cm. When the rice has fallen over, it is difficult to harvest only around the seeds, so a very large amount of straw gets into the reaper. Long straw tends to wrap around the rotating transport mechanism and cause jams during conveyance from the reaper to the thresher (Fig. 4), resulting in reduced efficiency. Since clearing jams is a time-consuming process, reducing the frequency of jams will greatly improve work efficiency. In this development, we focused on reducing jams in the feeder-to-thresher transition section, where jams occur most frequently.

Fig. 3 Long-culm Lodging Rice

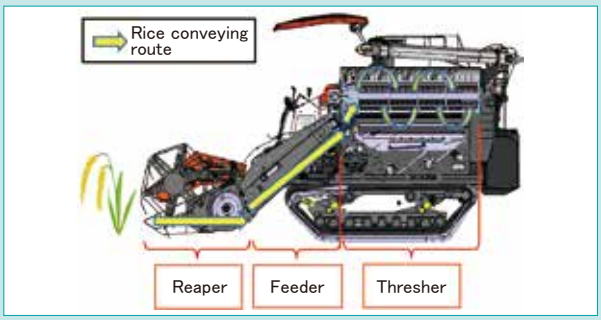

Fig. 4 Transport Path of Rice

3-2 Wet field performance

In wet fields with large foot sinkage, as shown in Fig. 1, it becomes difficult to move forward with crawler tracks when the vehicle sinks and its bottom becomes stuck in the mud. Once stuck in a wet field, the vehicle must move back and forth repeatedly to free itself, ruining the field, and if the vehicle still cannot get out, it must be towed by another machine, resulting in a significant loss of work efficiency. In addition, the transmissions of Kubota's existing machines in Thailand use a turning system called a brake-turn system, which cuts off the power to the inside crawler track when turning, and even if the vehicle can move straight in a wet field, the driving-side crawler track tends to slip when turning due to insufficient drive power.

4. Developed technology

4-1 Improvement of long-culm lodging performance

4.1.1 Flow analysis of the feeder-to-thresher transition section

To get through the transition section with fewer jams and windings, it is necessary to determine the optimum shape and combination of the various elements that make up the transition section. However, it would take too many man-hours to harvest and check for jams in all the possible combinations. To study the elements of the transition section that have a significant impact on performance, we modeled the conveying path and rice plants to conduct a rice flow analysis in collaboration with the Analysis Center (Fig. 5). After trying various combinations in this analysis, the following three elements were found to be important in the transition section (Fig. 6):

(1) The angle of the rice plants thrown into the thresher

(2) The speed of the conveyance to the thresher

(3) The shape of the drum and screw at the front end of the threshing cylinder (rice threshing part)

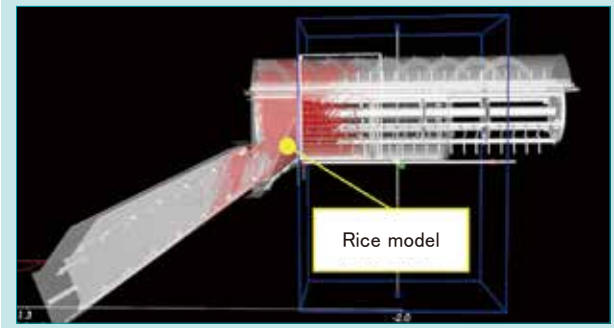

Fig. 5 Flow Analysis Model

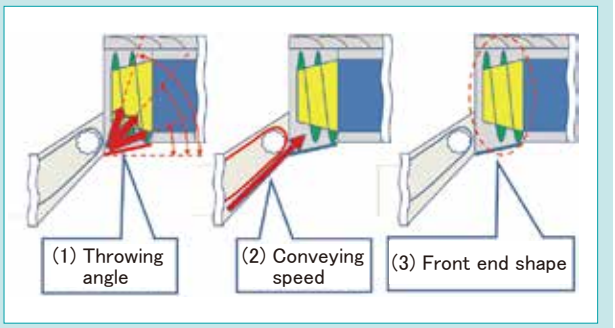

Fig. 6 Key Elements in Baton Touch

4.1.2 Bench test

To select the optimal shape and optimal combination of the above three elements in actual rice conveyance based on the results of the analysis, a bench test was conducted using reproduced Thai long culms, which were conveyed from the feeder to the thresher (Fig. 7). The content of the investigation for each element was as follows:

(1) Changing the relative positions of the feeder and thresher (two cases) and changing the thresher entrance plate angle (two cases)

(2) Changing the speed of the feeder chain for conveying rice inside the feeder (two cases)

(3) Changing the shape of the drum and screw at the front end of the threshing cylinder (three cases each)

From a total of 72 combinations tested in the bench test, those that did not cause jamming were selected. Jamming was reduced by lowering the feeder outlet by 76 mm from the current level and increasing the inlet plate angle by a factor of approximately 2.1 for above (1) (Fig. 8), and also increasing the conveying speed by 30% for above (2). This is believed to be due to the rice being raked up in front of the screw at the front end of the threshing cylinder, causing the conveyance to occur at an earlier stage. As regards the shape in above (3), it was possible to narrow down the combinations of above (1) and (2) to the three that would allow transition without jamming. These combinations were actually used to harvest long-culm lodging rice in a field in Thailand to compare the transition performance.

Fig. 7 Bench Test

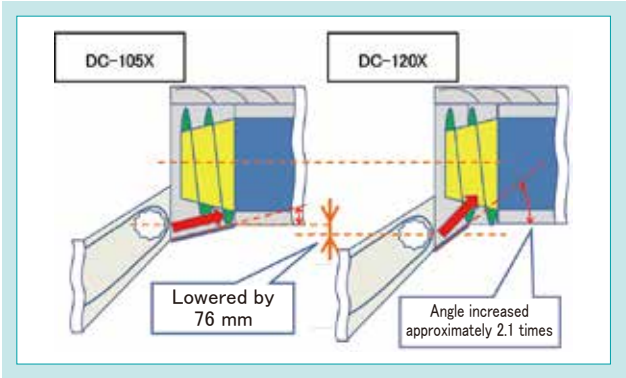

Fig. 8 Changing the Throwing Angle of Rice

4.1.3 Field test

Rice plants with a total length of approximately 200 cm and a lodging rate of 100% were harvested with three different front-end shapes of the threshing cylinder to determine the combination of drum and screw shapes with the best transition performance. Compared to the existing DC-105X machine, the new model with this combination delivered a 1.65-fold increase in work efficiency, achieving the target factor of 1.60 or more (Table 2).

Table 2 Results of an Efficiency Comparison

Item	Field area [ha]	Time required [s]	Efficiency [ha/h]	Efficiency ratio compared to the existing machine
DC-105X	0.11	1921	0.206	1
DC-120X	0.09	956	0.339	1.65

4-2 Improvement of wet field performance

4.2.1 Mounting 2P2M transmissions

This system has high traction because it is driven by two hydrostatic transmissions (HSTs) and, unlike the conventional transmissions mounted on existing machines, power is also transmitted to the inside crawler track when turning, so that road surface resistance is shared by both crawler tracks to reduce slippage in wet fields. Whereas previously only brake-turn was available, soft-turn and spin-turn have been added to provide three turning modes, improving maneuverability and turning performance (Fig. 9).

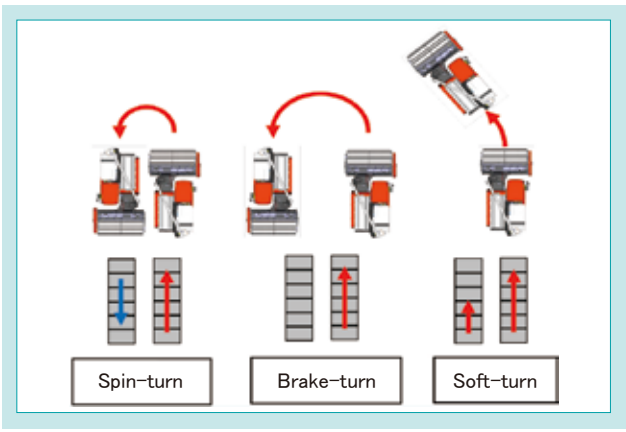

Fig. 9 Turning Systems

4.2.2 Increasing the minimum ground clearance

The minimum ground clearance (distance from the ground surface beneath the crawler track to the bottom of the transmission) of the DC-120X is 75 mm greater than that of the existing DC-105X to reduce the likelihood of the vehicle bottom getting stuck in the mud in wet fields where foot sinkage is large (Fig. 10).

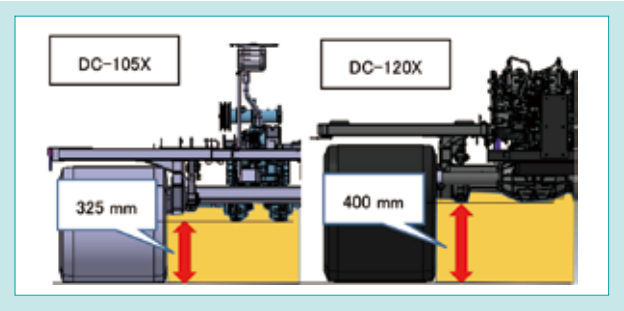

Fig. 10 Ground Clearance Comparison

4.2.3 Rear-wheel drive

In a conventional ordinary combine harvester, the engine, transmission, and driver's seat are located at the front of the machine, and the feeder and harvester are overhung in front of the machine, resulting in weight concentration at the front of the machine (Fig. 11). Some models carry weights in the rear of the machine only to adjust the front-rear balance. Since the 2P2M transmissions are approximately 25% heavier than the existing transmissions, installing them in the original position on the existing DC-105X will make the front of the machine correspondingly heavier. Therefore, the DC-120X was designed with a rear-mounted transmission and rear-wheel drive to achieve the same level of front-rear balance as the DC-105X without the need for balance weights (Fig. 12).

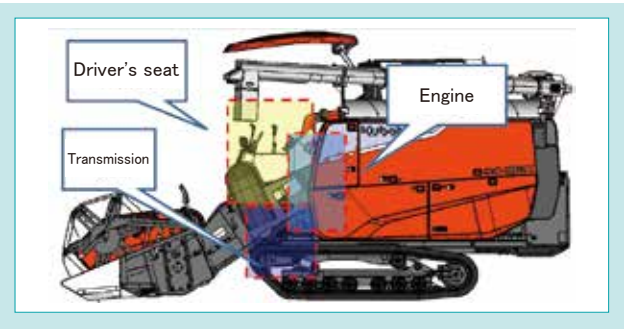

Fig. 11 Ordinary Combine Layout

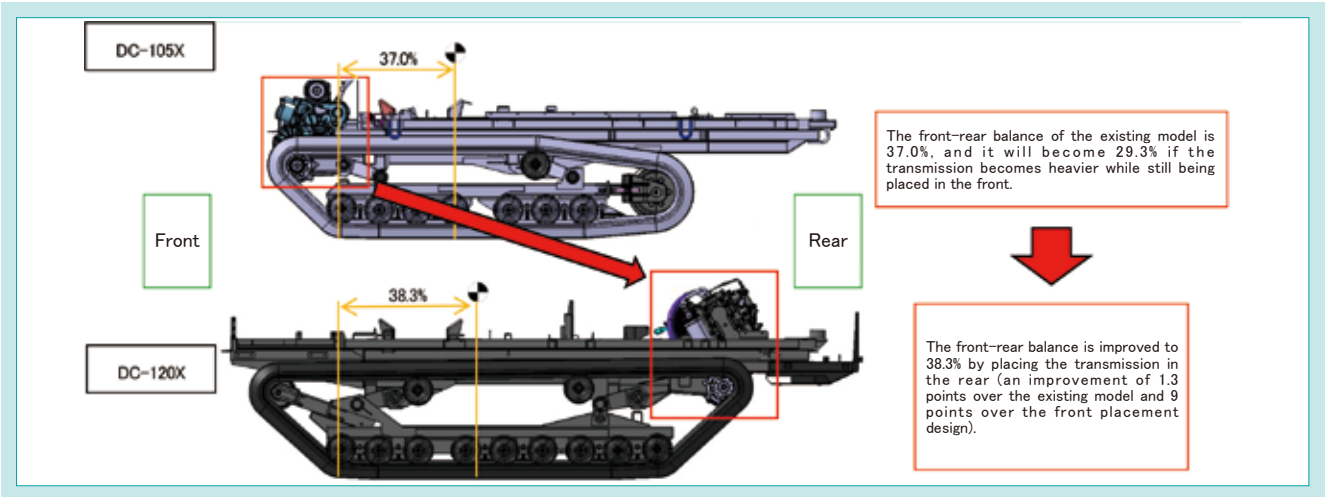

Fig. 12 Comparison of the Anteroposterior Balance

4.2.4 Front/rear boat-shaped crawler track profile

In a wet field, the smaller the angle θ that the crawler track surface makes with the ground in the direction of travel, the smaller the force of the machine going over the mud when the machine sinks (Fig. 13). Conventional machines increase this angle by designing the crawler tracks to have a boat-shaped profile on the front side. On the other hand, the DC-120X has crawler tracks whose profile is boat-shaped on both front and rear sides to achieve high drivability in wet fields in both forward and reverse directions (Fig. 14). This profile was achieved by changing the tensioning direction of the crawler tracks.

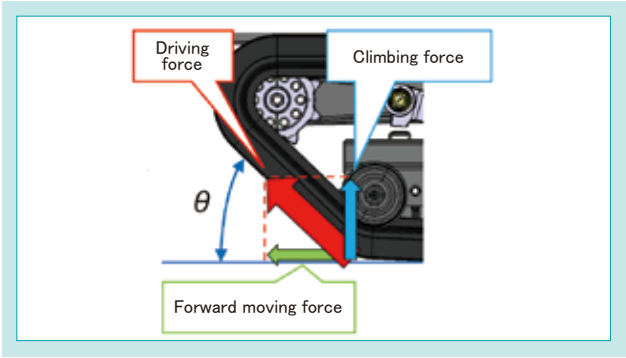

Fig. 13 Boat Shape Angle of the Crawler

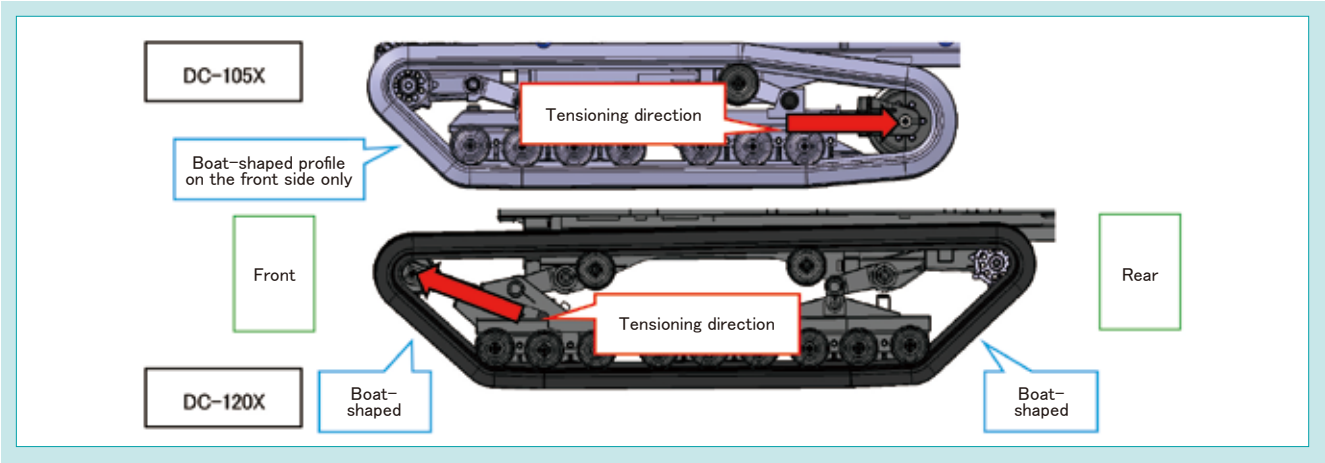

Fig. 14 Front and Rear Boat Shape of the Crawler

4.2.5 Field test

The wet field performance of the existing DC-105X and the DC-120X was compared in a wet field with a foot sinkage of 45 cm by measuring the time required to make a round trip along a straight 100 m line while harvesting. As a result, the DC-105X got stuck in the wet field once while harvesting and took 65 seconds to escape, while the DC-120X did not get stuck at all. The DC-120X also took less time to turn and was 1.86 times more efficient (Table 3). To test the limits of the DC-120X's wet field performance, it was run harvesting in even deeper wet fields and was confirmed to operate at a foot sinkage of up to 55 cm and could run at a foot sinkage of up to 60 cm, achieving the target of 40 cm or more.

Table 3 Results of an Efficiency Comparison

Item	Time required [s]	Time stuck in the wet field out of the total time required [s]	Efficiency ratio compared to the existing machine
DC-105X	414	65	1
DC-120X	222	0	1.86

4-3 Development results

In the developed DC-120X, the target work efficiency and the target workable foot sinkage were achieved by improving the long-culm lodging performance and wet field performance. In achieving the goal, flow analysis and bench testing conducted jointly with the Analysis Center enabled us to significantly reduce the cost and man-hours required to conduct field testing. In the conventional layout of ordinary combine harvesters, the adoption of 2P2M transmissions to improve wet field performance has sometimes been difficult because of the negative impact of weight imbalance. However, the new layout with the transmissions positioned at the rear of the machine has allowed us to demonstrate improved wet field performance in regions other than Thailand and for different classes of combine harvesters.

5. Conclusion

We have developed a technology that can attract new users, focusing on users who use locally available machines in adverse conditions such as long-culm lodging rice and deep wet fields.

Therefore, in the future, we will apply this analysis and the bench test results to wheat, corn, beans, buckwheat, etc., and study the adaptation and shape optimization for different crops. Although we were able to achieve wet field performance well above the target foot sinkage in this study, it is also true that there are much deeper wet fields. We will consider developing new technologies to address this issue and further improve wet field performance.

Contribution to SDG targets

2.3 Increased agricultural productivity and income
Contributing to labor-saving and lightening of harvesting work by improving work efficiency

8.2 Increased productivity through innovation
Contributing to improved work efficiency in deep wet fields with 2P2M transmissions and rear-wheel drive

9.2 Strengthening of inclusive and sustainable industrial infrastructure
Addressing the issue of labor shortages in agriculture by saving labor in the harvesting of long-culm lodging crops

Development of the Unmanned Autonomous Combine Harvester “DRH1200A-A”

Farm and Industrial Machinery R&D Dept. Ⅵ／ Farm and Industrial Machinery R&D Dept. Ⅰ
Technology Innovation R&D Dept. Ⅱ／ Combine Harvester Engineering Dept.

The level of automatic operation of agricultural machines is roughly divided into three levels: Level 1 is automatic steering with the user on board, Level 2 is automatic operation with the user off board and monitoring from a visible location, and Level 3 is automatic operation with remote monitoring[1]. The combine harvester, which is run while harvesting rice and wheat, has problems such as monitoring the surrounding area during operation, a high level of difficulty in operation, and continuity of operation. It was difficult to achieve Level 2, but advanced technology and control technology overcame these problems and succeeded in commercialization. This paper introduces the obstacle detection technology in the working environment and the technology to automate reaping work, as well as the technology to improve the efficiency of automatic operation work, which were developed to realize this automatic operation Level 2 combine.

【Key Word】
Combine Harvester, Autonomous Driving, Obstacle Detection, 2D-LiDAR, Millimeter-wave Radar

Related SDGs

1. Introduction

As Japanese agriculture faces a decline in the number of workers and an aging workforce, the consolidation of farmland and expansion of farming scale are accelerating. Under these circumstances, the development of robotic agricultural machines that perform tasks automatically is being promoted to increase efficiency and save labor. Kubota has been selling unmanned Level 2 automatic operation models for tractors and rice transplanters, but has not been able to do so for combine harvesters that travel while harvesting crops due to problems with detecting surrounding obstacles and ensuring continuous operation.

We have recently developed the DRH1200A-A automatic combine harvester for unmanned harvesting of rice and wheat by developing new sensor and control technology (Fig. 1) .

Fig. 1 Unmanned Autonomous Combine Harvester “DRH1200A-A”

2. Development concept and target values

2-1 Development concept

Since 2018, Kubota has been selling automated combine harvesters. With previous models, the operator had to perform some tasks, such as monitoring people and obstacles around the machine during automatic operation, adjusting the position of the reaper according to the crop, and performing recovery operations when the reaper became jammed. It was also necessary to manually drive and reap around the field perimeter three times in advance to create a field map needed for automatic operation. As a result, the market demanded a combine harvester that could operate automatically without an operator in the cab, expand the harvesting area, and further reduce the workload.

Therefore, the concept of this product was to develop an unmanned combine harvester that could perform harvesting operations like a skilled operator and expand the area of automatic operation.

2-2 Development goals

Based on the development concept, the following development goals were set:

(1) A surroundings monitoring system ideal for harvesting operations

The goal is to develop a surroundings monitoring system that detects people and obstacles without detecting crops, weeds, birds, etc., present in the field during harvesting operations.

(2) Automated harvesting operation technology necessary for unmanned harvesting

(i) An automatic reel control function

Skilled operators adjust the reel position of the harvester according to the ear height of the crop (Fig. 2). Therefore, the goal is to develop a function that automatically controls the reel position during harvesting.

(ii) An automatic unjamming function

In some cases, crops get stuck in the reaper during harvesting operations (Fig. 2). The goal is to develop an automatic unjamming function so that unmanned automatic operation can continue without stopping the machine in such cases.

(3) Expansion of the area of automatic operation and an improvement of efficiency

With the existing machine, three laps of reaping were required in manual operation to create a field map for automatic operation, and the area of automatic operation was only 71%.* The new machine aims to reduce the required number of laps in manual operation to one, and to perform automatic operation in 90%* or more of the area (Fig. 3). Another goal is to achieve the same efficiency as a skilled operator (5% or less increase in work time compared to a skilled operator).

* Conditions for calculating the automatic operation area
  - Field size: 1 ha (100 m × 100 m)
  - Header size: 2.6 m

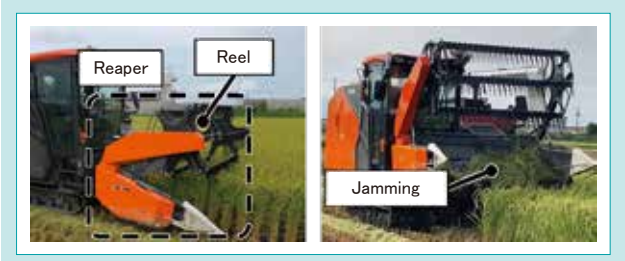

Fig. 2 Reaping Part and Clog

Fig. 3 Autonomous Work Area

3. Technical issues to be solved

3-1 A surroundings monitoring system ideal for harvesting operations

Unmanned automatic tractors and rice transplanters are equipped with obstacle detection technology using laser sensors (laser light) and sonar (sound waves). However, because combine harvesters travel through crops during harvesting, laser sensors or sonar would incorrectly detect crops as obstacles, as shown in Fig. 4. Therefore, a new obstacle detection system was needed that could adapt to the combine harvester's working environment and accurately detect people and obstacles without misidentifying crops as obstacles.

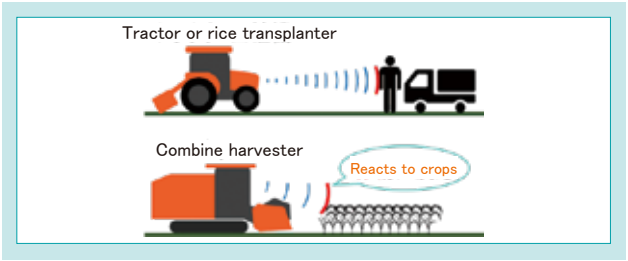

Fig. 4 Difference of the Environment Tractors and Combines

3-2 Automated harvesting operation technology

3.2.1 The automatic reel control function

To automatically control the reel position according to the crop height, it is necessary to develop new technology to detect the crop height in front of the vehicle.

3.2.2 The automatic unjamming function

In manual operation, if the reaper is jammed, the operator pulls up the lever that rotates the reaper in reverse to remove the jammed crop from the reaper. This process needs to be automated.

3-3 Expansion of the automatic operation area

With the existing machine, three laps of perimeter reaping are performed in manual operation to map the field, followed by automatic operation. Reducing manual operation to one lap will cause automatic operation to start without having enough space for a turn. Therefore, a new automated technology was needed to achieve efficient turning in a confined space (Fig. 5).

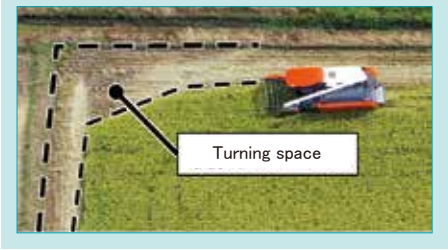

Fig. 5 Turning Space After One Lap

4. Developed technology

4-1 A surroundings monitoring system ideal for harvesting operations

4.1.1 Person detection technology

To detect people during harvesting, we developed a sensor system that uses AI to detect people from image data captured by the cameras (Fig. 6). First, we corrected a large amount of image data of people in the harvesting work environment to teach the features of people to AI. This trained AI model is specialized in detecting people from images captured by the cameras mounted in four directions on the machine (Fig. 7).

However, when this AI runs on its own, several types of objects could be mistakenly identified (false-positive) as people. Through the analysis of factors causing misidentification, we revealed that many misidentification cases were caused by a combination

of features, including parts of the machine itself, shadows, and backgrounds. Therefore, to reduce the effects of machine parts, shadows, and backgrounds, masking was applied to the captured images to hide the area of the machine itself. To cope with variability in the camera mounting posture and lens, we also developed a technique to dynamically generate a mask area from feature points of the machine itself that were captured by the cameras.

Furthermore, detection accuracy in diverse environments was improved by analyzing the color distribution of training data, as well as the positions of objects and cameras, and by statistically collecting data without bias. For objects detected as people, stable detection performance was pursued by scoring the objects according to the level of collision risk and deciding whether to stop the machine based on the results.

As a result of the technological developments above, we have developed an AI-based person detection system with high accuracy, which suppresses false detection of objects such as crops, weeds, and birds.

Fig. 6 Camera Mounted Around the Combine Harvester and Person Detection

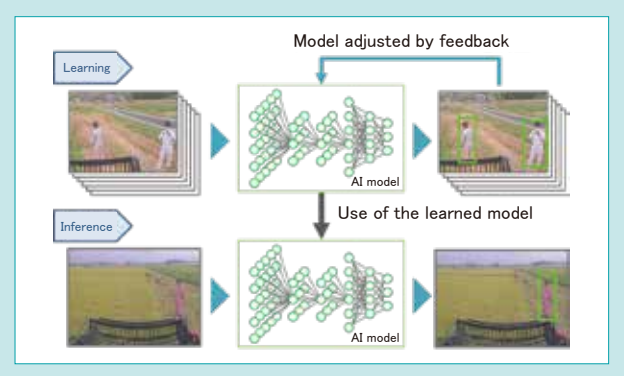

Fig. 7 Learning and Inference with AI

4.1.2 Vehicle detection technology

Vehicles and other objects entering the field are detected by a sensor system using millimeter wave radar mounted at the front and rear of the machine (Fig. 8).

Millimeter wave radar can measure the distance and direction to an object by emitting radio waves in the millimeter wave band and measuring the reflected waves. In the harvesting environment, the reflected wave includes those reflected from vehicles and those reflected from crops and weeds that are not targeted for detection. Therefore, the signal strength of the reflected waves is used to distinguish the measurement points of vehicles from those of crops and weeds. Since there are cases in which nontarget objects cannot be identified and removed simply by setting a threshold value, the detection area of the millimeter wave radar is divided into multiple areas, and an object is judged to be an obstacle when the number of measurement points detected in the same area for a certain period or longer exceeds the threshold value (Fig. 9).

If there are vehicles or metal structures with high reflectivity in the vicinity of the field, the scope of detection is limited to within the field map for automatic operation in order to avoid false detection of these objects. To avoid false detection associated with measurement points other than those relevant to the machine's direction of travel, the scope of detection is changed dynamically based on the direction of travel.

With these technologies, we have developed a sensor system that detects vehicles in the field while avoiding false detections caused by crops and weeds in the field and objects outside the field.

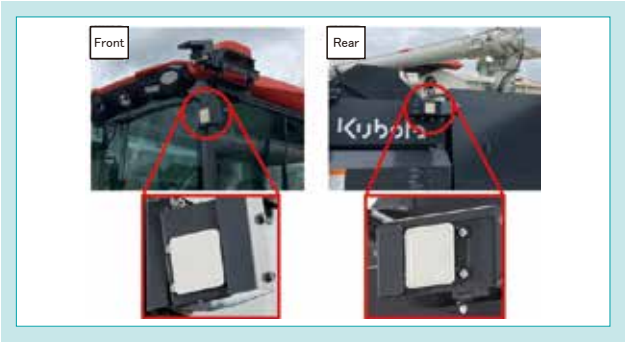

Fig. 8 Millimeter-wave Radar

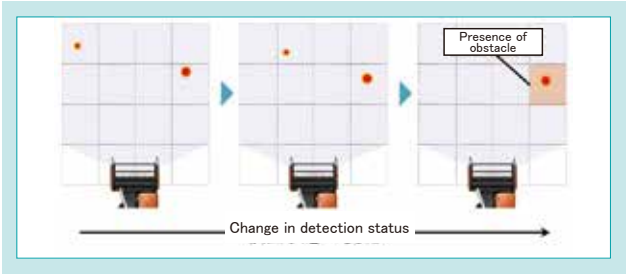

Fig. 9 Detection Area and Obstacles

4-2 Automation of harvesting operations

4.2.1 Reaper control based on the height of harvested crops

To automatically control the reel position according to the crop height, a laser sensor (2D-LiDAR) was mounted on the upper front of the machine and a new control technology was developed.

As the machine automatically harvests crops, it acquires the position of the machine using Real Time Kinematic GNSS (RTK GNSS), the posture of the machine using an Inertial Measurement Unit (IMU), and three-dimensional point cloud data in front of the machine using laser sensors (Fig. 10).

After noise removal, this data is converted to data for each coordinate point in the forward region and stored. From the accumulated data, the median crop height is calculated at regular intervals to create a crop height map (Fig. 11). Based on the generated crop height map, the reel fore/aft position, up/down position, reel speed, and vehicle speed are automatically controlled.

The automatic control set points corresponding to crop height were determined by analyzing the operating data of experienced operators. Since the time required to move the reel back and forth or up and down, to adjust the reel speed, or to increase or decrease the vehicle speed varies, the crop height information at the optimum point for each relevant section was used to control the operation.

This crop height sensing technology allows the reaper to be operated according to the crop height, just as an experienced operator would.

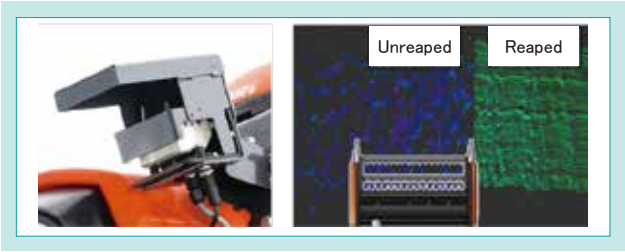

Fig. 10 Laser Sensor and Measurement Data

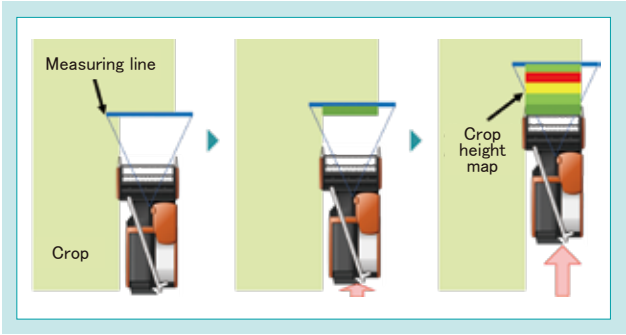

Fig. 11 Generated Image of the Crop Height Map

4.2.2 Automatic unjamming of the reaper

We have developed an electric reaper reversing device and automatic unjamming control that can automatically unjam and resume operation when the reaper is jammed.

Since a large instantaneous torque is required to unjam the reaper, an engine starter motor is used as the drive unit, and a gear train mechanism is used to reverse the drive of the reaper (Fig. 12).

When the rotation sensor on the reaper detects that the reaper has stopped rotating due to a crop jam, the harvesting travel stops and backward movement begins. In this case, the reaper rises, the machine moves backwards, and then the reaper rotates in reverse to release the jammed crop forward, so that the cutting blades do not cut the tips of the crop in front of them during reverse operation. After release, the reaper is rotated forward, and harvesting travel resumes when the jam is cleared (Fig. 13). Immediately after resuming, the reaper and reel positions are lowered to the lowest limit to collect the crop released in front of the machine during the reverse movement.

The reaper's automatic unjamming feature allows unjamming and resumption to occur without human intervention, improving the continuity of unmanned operations.

Fig. 12 Electric Reaping Reversing Device and Unclogging

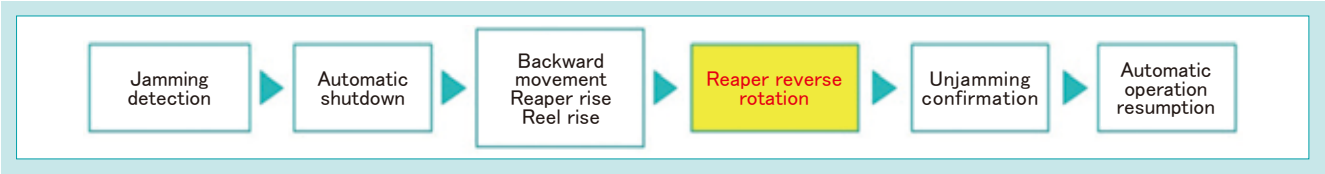

Fig. 13 Automatic Release Flow for a Clogged Cutting Part

4-3 Expansion of the automatic operation area

4.3.1 Field corner harvesting technology

Generally, when harvesting in a situation where there is not enough space to turn, such as at the very edge of a field, harvesting is performed by repeatedly driving back and forth around corners to gradually create space for turning. As a result, the remaining unharvested area has a complex polygonal shape. We have developed a harvesting technique for the corners of this polygonal field (Fig. 14).

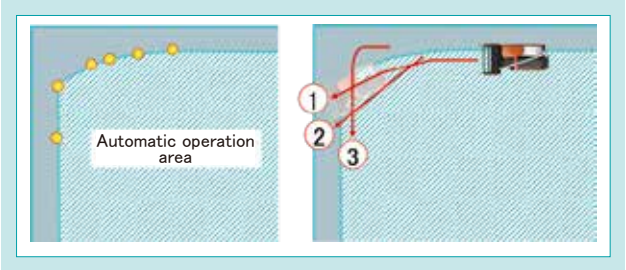

Fig. 14 Recognition and Reaping Method of a Corner Section

First, the unharvested area of the field is shaped in detail by connecting vertexes (up to 64 points) with straight lines. Next, the field outline and the unharvested area at the field corners are checked to determine if there is a turning area, and if there is not enough turning area, a harvest path is generated along the unharvested area. The forward/backward harvesting motion is repeated until a turning area is secured, then the machine turns.

In this way, the corners of the field can be harvested as an expert operator would do. By harvesting only the outermost perimeter in manual mode, the second and subsequent rounds can be done in automatic mode, increasing the area of automatic operation in the field to 90%.

4.3.2 Ridge height map

When harvesting the corner of a field, an experienced operator will turn the machine while allowing the front and rear of the machine to partially overhang the peripheral field ridge if the ridge is low. This reduces the number of back and forth movements, resulting in more efficient movement. To enable efficient turning in automatic mode comparable to the performance of an experienced operator, we have developed technology that detects the height of the peripheral ridges. If a ridge is low, the machine is able to turn efficiently with its front and rear partially overhanging the ridge.

First, when harvesting the outermost edge of the field in manual mode, a laser sensor is used to capture three-dimensional point cloud data in front of the machine (Fig. 15). This point cloud data is converted to coordinate data to create a raster height map. A ridge height map is then created, treating the outside of the area where the combine harvester has traveled as the ridge area. If there are weeds growing on the ridge or crops lying on the ridge, the height including them will be recognized as the height of the ridge. To prevent this, a filtering process is applied to remove point clouds with low spatial density, allowing the ridge height to be determined with minimal influence from weeds and fallen crops on the ridge.

Based on this ridge height map, the system determines if it is possible for the front and rear of the machine to overhang the ridge and allows overhanging if possible, providing automated operation comparable to that of a skilled operator (Fig. 16).

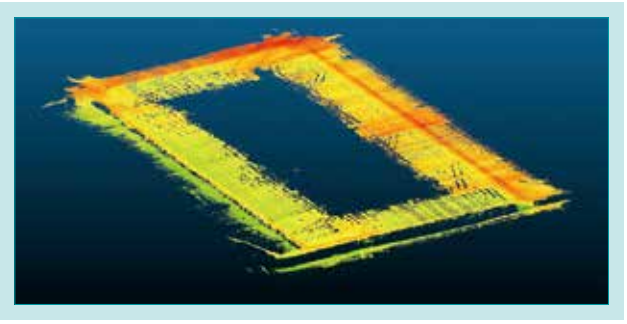

Fig. 15 Measurement Data Around the Field

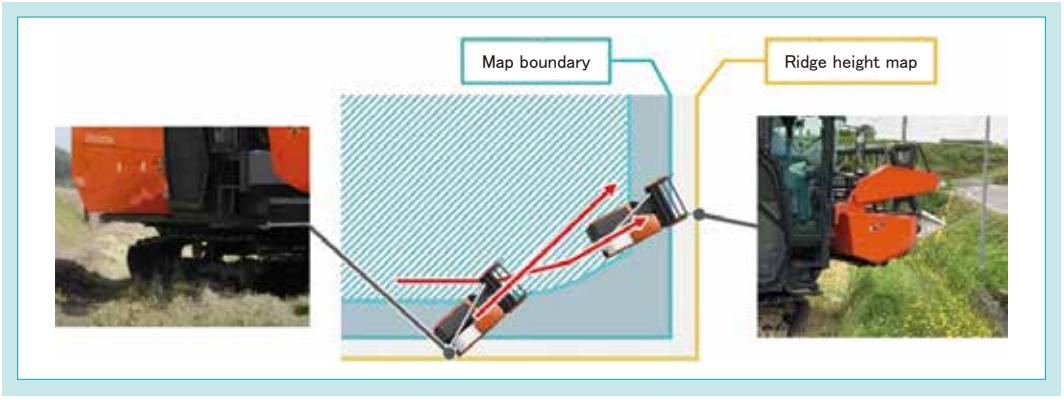

Fig. 16 Turning Using a Ridge Height Map

5. Conclusion

We have developed various new technologies that have enabled the introduction of the industry's first unmanned combine harvester to the market. They include person and obstacle detection sensors suitable for harvesting operations, crop and field ridge height detection technology, and an automated unjamming function in the reaper. We have also made it possible to harvest an unharvested area with a complex shape and improved the percentage of the automatic operation area to 90%. We hope that the product we have developed will help farmers overcome labor shortages and improve work efficiency.

Contribution to SDG targets

2.4 Realization of sustainable and robust agriculture
Unmanned harvesting that contributes to labor-saving and lightening of harvesting work

8.2 Increased productivity through innovation
Contributing to increased efficiency in farm management with the industry's first unmanned automatic combine harvester.

9.2 Strengthening of inclusive and sustainable industrial infrastructure
Helping to solve the agricultural labor shortage through unmanned harvesting

Reference

1) Ministry of Agriculture, Forestry and Fisheries: "Automation Level of Safety Assurance of Agricultural Machinery" https://www.maff.go.jp/j/kanbo/kihyo03/gityo/g_smart_nougyo/pdf/04_jidouka.pdf (referenced on September 30, 2024)

Development of the Riding Type Rice Transplanter KA Series for China

Transplanter Engineering Dept. ／ Analysis Center

In the Chinese market, the main stream is contractors, in which farmers entrust rice transplanting to companies. Larger machines with higher efficiency are needed against the backdrop of an expansion in the scale of wage planting and a shortage of labor due to a declining rural population. To meet these needs, we developed a riding type rice transplanter for China based on the concept of "a rice transplanter that can improve the efficiency of large-scale contract transplanters." In this paper, we introduce the development of a wheel for improved paddy field driving and a new horizontal control mechanism for improved planting accuracy in order to cope with increasing size.

【Key Word】
Riding Type Rice Transplanter, High Efficiency, Planting Part Horizontal Control, Analysis

Related SDGs

1. Introduction

In the Chinese market, rice planting is mostly done by contractors, known as "contract transplanters." They are very business-minded and are looking for machines that are more efficient and can expand contracted acreage and increase profits. In addition, the labor force is decreasing due to the decline in the rural population and rice transplanting machines are shifting from walking types to riding types, so further enlargement of machines is required. The percentage of Kubota's eight-row machine sales relative to the company's total sales of six-row and eight-row machines has been increasing, and this trend is expected to continue.

To meet these needs, we developed the KA series riding type rice transplanters for the Chinese market, which are larger machines with improved basic performance (Fig. 1) .

Fig. 1 Riding Type Rice Transplanter KA Series for China

2. Development concept and target values

2-1 Development concept

Given the Chinese market's need for larger rice transplanters, we set the following development concept: a rice transplanter that improves the work efficiency of large-scale contract transplanters. The following four major efforts were made to improve the efficiency of the developed machine:

(1) Improved wet field driving performance
(2) Improved planting accuracy
(3) A larger vehicle size that allows increased loading of seedlings
(4) Increased speed

Of these four, we focus in this paper on achieving the following two:

(1) Improved wet field driving performance
(2) Improved planting accuracy

2-2 Development goals

(1) Improved wet field driving performance

In uneven and deep fields, the following is required:

(i) It be possible to drive in fields where previous machines sank.

(ii) Achieve work efficiency exceeding that of existing machines by at least 5%.

(2) Improved planting accuracy

(i) Reduce the settling time for the horizontal control of the planting section to at least 50% less than that of existing machines.

(ii) Achieve planting accuracy exceeding that of existing machines.

3. Technical issues to be solved

3-1 Driving performance issues associated with larger rice transplanters

The wheels of a rice transplanter sink into the hardpan when traveling in the field, and as the amount of sinkage increases, the load torque increases, causing a reduction in vehicle speed. Driving force is generated as the wheels sink into the hardpan, but the reaction force causes the front side of the machine to rise (Fig. 2) . As the vehicle's weight increases, the amount of sinkage increases, as does the reaction force, causing the front of the vehicle to rise, and the vehicle eventually sinks into the field, unable to move on its own. If the vehicle sinks, it must be pulled up, which causes time loss and greatly reduces work efficiency. The challenge is to improve the driving performance of the vehicle without sinking, even as the rice transplanter becomes larger and heavier. This development primarily addressed the following:

- Development of wheels with improved wet field driving performance
- Improvement of the vehicle front-rear weight balance
- Be equipped with the largest engine in the same class

In section 4-1, we will mainly describe the development of wheels with improved wet field driving performance.

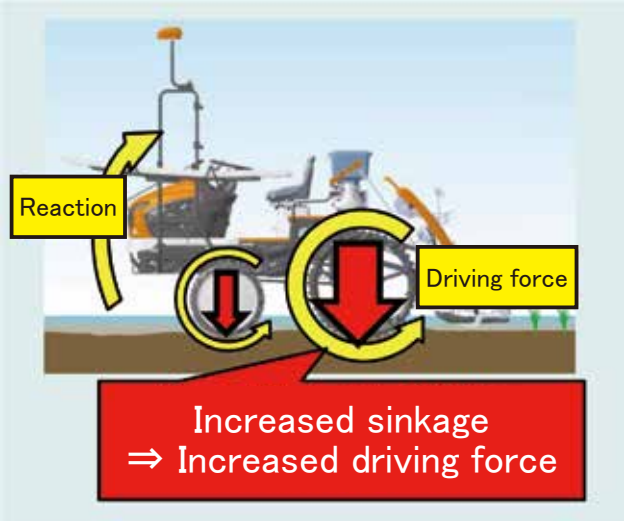

Fig. 2 Mechanism That Lifts Forward When Driving

3-2 Planting accuracy issues associated with larger rice transplanters

Since the planting section of a rice transplanter has a structure that pivots around a central support, when the number of rows is increased from six to eight and the width of the section is increased, the weight imbalance of the section increases during the feeding of seedlings for planting, and the section tends to wobble (Fig. 3) . When the rice transplanter tilts due to unevenness of the hard board, the distance between the mud surface and the planting claw differs greatly between the row at one end and the row at the other end of the planting section, resulting in a greater variation in the planting depth, which is one of the indicators of planting accuracy. In making the machine larger, the challenge was to improve the stability of the planting section (Fig. 4) .

Therefore, in this development, we worked to improve the horizontal control of the planting section.

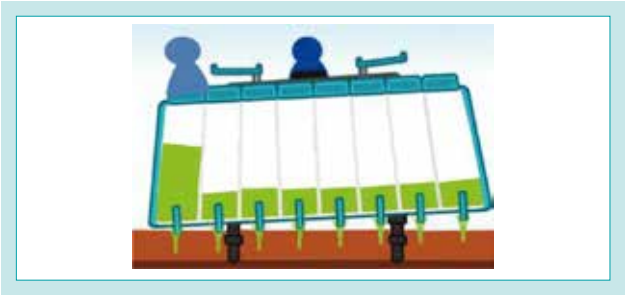

Fig. 3 Weight Imbalance During Seedling Supply

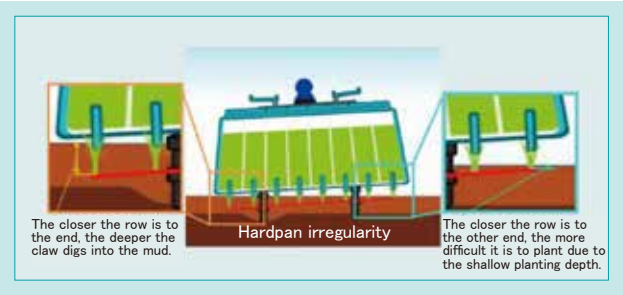

Fig. 4 Effect of an Irregularity of Hardboard on Planting Accuracy

4. Developed technology

4-1 Development of new wheels for improved wet field driving performance

4.1.1 Challenges in the development of new wheels for improved wet field driving performance

Unlike an automobile, the wheels of a rice transplanter get their traction from the reaction force of the wheel lugs, which sink into the soil and compress it (Fig. 5). The shape and angle of the lugs are important for obtaining this traction. In the past, wheel prototypes of different shapes were made to study and confirm their effectiveness and determine an appropriate shape, which took time for prototyping and verification. It was necessary to prototype and verify in a short time to develop a shape suitable for running in wet fields.

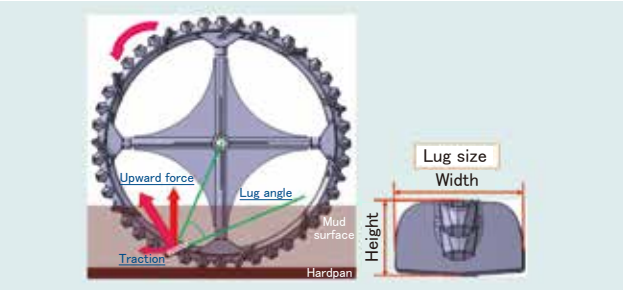

Fig. 5 Running Principle of the Rice Transplanter Wheel

4.1.2 Solutions for developing new wheels for improved wet field driving performance

In this development, we used analytical technology to analyze the running performance of wheels on wet fields and optimize their lug shapes. To study the behavior of a single wheel in the field, we performed a coupled analysis of soils using a wheel behavior mechanism and a Digital Elevation Model (DEM) (Fig. 6). This analysis quantifies three driving performance indicators (traction force, upward force, and drive torque) by applying a rotational force to the wheel to generate a reaction force from DEM particles

that mimic muddy water.

This analysis was used to optimize each driving performance index by varying three parameters: wheel lug angle, width, and height. The characteristics of each parameter are as follows:

Lug angle: The traction force increases as the angle increases, and the upward force increases as the angle decreases. Lug angle has a significant effect on all driving indicators, with the most pronounced effect on traction.

Lug width and height (lug size): Increasing the lug size has a large effect on the upward force, whereas it decreases traction because the increased resistance of the peripheral lugs in muddy water exceeds the increased traction.

In fact, locally made wheels were used in wet field areas where sinking was common because Kubota's existing wheels could not work in such areas. The locally made wheels had extremely large lugs to improve driving performance. On the other hand, they disregarded the planting performance. This caused large wheel tracks due to the lugs, which disturbed the mud surface of the adjacent planting areas and made the planting unstable.

Under these circumstances, the maximum lug width was set so that the wheel tracks would not interfere with planting. Wheels were modeled and a reference upward force was established from the aforementioned analysis. The lug height and angle were then determined to achieve an equivalent upward force (Fig. 7).

As a result of focusing on the upward force with reference to local wheels, the traction of the wheels alone was reduced. However, the overall driving performance of the machine was improved by improving the following items, apart from changing the wheel lugs:

(1) Increasing engine output by 12%

(2) Reducing the load on the rear wheels by improving the balance of the body

To verify their effectiveness, a field driving test was conducted in an actual wet field. A comparison of different wheels showed that the machine with the newly developed wheels could run in a field in which the machine with the existing wheels could not. In another field, the machine's posture was improved from an elevation angle of 2.1° to 1.1°, demonstrating the low sinkage and usefulness of the developed wheels (Table 1).

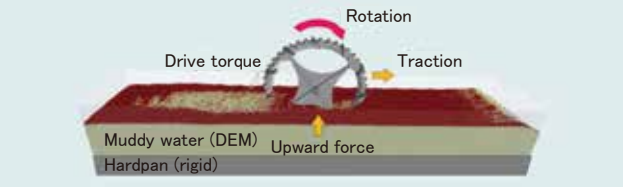

Fig. 6 Analytical Model of the Wheel

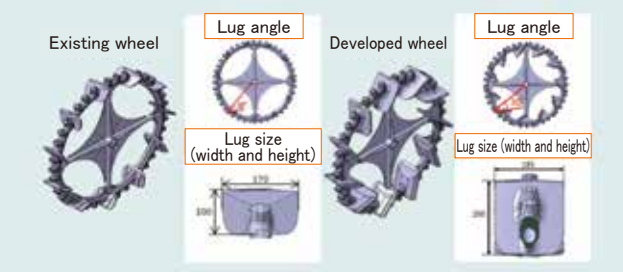

Fig. 7 Current Wheels and Improved Wheels

Tests were conducted to compare the actual work efficiency of the developed machine and the existing machine in a wet field under the same settings. Despite the same speed on the road, the developed machine achieved a 7% increase in work efficiency over the existing machine, demonstrating its superior driving performance (Table 2).

Table 1 Results of a Wet Field Running Comparison Test

Field	Machine posture	
	Existing wheels	Developed wheels
Y	Sunk	1.5°
Z	2.1°	1.1°

Table 2 Results of an Actual Work Efficiency Comparison Test

	Existing machine	Developed machine
Work efficiency [a/hr]	72.3	77.4
Relative to existing machine	–	+7%

4-2 Improved horizontal control of the planting section

4.2.1 Improved horizontal control of the planting section

In the horizontal control of the planting section, it is necessary to control the planting depth at a constant level against the following two main disturbances:

(1) Weight imbalance during seedling replenishment

(2) Field unevenness

The challenge was to achieve two contradictory things: good responsiveness to correct the weight imbalance, and tilting of the planting section to follow the unevenness of the field.

The horizontal control mechanism of Kubota's existing machines was designed to pull up the lowered side of the tilted planting section with a motor via a tension spring and wire cable (Fig. 8).

The spring allows the planting section to tilt and follow the unevenness of the field freely to a certain extent. If the planting section tilts due to a weight imbalance, an angle sensor mounted on the planting section measures the tilt and the motor mounted on the machine pulls the spring to keep the planting section horizontal. For example, if the right side of the planting section tilts down, the motor will pull the spring to lift the left side to keep the planting section horizontal (Fig. 8(a)). However, when the planting section becomes horizontal, the loads of the left and right tension springs balance each other, so that no balancing force is generated when the planting section is near horizontal, making the planting section susceptible to wobbling (Fig. 8(b)).

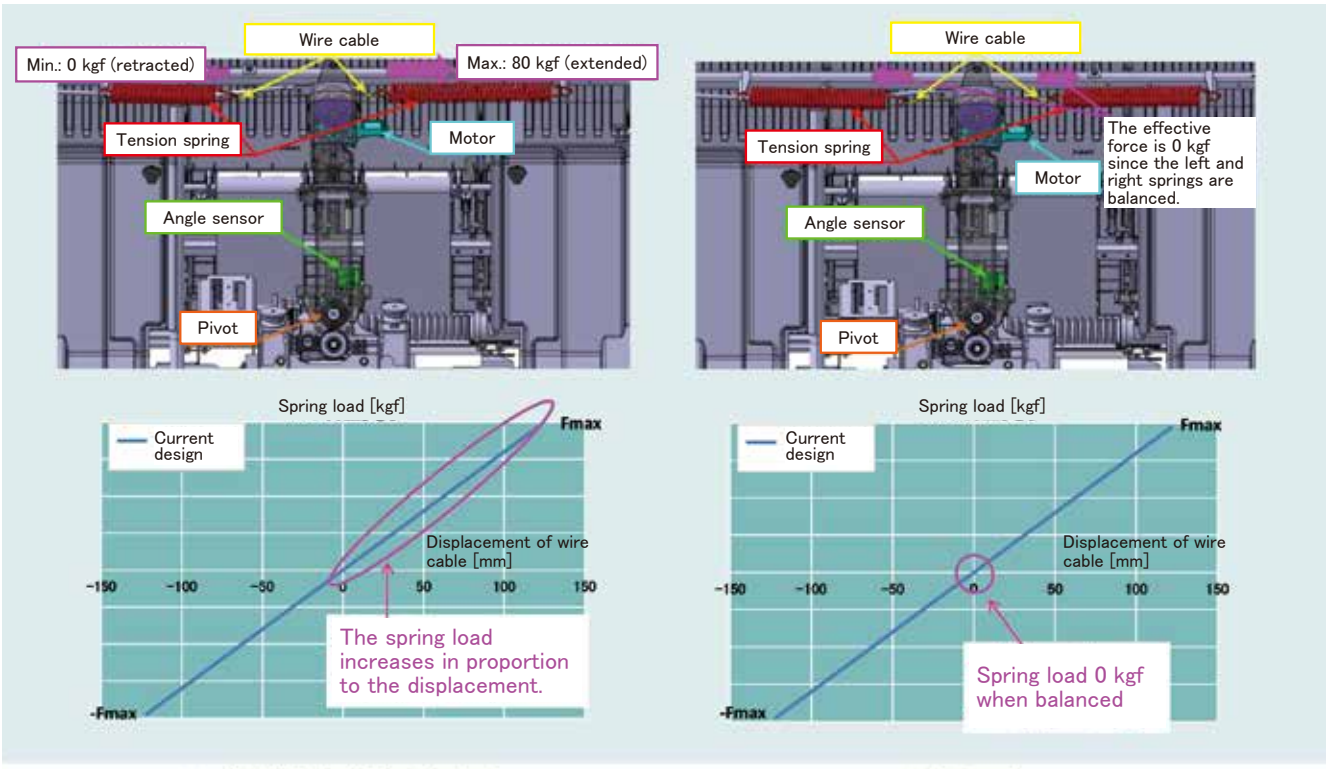

(a) When the right side of the planting section tilts down

(b) When Horizontal

Fig. 8 Horizontal Control Mechanism of a Conventional Structure

4.2.2 Solutions to improve the horizontal control of the planting section

The newly developed mechanism uses compression springs to generate a preset load (Fpre) when horizontal, so that it has a balancing force even when the planting section is near horizontal (Fig. 9). When horizontal, the left and right metal fittings attached to the planting section push the gear pin on the machine side, ensuring that the planting section has a preset load applied to it from both the left and right sides (Fig. 9-(b)). For example, if the left side is tilted down, the motor will move the gear with the pin to the right. The left side metal plate (yellow-painted part in Fig. 9(a)) is designed to go through the long hole so that it does not hit the pin and does not transfer any load to the planting section. The right side metal plate (pink-painted part in Fig. 9(a)) receives the load from the pin and transfers the spring load to the planting section to lower the raised right side of the planting section for balance compensation. The structure is such that the planting section does not move until the preset load is exceeded, and after it is exceeded, the spring load increases according to the amount of displacement to provide balance compensation (Fig. 9(a)). This has the advantage, as in the existing machine, of allowing the spring to follow the unevenness of the field while maintaining the preset load when the planting section is near horizontal, thereby reducing wobble.

To verify the effectiveness, a horizontal settling test was performed with a 10 kgf load applied to one end while the planting section was lifted in the air. The test results are shown in Fig. 10. The tilt angle of the planting section increased significantly 2 seconds after the load was applied, confirming that the planting section followed the loading. In addition, the horizontal settling time was reduced by approximately 80%, from approximately 10 seconds in the existing model to approximately 2 seconds in the new model.

As a result of conducting a test to compare the planting accuracy of the developed machine with that of the existing machine, it was confirmed that the standard deviation of the planting depth in the developed machine was reduced by about 30%, and that the planting was performed accurately according to the unevenness of the field (Table 3).

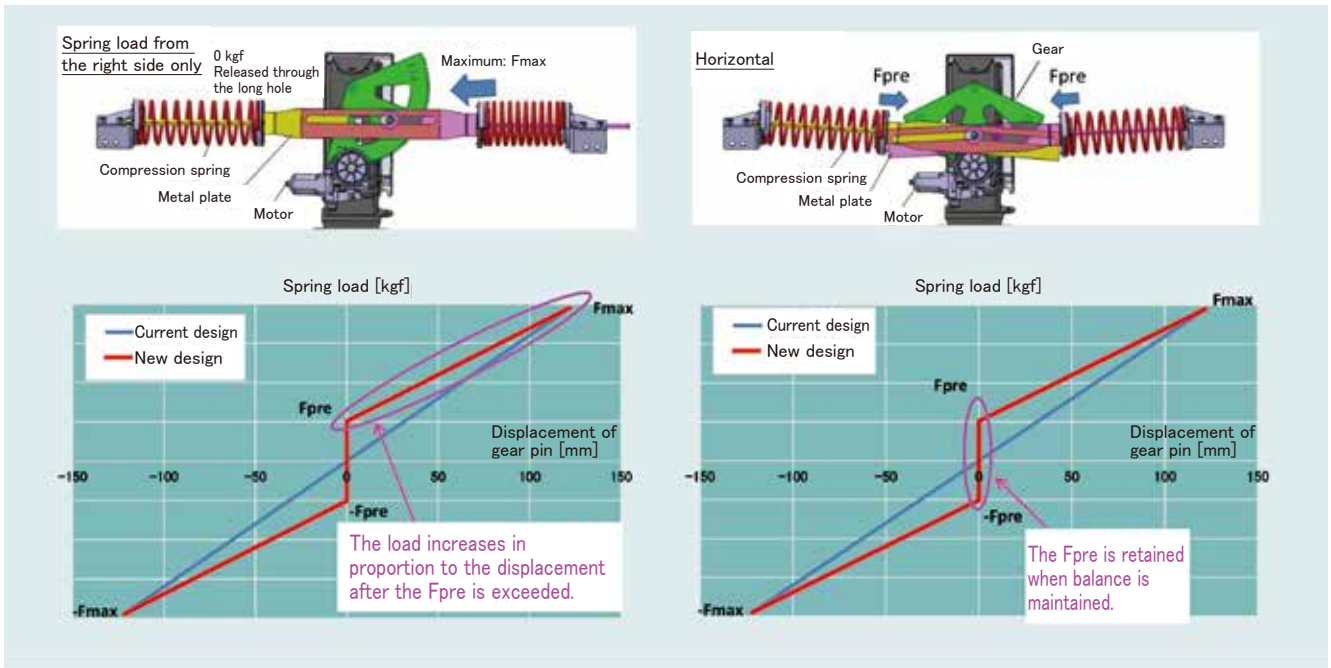

(a) When the left side of the planting section tilts down

(b) When horizontal

Fig. 9 New Horizontal Control Mechanism Developed

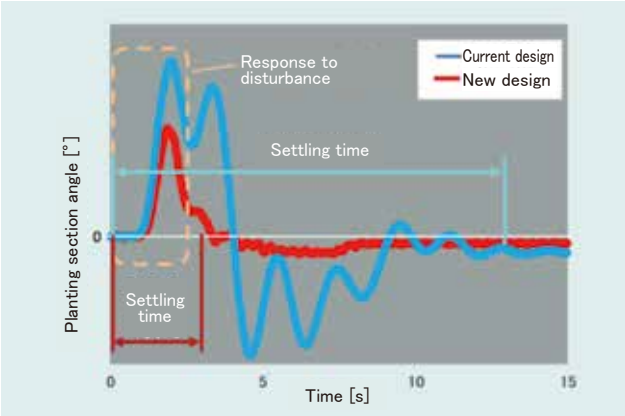

Fig. 10 Horizontal Setting Test Result

Table 3 Results of a Comparative Planting Accuracy Test

	Existing machine	Developed machine
Standard deviation of planting depth [mm]	8.38	5.87
Relative to the existing machine	–	−30%

5. Conclusion

To meet the needs of the Chinese market, the KA series was developed with the following concept: a rice transplanter that can improve the efficiency of large-scale contract transplanters. The KA series was highly praised for its improved driving performance and horizontal control of the planting section, resulting in the desired increase in efficiency.

As there are many wet rice fields in ASEAN and other markets due to insufficient infrastructure development, a rice transplanter equipped with our newly developed technology to improve work efficiency is expected to be widely accepted. In the future, we plan to use the KA series as a base and sequentially develop products with specifications tailored to the needs of the ASEAN and Indian markets.

Contribution to SDG targets

2.3 Increased agricultural productivity and incomes
Contributing to increased productivity through improved planting accuracy

2.4 Realization of sustainable and robust agriculture
Contributing to improved rice planting efficiency through improved driving performance

8.2 Increased productivity through innovation
Contributing to improved work efficiency by increasing the number of rows harvested with the KA series models, which are suitable for an increasing machine size

Development of the Gasoline Engine GZ850H

Engine Engineering Dept. Ⅰ

Development of the gasoline engine GZ850H for use in the Utility Vehicle RTV-XG850 enabled us to expand our business domain. This is Kubota's first development of a high-speed gasoline engine. The air intake system was changed from the conventional model to achieve higher output and lower fuel consumption. Competitiveness was strengthened by improving engine stall resistance. In order to comply with exhaust gas regulations, a new test method using intake pressure control was established, and efforts were made to ensure quality by measuring exhaust gas on a non-consolidated basis at the engine.

【Key Word】
GZ850H, High-speed Gasoline Engine, Increased Output, Improved Fuel Consumption, Emission Regulation

Related SDGs

1. Introduction

The GZ850H is a high-speed, water-cooled, two-cylinder gasoline engine mounted on the RTV-XG850 utility vehicle developed by the Tractor Division. While previous machines were equipped with engines produced by other companies, new machines will have their engines produced by Kubota.

Seizing this opportunity, Kubota will develop its new business field of high-speed engines. To realize the product concept of enhanced workability and recreational performance for hobby farmers and residential customers, we will work to improve the performance of existing machines, thereby securing the utility vehicle (UV) business field and further expanding our engine business.

2.Development concept and target values

2-1 Development concept

The concept is to develop an engine with high power, high performance, and high reliability to achieve stable driving performance and driving comfort even on rough roads and at low temperatures, thereby strengthening product competitiveness and contributing to business expansion.

2-2 Development goals

The specifications of the newly developed engine and its external view are shown in Table 1 and Fig. 1, respectively. The development goal is to improve engine performance and add value according to the above concept. In addition, a system will be developed to control emission quality by establishing a new emission measurement method.

- Increased power output and improved fuel efficiency
- Improved engine stall resistance

The goal is to ensure that the engine does not stall even under the most severe conditions of vehicle driving: hard braking at low temperatures causing the tires to lock.

- Establishment of a method for measuring emissions from stand-alone engines

Table. 1 Engine Specification

Item	Specifications
Valve train	DOHC
Displacement (L)	0.851
Bore diameter / Stroke (mm)	92 / 64
No. of cylinders	2
Output [kW]	40.3

Fig. 1 GZ850H

3. Technical issues to be solved

3-1 Improved power output and fuel economy

Conventional engines had difficulty in distributing the intake airflow evenly to each cylinder due to the continuous intake process characteristic of two-cylinder engines, and their low volumetric efficiency made it difficult to improve the power output and fuel economy.

By optimizing the intake system, the goal is to evenly distribute the intake air between the cylinders and increase power from 36 kW at 5,750 rpm to 40.3 kW at 6,000 rpm. Another goal is to improve the fuel economy by improving the intake efficiency.

3-2 Improved engine stall resistance

Conventional engines are designed with a low moment of inertia for flywheels and other rotating systems to improve acceleration response. In addition, they have no governor mechanism or other speed control device, and the throttle opening during deceleration corresponds one-to-one with the accelerator pedal depression, resulting in low engine stall resistance. This characteristic is especially noticeable at low temperatures. Therefore, in order to achieve smoother acceleration without compromising the operability of conventional engines, we have designed the idle speed control (ISC) valve to be controlled by the electronic control unit (ECU) without adding a moment of inertia or a governor, thereby improving stall resistance.

3-3 Compliance with vehicle emission regulations and measurement of the emission performance of stand-alone engines

This engine application is subject to vehicle-mounted emission regulations, which are different from the emission regulations applied to conventional Kubota engines (stand-alone engine regulation). The emission regulations require that emissions be measured when the vehicle is placed on a chassis dynamometer and driven in acceleration and deceleration modes. As a result, a method for evaluating emissions for stand-alone engines has not been established, and quality control of the emission performance of stand-alone engines has been a challenge.

4. Developed technology

4-1 Technology to improve the intake balance between cylinders by improving the intake system

4.1.1 Intake balance of conventional engines

Conventional engines had the intake flow imbalance characteristic of 180-degree crank two-cylinder engines, with the intake flow of cylinder 2 being extremely low compared to that of cylinder 1. As a result, the workload of cylinder 2 was low and engine performance was not maximized.

Test No ①Idle ②4000rpm 500hPa
③4250rpm 650hPa ④5400rpm WOT

4.1.2 Solutions for intake imbalance

To improve the inter-cylinder balance of the intake flow, we investigated ways to increase the capacity of the intake manifold compared to conventional engines. Figure 2 shows the results of the intake flow ratios (intake flow of cylinder 1 divided by that of cylinder 2) calculated for a conventional engine and the GZ850H using the 1D-CAE approach. The intake flow ratio of the conventional engine is greater than 1 throughout the entire load range and is greater than 1.3 at idle, indicating a relatively low intake flow in cylinder 2. On the other hand, the intake flow ratio of the GZ850H is closer to 1, which represents the optimum value of balance, and below 1.1 throughout the load range, indicating an improvement in the intake flow balance. The results also show an increase in volumetric efficiency (intake flow divided by exhaust flow).

Based on this, a prototype intake manifold with improved specifications was built for verification on actual engines, with the results shown in Fig. 3. The results show the same trend as the 1D-CAE analysis results, achieving improved cylinder balance and increased volumetric efficiency by increasing the intake manifold capacity.

Figure 4 compares the full-throttle performance curves obtained. The absolute amount of intake flow increased due to the improved volumetric efficiency, resulting in a power increase of approximately 11% from 36.0 kW at 5,750 rpm to 40.3 kW at 6,000 rpm.

The improved intake efficiency also resulted in improved fuel economy, achieving a 10% improvement when running in emissions mode.

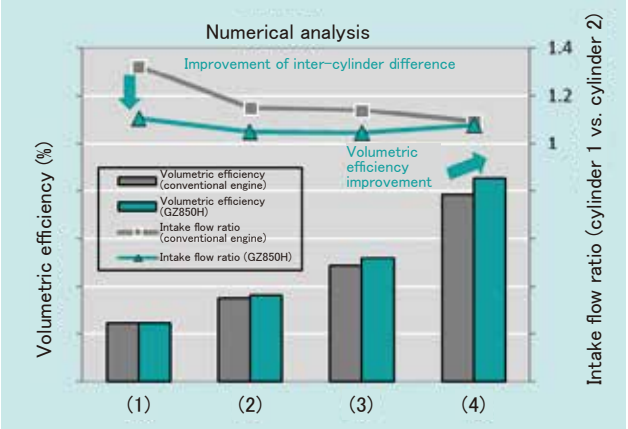

Fig. 2 Intake Flow Comparison (Numerical Analysis)

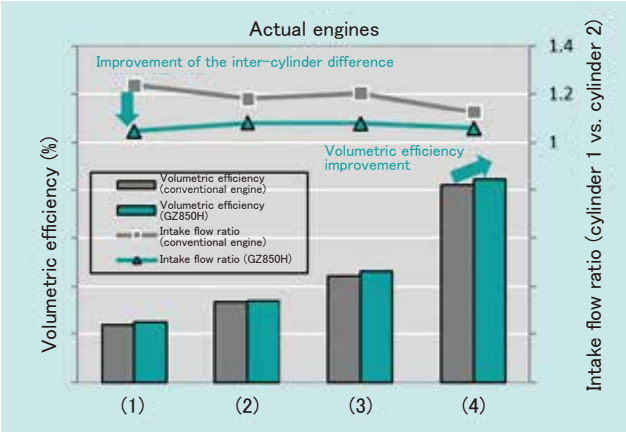

Fig. 3 Intake Flow Comparison (Actual)

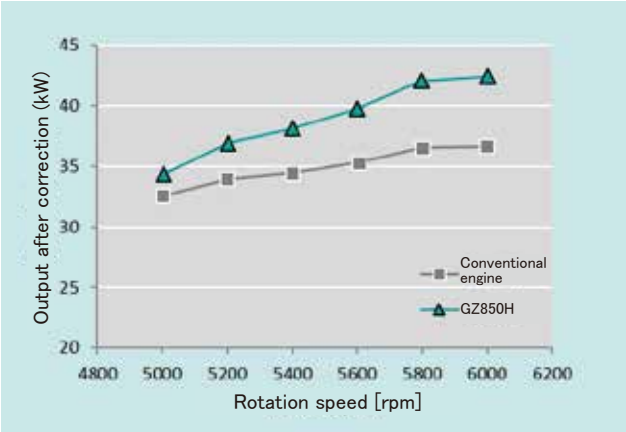

Fig. 4 Output Curve

4-2 Improvement of engine stall resistance

4.2.1 Engine stall resistance

The majority of Kubota's conventional engines have been used in industrial machinery such as agricultural and construction equipment. Engines for industrial machinery are equipped with a flywheel with a large moment of inertia or a governor in the rotating system to reduce speed drops caused by a sudden load or a sudden increase in engine rotation when a load is instantly removed. However, in order to achieve a direct drive that responds immediately to gas pedal operation, the engine under consideration has a small flywheel moment of inertia and is not equipped with a governor. As a result, the rotation fluctuation is large in relation to the load fluctuation, making it difficult to ensure stall resistance. Figure 5 schematically shows the throttle response of a Kubota engine equipped with a typical governor and that of the GZ850H. In the engine with a governor, when the driver releases the accelerator pedal, the throttle reaches the fully closed position once, but as the engine speed drops, the governor is activated and the throttle moves in the open direction, providing a constant intake flow. On the other hand, the GZ850H has low stall resistance because the throttle valve remains fully closed when the accelerator pedal is released, resulting in insufficient intake flow.

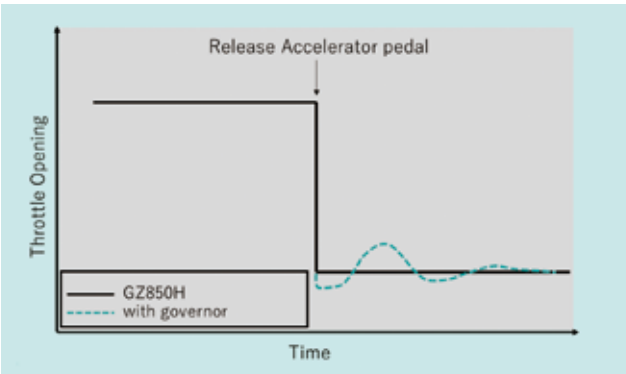

Fig. 5 Throttle Behavior

4.2.2 Improved engine stall resistance

The throttle body of this engine is equipped with a solenoid valve called the ISC valve, which is designed to adjust the airflow at idle. Figure 6 shows the structure of the throttle body. The ISC valve supplements the intake airflow during deceleration to improve stall resistance.

Figure 7 shows the engine speed and ISC valve behavior of the GZ850H during hard braking deceleration, comparing before and after the improvement. Before the improvement, when the engine speed dropped during hard braking, the ISC valve opened slowly, as indicated by the white arrow in the figure, resulting in insufficient intake air (insufficient engine torque) and an engine stall. On the other hand, when a decrease in the engine speed was detected, the ISC valve responded immediately to increase its opening, as shown by the blue arrow in the figure. This allowed the intake air to be secured before the engine speed dropped, resulting in the engine maintaining torque persistently and not stalling even during hard braking.

In addition, in order to avoid an extreme reduction in engine braking performance during deceleration, the timing at which the ISC valve began to open was set below the centrifugal clutch engagement speed of 1,800 rpm, i.e., the speed at which drive torque was transferred to the transmission.

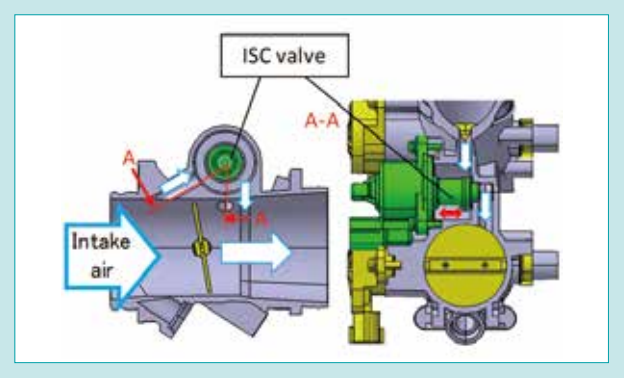

Fig. 6 Throttle Body

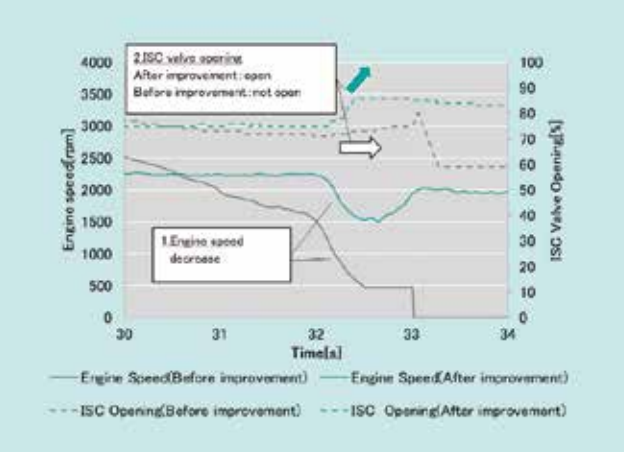

Fig. 7 Behavior of the ISC Valve During Deceleration

4-3 Compliance with vehicle emission regulations

4.3.1 Creation of an emission simulation mode for stand-alone engines

Vehicle emission regulations are based on a defined pattern of driving on a chassis dynamometer and do not specify a measurement pattern for a stand-alone engine. Therefore, engine data (rpm and load data) obtained during vehicle emissions measurement is used to create an emission simulation mode. Figure 8 schematically shows the emission simulation mode. In measuring a stand-alone engine, vehicle speed data is converted to engine speed and intake pressure.

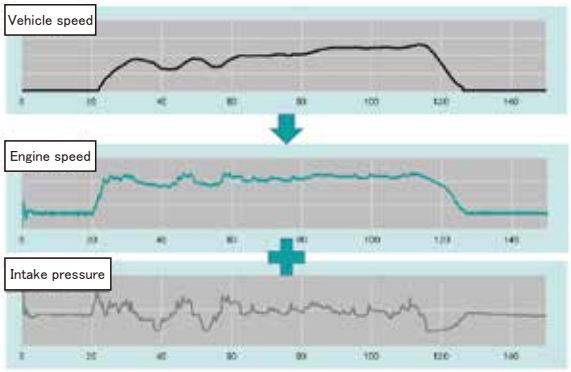

Fig. 8 Exhaust Gas Simulation Mode

4.3.2 Reproduction of the engine load during vehicle testing using the intake pressure control method

In general, torque is the control target when an engine on a bench is loaded from a dynamometer. However, under in-vehicle conditions, it is difficult to install a torque meter and measure the engine torque directly. Therefore, intake pressure was used as a substitute for torque to perform load control (TH-ABR). TH-ABR is a method of approaching the target value of intake pressure by operating the opening of the intake throttle by feedback control. This was combined with control of the dynamometer speed to match the engine speed (DY-ASR), thereby reproducing the engine load during vehicle testing.

4.3.3 Reproduction of negative torque by a newly introduced AC dynamometer

The existing engine bench (eddy current dynamometer) can absorb torque, but cannot drive the engine from the dynamometer to generate negative torque (torque transfer from the vehicle to the engine side, e.g., engine braking). We therefore installed an AC dynamometer capable of driving the engine from the dynamometer. The AC dynamometer is capable of both absorbing and generating torque. We created an automatic engine operation program with coordinated control that combines the distinct use of torque absorption and generation with the aforementioned engine intake pressure control to reproduce negative torque when the vehicle is running.

4.3.4 Determination and verification of the emission simulation mode

Figure 9 compares the emissions of stand-alone engines measured on an engine bench using the emission simulation mode with the emissions of the same engine mounted on a vehicle and run in FTP(b) mode on a chassis dynamometer. With reference to the regulation values, the emissions of the stand-alone engine and the engine mounted on the vehicle were close enough. Figure 10 is a graph comparing a time series of the exhaust gas concentrations and their cumulative values for the stand-alone engine and the engine mounted on the vehicle. The time series data of the stand-alone engine is also generally consistent with that of the engine mounted on the vehicle. The above results indicate that it is possible to control the emission quality of stand-alone engines.

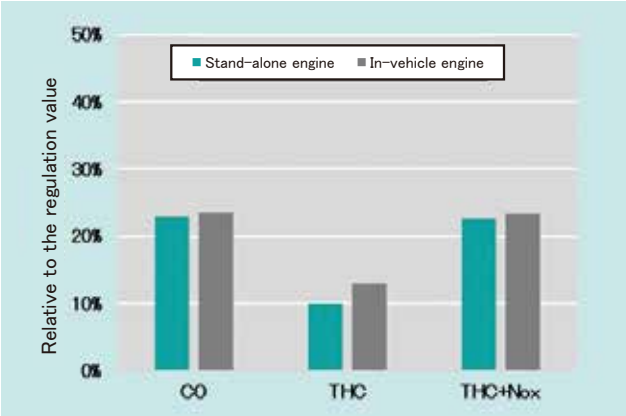

Fig. 9 Exhaust Gas During Mode Operation

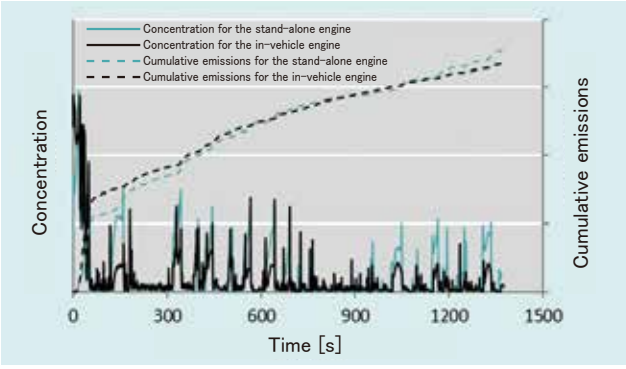

Fig. 10 Time Series Data of Exhaust Gas

Fig. 11 RTV-XG850

5. Conclusion

We have worked to improve a high-speed gasoline engine for utility vehicles (Fig. 11) to achieve both higher output and lower fuel consumption than conventional engines, thereby contributing to the reduction of CO_2 emissions.

In addition, by establishing a method for measuring emissions from stand-alone engines, we have created an environment in which emission quality can be controlled.

While the engine size is the same as conventional engines to ensure installation compatibility, the engine's competitiveness has been enhanced by the aforementioned increased power output and lower fuel consumption, as well as by improved stall resistance.

The development of this engine was a challenge for the Engine Division to enter a new business field. Based on the results of this development, we will contribute to the expansion of the high-speed gasoline engine business and help achieve the SDGs by developing high-performance engines with low fuel consumption.

Contribution to SDG targets

7.3 Improvement of energy efficiency
10% improvement in fuel consumption compared to conventional engines

8.2 Increased productivity through innovation
Helping to manage emission quality based on stand-alone engines

Development of the Diesel Engine for Industrial Use "V5009"

Engine Engineering Dept. Ⅲ

The V5009 engine boasts 200 PS, the largest horsepower in the Kubota series. To achieve the market need for low fuel consumption performance, it incorporates a basic structural design that can withstand high cylinder pressure, and high boost control technology with a VG turbo. In terms of regulatory compliance, the European Stage V Emission regulations have been implemented from 2019, and DOC+DPF/SCR after-treatment technology has successfully reduced NOx/PM. In addition to the fuel consumption and emission reduction requirements, the V5009 has achieved durability in the severe environments specific to large engines, strengthening the product's competitiveness.

【Key Word】
V5009, High Cylinder Pressure Design, High Power Density, VG Turbo Technology

Related SDGs

1. Introduction

Kubota's diesel engines were originally developed for small-farm tractors in Japan. Since then, the company has focused on expanding the installed applications and power range to meet the needs of large agricultural machines and overseas OEM customers. Recently, in 2020, in response to market demand for even higher power and lower fuel consumption, Kubota developed the V5009 engine with a displacement of 5.017 L and a power output of 200 hp, the largest in the company's lineup.

In the future, Kubota will continue to increase the power of its engines in order to capture a larger share of the overseas market for large agricultural machines, thereby contributing to the competitiveness of its products. Another important challenge is to expand business in the large diesel engine market. To achieve this, it is essential to utilize the high power and low fuel consumption technologies that Kubota has cultivated in the development of diesel engines, and to ensure reliability and durability. In addition, emission regulations for nitrogen oxides and soot, which are toxic substances in exhaust gases, are gradually being tightened in response to growing global environmental concerns. To comply with the European Stage V emissions standards that came into effect in 2019, it is essential to develop technology for after-treatment systems to purify emissions.[1)]

This paper presents the technologies cultivated during the development of the V5009 engine.

2. Development concept and engine specifications

2-1 Development concept

Based on the V6108 diesel engine, Kubota is developing an engine that complies with Tier 5 emission standards, achieves a significant increase in power, and can be adapted to large upland farming machinery.

The V5009 is Kubota's largest diesel engine, with a displacement of 5.017 L and four cylinders. The V5009 is a four-cylinder engine with excellent reliability, economy, and maintainability, as well as the compactness and ease of installation that is characteristic of Kubota's diesel engines. Its bed-plate crankcase and cast-iron oil pan provide structural strength sufficient for tractor mounting. This paper presents the development of the new V5009 engine as a high-end model in Kubota's engine lineup, with significantly increased power and the highest power and power density among the company's engines.

Fig. 1 V5009 External View

2-2 Engine specifications

With a target power output of 200 hp (155 kW), the engine will be Kubota's high-end model compliant with European Stage V emission standards. The specifications of the V5009, Kubota's highest power and displacement engine, are shown in Table 1.

As shown in the table, it is a vertical, water-cooled, 4-stroke, 4-cylinder diesel engine with a displacement of 5.017 L and a bore vs. stroke of 110 mm/132 mm. The supercharging system is a turbo inter-cooler system, the exhaust gas after-treatment system is DOC plus DPF/SCR, the combustion system is direct injection, and the fuel supply system is a common rail system. The engine specifications include a rated output of 157.3 kW at 2,200 rpm and a maximum torque of 883.1 Nm at 1,500–1,600 rpm.

Table 1 V5009 Engine Specifications

	Specifications
Name	V5009-TIE5
Conforming to emission regulations	EPA/CARB Tier4 + EU Stage V
Type	Vertical, water-cooled 4-stroke diesel engine
No. of cylinders	4
Bore/Stroke	110.0 mm / 132.0 mm
Displacement	5.017 L
Supercharging method	Turbo inter-cooler
Exhaust gas after-treatment system	DOC + DPF/SCR
Rated output / Speed*1	157.3 kW / 2,200 rpm
Maximum torque / Speed*1	883.1 Nm / 1,500-1,600 rpm
Combustion method / Fuel supply system	Direct injection common rail system
External dimensions	894 mm × 693 mm × 967 mm
Dry weight	632 kg

*1: Gross value based on SAE J1995

3. Technical issues to be solved

As Kubota's high-end model, there are three issues to be resolved.

3.1. Cooling technology for higher power output and increased heat load

Because the combustion heat load and the combustion pressure increase with a large increase in power, it is important to improve the cooling performance and ensure durability and reliability. This calls for the development of an efficient cooling system.

Another challenge is to optimize the flow path design using computational fluid dynamics (CFD) technology.

3.2. Engine and after-treatment system mounting technology

In designing a narrow engine, the conventional method of placing the balancer inside the crankcase increases the width of the crankcase. In addition, an oil cooler is required to handle the increased heat load, and a large exhaust gas recirculation (EGR) cooler is required to secure the EGR volume. Consequently, the conventional balancer arrangement requires further expansion of the engine width.

3.3. Technology with advanced turbocharging to respond to sudden loads

Engine speed drop due to sudden load changes is a problem in the construction equipment market. Sudden load changes cause the engine speed to drop instantly, reducing work efficiency and increasing the risk of equipment damage. The technological challenge is to address this situation by responding quickly to sudden load changes while maintaining engine durability and performance. It is expected that these initiatives will improve the operational efficiency and reliability of construction equipment.

4. Developed technology

4-1 Technology to improve the cooling performance for higher power output and increased heat load

4.1.1 Technology to improve the crankcase water jacket cooling performance

To ensure durability, the cooling performance must be improved to handle the increased heat load created by higher in-cylinder pressures. Coolant discharged from the water pump is distributed evenly to each cylinder in the distribution section in the center of the engine (Fig. 2).

To improve the cooling performance of the liner section, the V5009 separated the liners and head bolt bosses, which were previously joined, to provide a coolant passage around the liners (Fig. 3). This improved the cooling performance of the crankcase against the increased heat load and ensured durability.[2)]

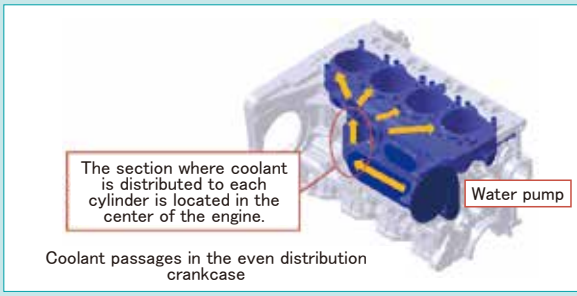

Fig. 2 Crankcase Coolant Passage

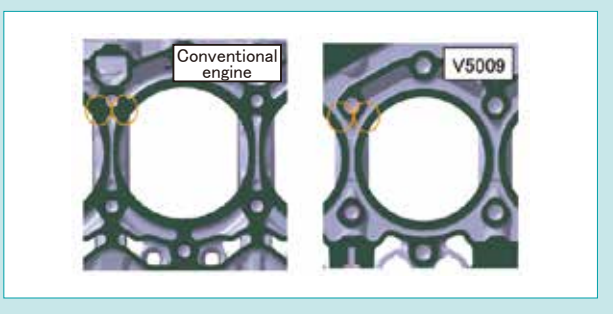

Fig. 3 Cylinder Liner Cooling Water Passage

4.1.2 Crankcase heat transfer analysis technology

Figure 4 is a contour plot of the results of crankcase heat transfer coefficient analysis for the V5009 compared to a conventional engine. The left side of the figure shows the analysis results for the conventional engine's crankcase, and the right side for the V5009's even distribution crankcase. The heat transfer coefficient is low in blue areas and high in red areas. The cooling structure of the conventional engine connects the coolant passage from the water pump with the coolant passage of each cylinder, so that the coolant flows from the front to the rear of the engine while being distributed to each cylinder. In the conventional model, the heat transfer coefficient between cylinders decreases toward the rear of the engine, whereas in the V5009, the heat transfer coefficient between cylinders 3 and 4 is the same as between cylinders 1 and 2.

This shows that by placing the distribution section in the center of the crankcase, the coolant can be evenly distributed to each cylinder. This has reduced variations in cooling performance between cylinders, suppressed liner wear, and improved head gasket durability.

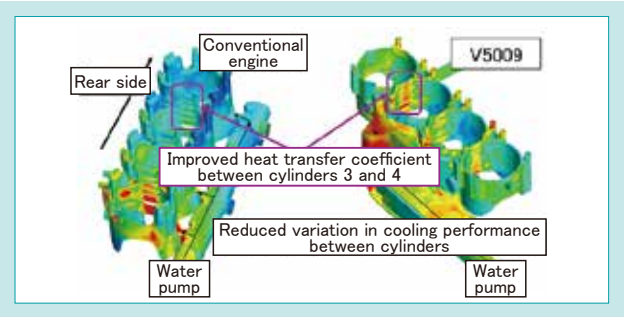

Fig. 4 Crankcase Heat Transfer Coefficient Analysis Results

4.1.3 Technology to improve the cylinder head cooling performance

This section describes the cooling structure of the cylinder head. The coolant passages in the cylinder head include a water jacket, intake and exhaust valves, and an injector sleeve for injector cooling. The injector and valve areas in the cylinder head are intensively cooled to handle the increased heat load.

Specifically, a coolant passage is provided between the intake and exhaust valves to cool the area around these valves, thereby reducing valve seat wear. In the past, an injector hole was machined directly into the cylinder head, but by providing a sleeve for injector cooling, the injector insertion area can be made thinner, improving cooling performance. In addition, a rib is provided on the exhaust side to allow coolant to flow underneath the explosion surface, where temperatures are higher (Fig. 5).

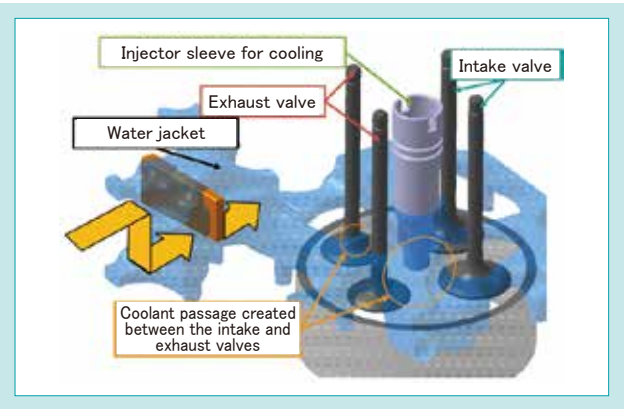

Fig. 5 Cylinder Head Cooling Structure

4-2 Engine and after-treatment system mounting technology

4.2.1 Narrow engine design

Technically, the introduction of the cassette balancer represents a revolutionary change in engine design. By using an externally placed balancer instead of the conventional built-in balancer, engines can be made more compact (Fig. 6). This improves the overall packaging of the engine and increases flexibility in vehicle design. In particular, the space around the engine can be increased, making it easier to place other important components. For example, it allows optimal positioning of the oil cooler and EGR cooler (Fig. 7). This improved the cooling performance and increased the engine durability and performance. The shortened EGR path also increased the EGR efficiency and improved the environmental performance. The introduction of the cassette balancer symbolizes the evolution of engine design and is expected to play an important role in future engine development.

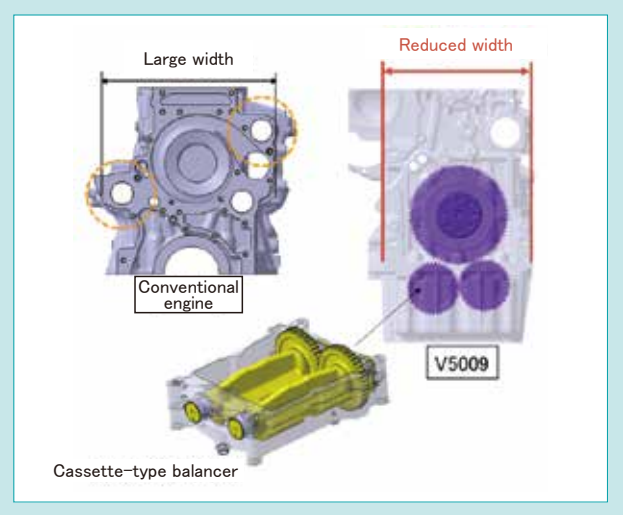

Fig. 6 Cassette Type Balancer

4.2.2 Compact appearance of the exhaust gas after-treatment system

Regarding the compact appearance of the exhaust gas after-treatment system, the width of the system must not exceed the width of the engine in order to fit the after-treatment system under the hood of the agricultural machine. There was concern that the higher power of the V5009 would increase the exhaust flow and make the machine larger. Therefore, the position and angle of the diesel exhaust fluid (DEF) injector were adjusted to create a mixing section to facilitate the mixing of DEF and exhaust gas (Fig. 8). These two measures have improved NOx removal and reduced the size of the selective catalytic reduction (SCR) system. Fluid analysis simulations were used to find the optimal placement and angle of the injector, and the shape and length of the mixing section were also optimized to promote efficient chemical reactions. Accordingly, the after-treatment system was downsized.

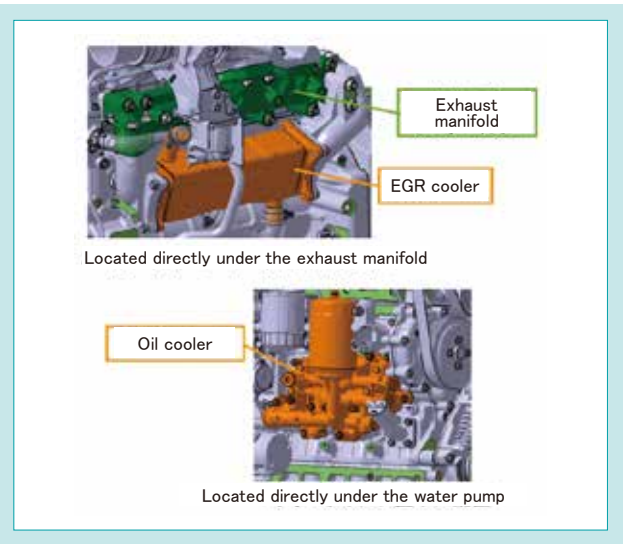

Fig. 7 Layout Adjustment of Engine Components

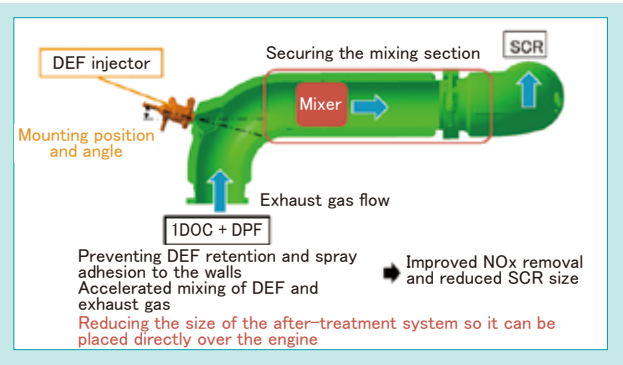

Fig. 8 Compact Post-processing

4.2.3 Maintainability

The V5009 achieves one-side maintenance by placing the maintenance parts shown in Fig. 9 on the intake side. The consolidated placement on the intake side improves work efficiency and helps reduce maintenance costs. While Kubota engines have traditionally required valve clearance adjustment, the use of hydraulic lash adjusters (HLAs), or hydraulic tappets, has eliminated the need for this adjustment and improved maintainability. We were particular about hydraulic tappets that were viable in the overhead valve (OHV) form.

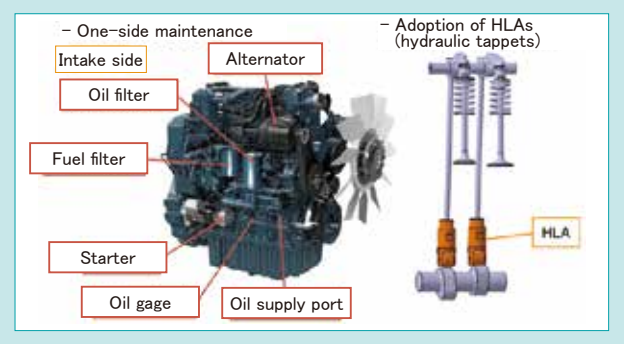

Fig. 9 Engine Maintainability

4-3 Advanced turbocharging technology for sudden load response

4.3.1 Engine speed drop due to load variation

In construction and agricultural machinery, engine performance and durability are extremely important. In particular, construction equipment such as excavators requires high engine responsiveness and operability in high-altitude and high-temperature environments due to the sudden load changes that occur during excavation. Turbocharger adaptation plays an important role in overcoming these challenges. The first problem is that sudden load changes cause a sudden drop in engine speed and an instantaneous lack of power, resulting in engine stalling and other operational degradation. To solve this problem, the speed drop must be reduced (Fig. 10).

Kubota selected turbochargers suitable for construction machinery. A conventionally used wastegate (WG) turbo and a new variable geometry (VG) turbo were compared from four perspectives: control of boost pressure, high output, workability, and emission performance. The results showed that the VG turbo can control boost pressure over the entire range and provide higher power output, achieving both workability and emission performance.

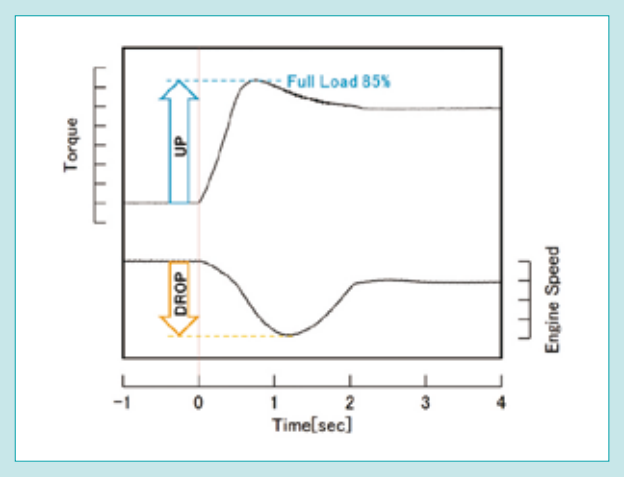

Fig. 10 Behavior of Engine Speed When Load Variation is Applied

4.3.2 Reduced engine speed drop by increasing the fuel injection

The conventional method of improving the speed drop by increasing the amount of fuel injection reduced the drop by 46%, but delayed the start of boost, resulting in insufficient airflow and the generation of a large amount of soot (Fig. 11). The generation of soot shortens the diesel particulate filter (DPF) regeneration interval and causes fuel consumption to deteriorate. The V5009, on the other hand, uses a method to improve the speed drop by controlling the boost pressure with a VG turbo.

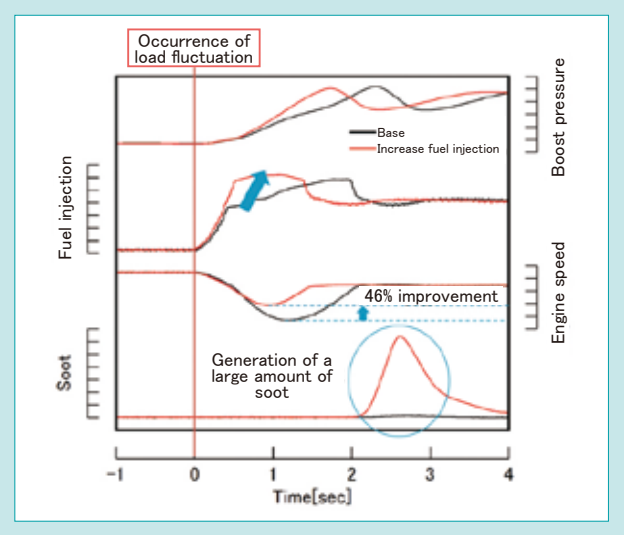

Fig. 11 Rotation Drop Variation with a Fuel Injection Increase

4.3.3 Reduction of engine speed drop by increasing the turbocharger pressure

With the introduction of the VG turbo, boost pressure can be controlled across the entire range, improving the speed drop associated with increased boost pressure. By increasing the boost pressure in advance, the amount of soot generated was significantly reduced while the speed drop was reduced, as was the case with increasing the fuel injection. Specifically, soot generation was reduced by 94%, the DPF regeneration interval was extended, and fuel consumption was improved. Figure 12 compares the amount of soot generated after an increase in the fuel injection with that generated after an increase in the boost pressure, with the green lines representing the case of boost pressure control. The results show that the engine efficiency and environmental performance were improved by the boost pressure control.

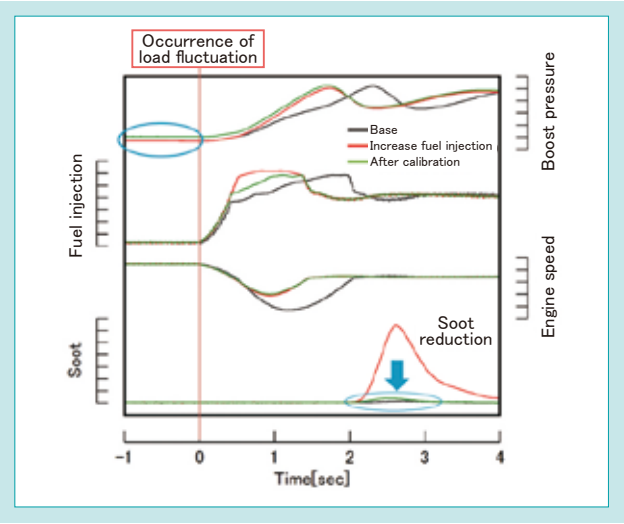

Fig. 12 Rotation Drop Variation with a Turbo Boost Pressure Increase

4.3.4 High-temperature and high-altitude performance

This section describes technology to ensure that construction equipment functions well in harsh conditions such as high temperatures and high altitudes. Construction equipment used in high-temperature environments, such as deserts, and in high-altitude mines is difficult to cool by the wind that the vehicle receives while running and therefore faces unfavorable cooling conditions. In a high-temperature environment, both the intake air temperature and the boost temperature rise. In a high-altitude environment, the boost temperature also increases as the pressure ratio increases due to lower atmospheric pressure. This also increases the exhaust temperature and reduces the power output due to the lower oxygen concentration. High-temperature and high-altitude environments increase boost and exhaust temperatures and reduce power output, limiting the heat resistance temperature of the turbo's compressor housing and turbine. The conventional method was to prevent the temperature rise by limiting the fuel and reducing the boost pressure, but this meant a reduction in power and worsened operability. We therefore used the VG turbo to improve the performance and operability in high-temperature and high-altitude environments. Specifically, Fig. 13 shows the relationship between the engine speed and power output at outdoor air temperatures of 25°C and 60°C. Prior to calibration, the power output at 60°C was as much as 23% lower than that at 25°C, but after calibration, the power output became equivalent to that of 25°C over the entire range. The figure also shows the relationship between the engine speed and power output at low altitude and under decompression corresponding to an altitude of 4,000 m. Here, boost pressure control lowered the boost temperature, improving power by 12% at rated output after calibration.

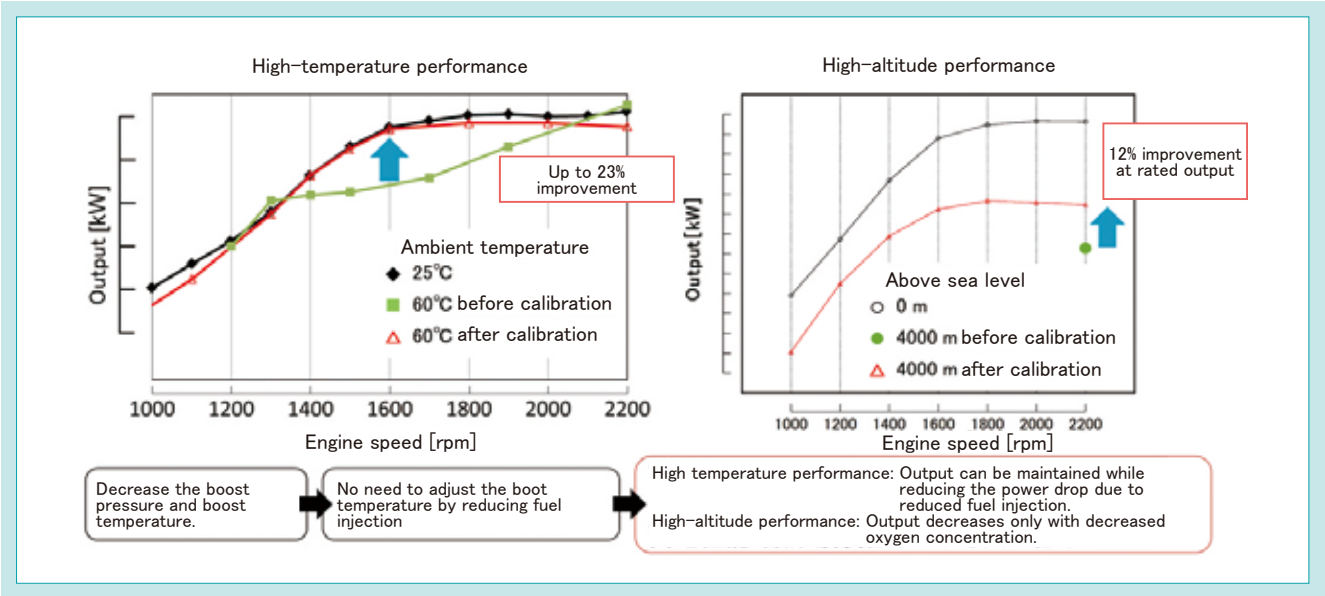

Fig. 13 High Temperature and High-altitude Performance

5. Conclusion

The following conclusions were reached as a result of this study:

- We have developed technologies to improve the cooling performance of the crankcase and cylinder head. In the crankcase, cooling water is evenly distributed to handle an increased heat load, and in the cylinder head, cooling around the intake and exhaust valves is improved by adding an injector sleeve and rib to guide the water flow.
- The introduction of a cassette balancer has resulted in a more compact engine and greater freedom in vehicle design. The exhaust gas after-treatment system has been downsized using fluid analysis simulation. In addition, maintenance parts have been concentrated on the intake side to achieve improved work efficiency.
- A VG turbocharger has been used to achieve high responsiveness to sudden load changes, and boost pressure control has reduced the speed drop while reducing soot generation by 94%. The use of VG turbo technology has improved engine performance and durability, even in high-altitude and high-temperature environments.

Kubota will continue to pursue low emission and low fuel consumption in its engines to strive for global environmental conservation and social needs.

Contribution to SDG targets

7.3 Improvement of energy efficiency
Kubota's first attempt to successfully reduce fuel the consumption rate using VG turbo technology

9.4 Improvement of infrastructure and industries by introducing environmentally friendly technologies and industrial processes
Helping to reduce hazardous substances emitted into the environment

Reference
1) Takayuki Suzuki, ed.: "Thorough Study of Diesel Engines" (2012)
2) Kei Watanabe: "Development of New V5009 Diesel Engine for Agricultural and Construction Machinery" JSAE Symposium on Newly Developed Engines (2021)

Development of SCR Catalyst Performance Degradation Prediction Technology

Engine Engineering Dept. Ⅲ

The after-treatment system of the V3, 08, and 09 series engines, covering an output range of 56-155 kW, has adopted “DOC+DPF/SCR” in compliance with the EPA/CARB Final Tier 4 emission regulations implemented in 2014. The degradation of the SCR catalyst directly affects exhaust gas performance. We conducted research on the optimal SCR catalyst for general-purpose engines and developed a new copper-based catalyst with high robustness against catalyst degradation. The development of the new catalyst required long-duration endurance testing for degradation evaluation, but we utilized a degradation prediction method. This allowed us to shorten the development time.

【Key Word】
SCR, Copper Catalyst, Exhaust Gas, After-treatment, Catalyst Degradation, Degradation Prediction

Related SDGs

1. Introduction

Kubota’s industrial diesel engines have been installed in a wide variety of machinery, such as agricultural and construction machines, with timely compliance with emission regulations enforced in various countries around the world. In particular, emission regulations in Europe, the U.S., and other developed countries are the most stringent, and after-treatment systems to clean engine emissions are mandatory to meet regulations in the 56 kW-plus category. Therefore, the after-treatment system of the V3, 08, and 09 series engines (Fig. 1) , which cover Kubota’s 56–155 kW output range, uses the “diesel oxidation catalyst (DOC) + diesel particulate filter (DPF) / selective catalytic reduction (SCR)” scheme as per the Environmental Protection Agency (EPA) / California Air Resources Board (CARB) Final Tier 4 standards. The new requirement from the CARB in 2020 to verify emission degradation factors has created an urgent need to develop a new after-treatment system with further improved degradation tolerance. The main contributor to emission degradation in engines equipped with SCR mufflers is the degradation of the SCR catalyst. Therefore, our goal is to make it possible to obtain certification in a short time using a new predictive method for after-treatment systems that improve the degradation tolerance of V3, 08, and 09 series engines, which cover the 56–155kW power range, thereby contributing to the creation and maintenance of comfortable living environments.

Fig. 1 V3800-TIE5H

2. Development concept and target values

2-1 Development concept

Catalyst manufacturers have little knowledge of predictive methods that correlate with actual engines. Therefore, in order to reduce development man-hours, Kubota is working to establish its own SCR catalyst degradation prediction technology.

2-2 Development goals

1) Enable rapid understanding of catalytic properties through improvement of chemical reaction analysis.

2) Enable highly accurate prediction of NOx emissions after degradation tolerance testing in SCR systems.

3. Technical issues to be solved

3-1 Establishing conditions for the preparation of catalysts with accelerated degradation

Since the range of ambient conditions that can be studied for the SCR catalyst characteristics depends on the actual engine, some conditions cannot be evaluated as parameters. Therefore, catalysts are selected within limited ambient conditions, and values suitable for control software are determined. In addition, the time to select and prepare a catalyst for an actual engine is long because the method for identifying characteristics other than the final NOx reduction performance and an appropriate evaluation method for the identified characteristics have not been established.

Therefore, in order to understand and select SCR catalyst characteristics, we will evaluate SCR catalysts with chemical reaction analysis from the viewpoint of physical property analysis and will establish conditions for preparing catalysts with accelerated degradation.

3-2 Prediction of the SCR catalyst performance after extended operation

Since there are no known methods correlated with actual engines to predict the SCR catalyst performance after extended operation, it is necessary to subject actual engines to extended operation to confirm SCR catalyst performance degradation.

Confirmation of catalytic performance degradation on actual engines involves repetition of work when the catalytic performance standard is not met in tests that require extended run times, as typified by degradation tolerance tests on actual engines required for certification (e.g., 8,000 hours required by CARB). There is concern that the target development time will be exceeded due to the long time required for the repetition of work.

Therefore, in terms of chemical changes that occur over time, SCR catalyst performance after a long period of operation is predicted based on the results of short-term accelerated tests.

4. Developed technology

4-1 Advanced chemical reaction analysis technology

To understand the characteristics of SCR catalysts for selection, SCR catalysts were evaluated with chemical reaction analysis from the viewpoint of physical property analysis through simulated exhaust gas testing on test pieces. Figure 2 shows a schematic diagram of the simulated exhaust gas test system.

The performance of the SCR catalysts varies depending on the catalyst species, such as copper and iron zeolites. Multiple SCR catalysts were evaluated using a simulated exhaust gas based on NOx reduction and NH_3 adsorption performance to develop SCR catalysts optimal for engine performance. The evaluation method and results (Fig. 3) for each performance item are shown below.[1)]

Evaluation method

(1) NOx reduction performance

- NOx reduction performance was measured as the temperature was gradually reduced from a high level.

(2) NH_3 adsorption performance

- After causing NH_3 to flow through the SCR catalyst at a low temperature, the temperature was gradually increased and the amount of NH_3 desorbed was measured to estimate the amount of NH_3 adsorbed.

The benefits of switching from an iron-based SCR catalyst to a copper-based SCR catalyst, as determined by chemical reaction analysis, are listed below:

(1) A high NOx purification rate in the low-temperature range, and no performance difference in the high-temperature range

(2) A low degradation rate of the SCR catalyst

(3) The NO_2/NOx ratio is less affected by DOC degradation

By understanding the chemical properties before and after SCR catalyst degradation, catalysts can be selected, selection time can be reduced, and values suitable for control software can be more accurately determined.

The simulated exhaust gas testing and NH_3 adsorption performance testing using test pieces in this study were conducted in cooperation with the energy research division of the National Institute of Advanced Industrial Science and Technology (AIST).

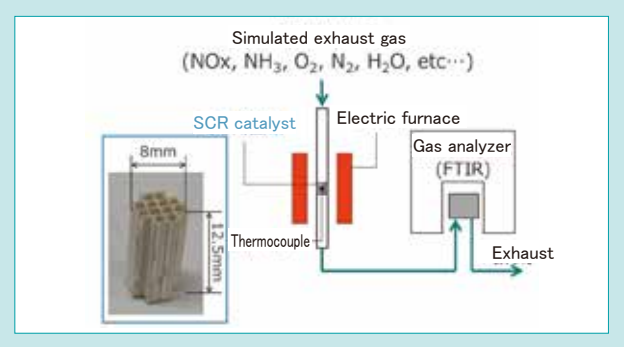

Fig. 2 The Simulated Exhaust Gas Testing Device

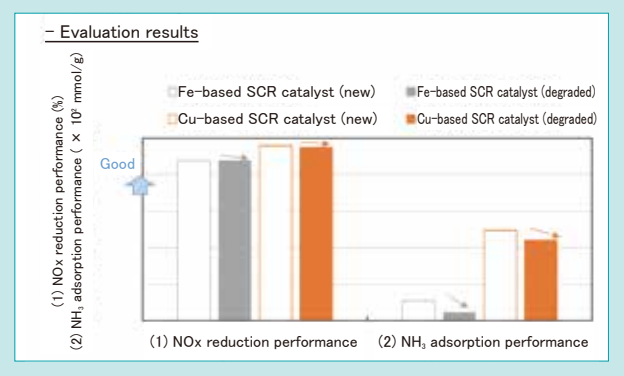

Fig. 3 Result of Mock Exhaust Gas Evaluation

4-2 Technology for predicting SCR catalyst degradation using the Arrhenius equation

As mentioned in section 3-2, to avoid repetition of work after actually operating the engine for many hours, it is necessary to accurately predict the degradation of SCR catalysts through predictive design studies. Therefore, the Arrhenius equation is used to predict long-term chemical changes from the results of short-term accelerated tests. The Arrhenius equation is defined as follows:

$$k = Aexp\left(\frac{-Ea}{RT}\right)$$

- Variables

k: Chemical reaction rate constant

T: Absolute temperature

- Constants

Ea: Activation energy (material specific)

R: Gas constant

A: Constant independent of temperature (frequency factor)

By applying this equation, the accelerated degradation time t_2 corresponding to long-term operation is determined based on the results of simulated exhaust gas tests using the test pieces for chemical reaction analysis in section 4-1 and the environmental conditions of the SCR catalyst during engine operation. Figure 4 shows a schematic of the calculation.

By constructing an SCR muffler using an SCR catalyst that has been degraded by exposure to the accelerated degradation temperature T_2 for the accelerated degradation time t_2 calculated from the above equation, and evaluating the emission tests on an actual engine, it is possible to simulate the performance of the SCR catalyst after long-term operation.

Based on the results calculated above, we compared the results of SCR muffler measurements using iron and copper catalysts when the catalysts were degraded under the following conditions and when they were subjected to actual operation for "A" and "B" hours[2]:

- Deterioration conditions

(1) Accelerated degradation temperature: A°C, accelerated degradation time: T_1 hours
(2) Accelerated degradation temperature: B°C, accelerated degradation time: T_2 hours

The results are shown in Fig. 5.

The results suggest the following:

(1) The NOx emissions obtained from the degradation tolerance test were nearly equal to those obtained from the accelerated degradation test and calculations resulted in an equivalent level of degradation, demonstrating the validity of the present calculation method.
(2) The heat-accelerated copper-based SCR catalyst, which was calculated to be equivalent to "B" hours of degradation tolerance operation, was confirmed to be in compliance with regulations within a sufficient margin.
(3) Compared with the iron-based SCR catalyst, the copper-based SCR catalyst showed a higher NOx purification performance and a lower degradation rate (slope of the first-order approximation for a new product and a product subjected to accelerated degradation) when subjected to both accelerated degradation and degradation tolerance operation. In other words, the copper-based SCR catalyst was found to have higher degradation tolerance.

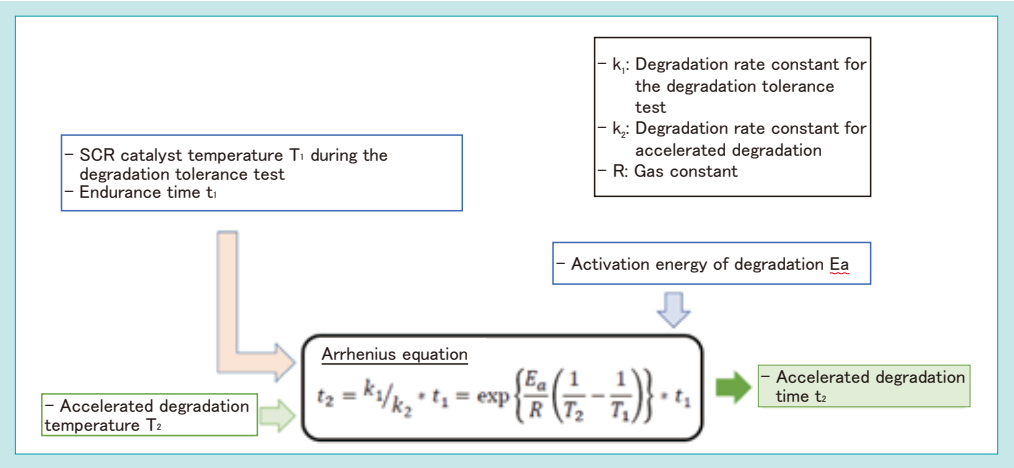

Fig. 4 Determination of Accelerated Degradation Time

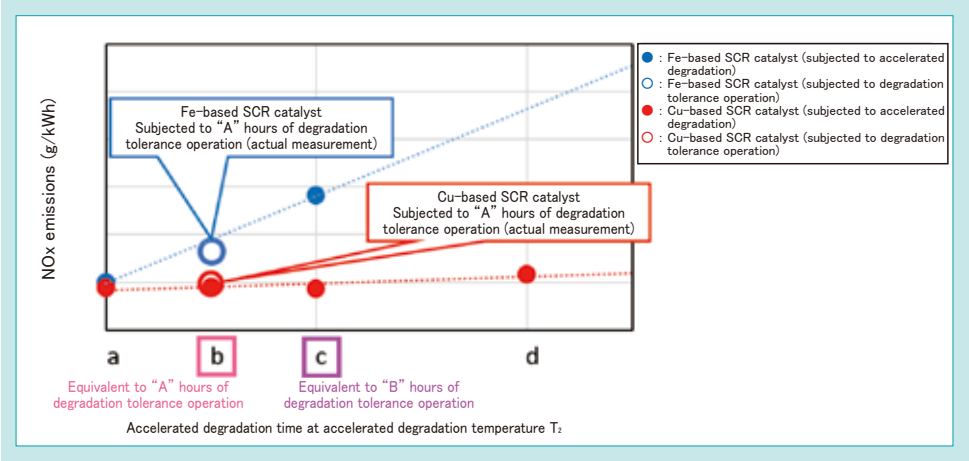

Fig. 5 Accelerated Degradation Time and NOx Emissions

5. Conclusion

We were able to develop a new catalyst for after-treatment systems that meet the European Stage V and Korean Tier 5 emission standards, which came into effect after the EPA/CARB Final Tier 4 emission regulations. By using technology to predict SCR catalyst degradation, we can achieve certification well before the start of emission regulations in each country and reduce development man-hours. This development contributes to strengthening the competitiveness of our engines.

Contribution to SDG targets

7.3 Improvement of energy efficiency
Improved SCR catalyst degradation tolerance compared to existing engines

9.5 Promotion of scientific research and innovation
Degradation prediction technology that reduces development time by more than 2 months

Reference
1) Y. Tsukamoto, et al,; "Reactivity Analysis and Modeling of NH_3-SCR Reaction at High Temperatures Considering Reactions on Cu Active Sites and Brønsted Acid Sites in a Cu-chabazite SCR Catalyst" Transactions of the Society of Automotive Engineers of Japan, Inc., 50, 6 (2019)
2) Takashi Tomiita, et al.: "Deterioration Simulation Based on Advanced Arrhenius' Model Combined with Environmental Degradation Factors" Journal of Materials Life Society, 14, 134–140 (2002)

Establishment of Design Guidelines of Casting Plans for Large Engine Castings

Materials & Castings Center ／ Machinery Castings Manufacturing Dept.

Engine castings are becoming larger, more complex in shape, and thinner-walled in recent years. On the other hand, as the shape factor (volume/minimum wall thickness) of engine castings increases, it becomes more difficult for molten metal to fill the mold quickly, so the gating system plans for castings have changed from the push-up plan to the flag-type plan and step-gate plan. Therefore, in this study, in order to establish design guidelines for the step-gate plan, we first clarified the effects of the sprue ratio and pouring velocity on the molten-metal filling behavior using methods such as flow simulation and water models, and then determined the appropriate sprue ratio range by verifying it through direct observation experiments.

【Key Word】
Engine Castings, Gating System Plan, Step Gate Plan, Flow Simulation, Filling Temperature, Gating Ratio

Related SDGs

1. Introduction

In recent years, engine castings have become larger, more complex in shape, and thinner-walled to accommodate the larger size of agricultural machinery and to achieve lower fuel consumption and a higher power density of engines. As the engine power increases, the shape factor (volume versus minimum wall thickness) of castings tends to increase (Fig. 1). This has led to a higher rate of defects in the casting line; namely, the occurrence of gas entrainment and slag during mold cavity filling, and an increase in the rate of defects caused by temperature drops. In response, the gating system plans for casting have changed from a push-up plan to a flag-type plan or step-gate plan, as shown in Fig. 2. These plan changes are primarily aimed at reducing the filling time and improving filling temperatures.

On the other hand, if the flow velocity is too high when filling the mold cavity, air and gas entrainment and a turbulent flow of molten metal in the cavity tend to occur, causing mold damage. Conversely, if the flow velocity is low, it is difficult to obtain a uniform flow, which leads to slag formation, and the cavity filling time is prolonged, resulting in a lower molten metal temperature.[1)] Therefore, when designing a gating system plan, the shape of the product and the casting conditions must be carefully considered before making a decision.

To establish design guidelines for the step-gate plan, this study first examines the effects of the gating ratio and pouring velocity on the molten-metal filling behavior using methods such as hot-metal flow simulation and water models.

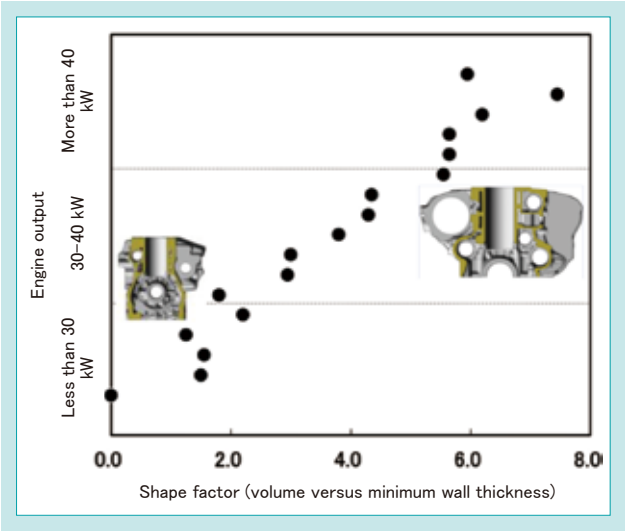

Fig. 1 Relationship Between Engine Power and the Shape Factor

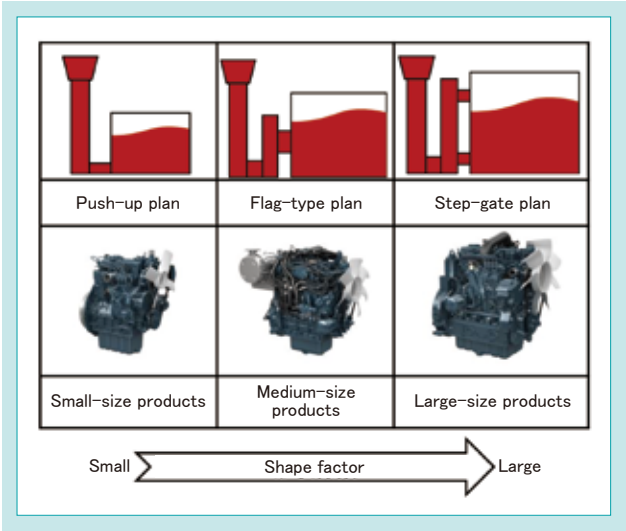

Fig. 2 Changes in the Gating System Plan According to Engine Power

2. Development approach and target values

2-1 Development approach

In order to determine an optimal step-gate plan, this study follows the steps below:

(1) Conduct a flow simulation of mass-produced products using casting CAE to identify problems with the current plan.

(2) Conduct a basic study using the theoretical equation for molten metal distribution, examine the effects of the gating ratio and the upper and lower gate area ratio on the molten metal distribution during molten metal filling, and develop a water model experimental plan.

(3) Change the sprue of the step-gate plan according to the water model, observe the molten metal filling behavior, and determine the optimal gating ratio range.

(4) Perform pouring experiments and verify the water model study results through direct observation experiments.

(5) Establish design guidelines for the plan and apply them to mass production.

2-2 Target values

Ideally, the gating system plan should control the velocity and flow rate of molten metal flowing into the cavity for rapid cavity filling. This study aims to reduce the incidence of dent defects to less than 50% by properly designing a runner plan and achieving the following three points:

(1) No turbulence occurs during molten metal inflow

(2) Up to the upper gate level, the cavity is filled with molten metal primarily from the lower gate

(3) The molten metal temperature does not drop immediately after filling

3. Technical issues to be solved

To identify challenges with the conventional method, the filling behavior of molten metal was observed by flow simulation using casting CAE, and the temperature of the molten metal after filling was measured by a temperature measurement experiment. The results of the flow simulation and the temperature measurement experiment are shown in Figs. 3 and 4. These results revealed the following technical challenges:

(1) Reduce the flow velocity of the molten metal as it enters the lower gate.

According to the flow simulation, the flow velocity at the time of molten metal entry is 1 m/s or more, which is much higher than the conventionally recommended 0.4 m/s or less.

(2) Properly adjust the timing of molten metal entry through the upper gate.

As shown in Fig. 3, the molten metal flows into the cavity through the upper and lower gates almost simultaneously, and the height of the upper gate causes the molten metal to spatter as it falls.

(3) Raise the molten metal temperature at the end of cavity filling.

The results of the temperature measurement in Fig. 4 show that the molten metal temperature on the top surface was approximately 1,243°C immediately after the completion of filling. At this temperature, it can be inferred that many temperature-induced defects, such as cold shuts and dents, will occur.

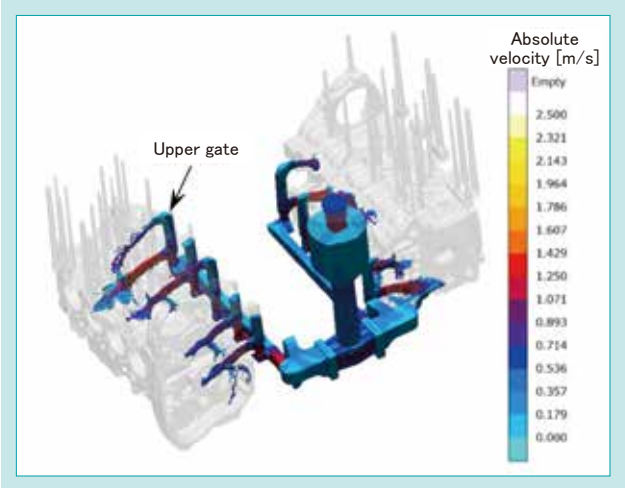

Fig. 3 Results of the Molten Metal Flow Simulation

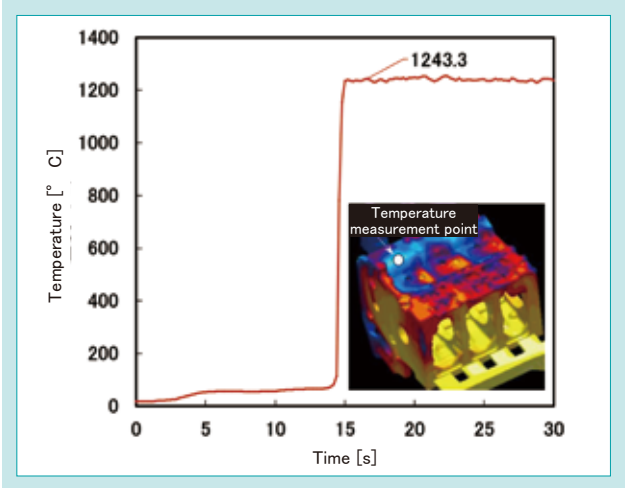

Fig. 4 Filling Temperature Measurement Results

4. Developed technology

4-1 Examination of the sprue ratio and flow velocity using water models

To address the technical challenges above, we evaluated the effect of the sprue ratio on the molten metal filling behavior using water models. Metal was poured using a pouring basin with a stopper. The runner dimensions were kept constant, and the gating ratio was adjusted by changing the diameter of the stopper (pouring flow diameter) and the cross-sectional area of the gate.

Two examples of molten metal filling are shown in Fig. 5, with their relative cross-sectional sizes as follows: an unpressurized plan (sprue cross-section < runner cross-section < gate cross-section) and a pressurized plan (sprue cross-section > runner cross-section > gate cross-section). In the unpressurized plan, the cavity was filled with molten metal flowing from the lower gate up to the upper gate level. In the pressurized plan, molten metal began to flow from the upper gate early, and spattering was observed during filling. Therefore, the unpressurized plan is essential to achieve the targets presented in section 2-2.

The relationship between the pouring flow diameter and the cavity filling time is shown in Fig. 6 for different gate dimensions. For the same pouring flow diameter (pouring velocity), the cavity filling time varied little with changes in the gate dimensions, indicating that the filling time is governed by the pouring velocity.

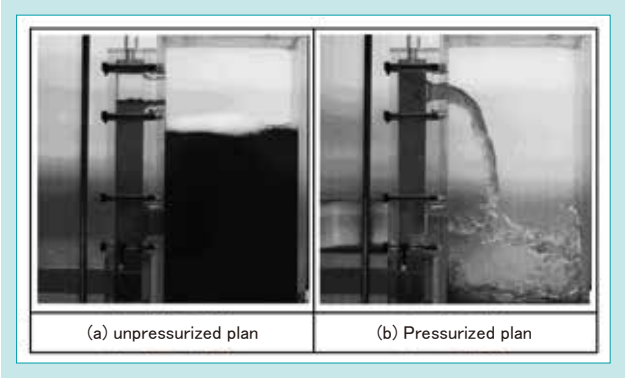

Fig. 5 Examples of Molten Metal Filling Using Pressurized and unpressurized Plans

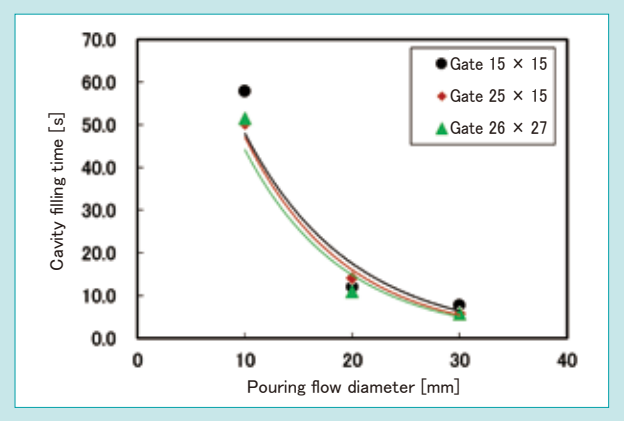

Fig. 6 Relationship Between the Pouring Flow Diameter and the Cavity Filling Time

4-2 Verification of the sprue ratio through pouring

To verify the experimental results of the above water models, casting experiments were conducted under three conditions of gating ratio (sprue cross-sectional area to lower gate cross-sectional area): 1:0.9 (mass production plan), 1:1.6, and 1:2. The upper mold of the casting was opened to directly observe the filling behavior of the molten metal. The results of direct observation of the molten metal filling are shown in Fig. 7. In the mass production plan with gating ratio of 1:0.9, molten metal flowed in vigorously from the lower gate, and shortly thereafter, it flowed in from the upper gate. It was also observed that the molten metal flowing in from the upper gate, located at a high level, hit the molten metal surface in the cavity, causing it to wobble. As the gating ratio increased, the flow velocity of the molten metal entering the upper gate decreased and the drop height decreased. These experimental results are in good agreement with those of the water models described above. The results of observing the molten metal surface at the end of the pouring process showed the presence of slag on the surface for the 1:0.9 and 1:1.6 gating ratios, but not for the 1:2 ratio. It was also found that the molten metal temperature increased in the latter case, achieving the development target (Fig. 8).

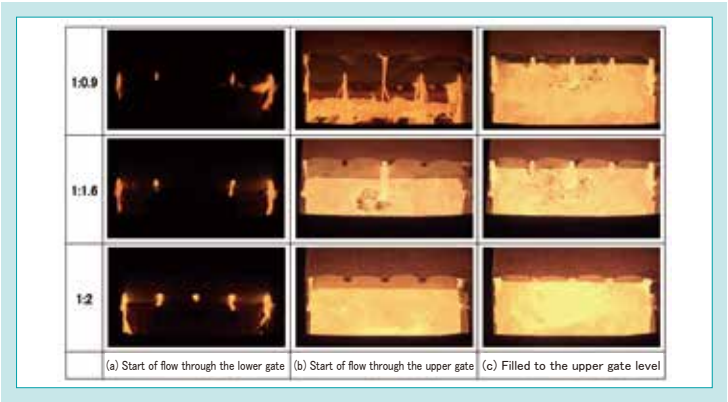

Fig. 7 Observation Results of Molten Metal Filling by Direct Observation

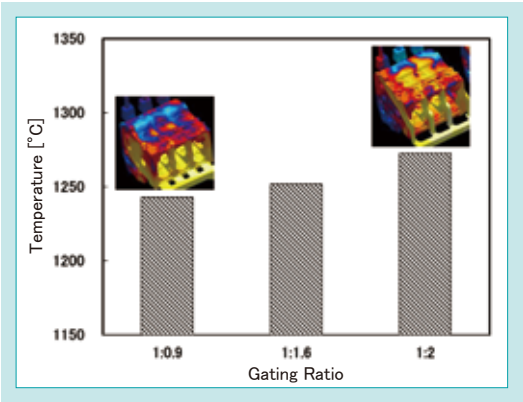

Fig. 8 Temperature Measurement Results After Filling

4-3 Application to mass production plan

Since the above water model and pouring experiments had clarified the effect of the gating ratio, the next step was to conduct evaluation tests for mass production use. The V3307 crankcase, a large mass-produced product, was selected as the evaluation model.

The V3307 crankcase was cast in July 2023 with a change in the gating ratio from the pressurized to unpressurized plan, and a total of 460 units were cast to evaluate the effect of the plan improvements on defect reduction. Evaluation items included slag inclusion and dent defects caused by a melt temperature drop. As shown in Fig. 9, the incidence of dent defects was reduced by 72%. It was confirmed that the incidence of dent defects could be reduced by improving the gating system plan to change the gating ratio.

Based on these results, we are applying the results of the gating ratio study to the design of mass production plans and continuously monitoring the occurrence of defects.

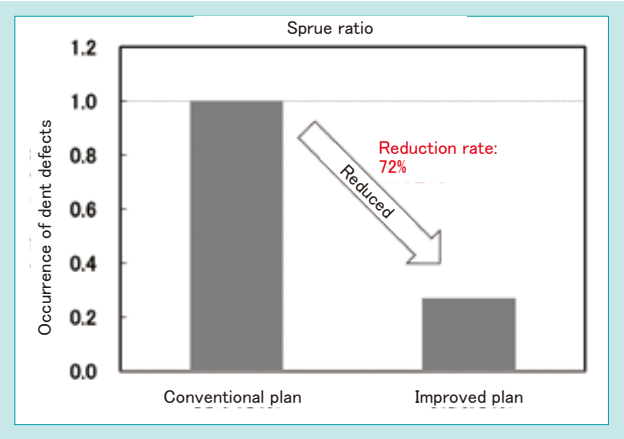

Fig. 9 Effect of Reducing Dent Defects by Improving the Gating System Plan

5. Conclusion

To establish guidelines for designing a step-gate plan for large engine castings, we conducted various experiments and obtained the following results:

(1) In the unpressurized plan, the cavity was filled with molten metal flowing from the lower gate up to the upper gate level.

(2) The gate dimensions had little effect on the cavity filling time, which was governed by the pouring velocity.

(3) The results of a direct observation experiment were in good agreement with the results of a water model experiment.

The study results above will be applied to mass production to help reduce the incidence of dent defects.

Contribution to SDG targets

7.a Promotion of investment in energy-related infrastructure
Reduction of electricity consumption by reducing the rate of defects

9.4 Infrastructure improvement by introducing environmentally friendly technologies
Reduction of the defect rate by introducing optimal gating system plans

12.5 Prevention of waste generation and implementation of reuse
Contributing to waste reduction by reducing the rate of defects

Reference

1) Lin Wang, Toshiki Tamura, and Keiji Matsumoto: 183rd National Conference of the Japan Foundry Engineering Society, No. 58

Development of the Expanding Working Range Technique for Mini Excavators

Construction Machinery Base Technology Engineering Dept.
Construction Machinery Engineering Dept. for Excavator

While the mini excavator is highly evaluated for its wide working range, it is also required to work in a narrow space at the same time. In order to improve the narrow-space workability while maintaining the working range, a new working machine design method utilizing electronic control is necessary. However, regarding the angle detection of the working machine, the conditions near the bucket, such as breakage and submergence, are severe, and installation is difficult. In recent years, expensive detection methods that avoid environmental conditions near buckets have been adopted in ICT construction equipment. However, adoption is difficult for mini-excavators because of the large cost burden. This paper introduces the anti-interference control of the working machine to achieve the required narrow-field workability, and the method to realize bucket angle detection, which is key for control by the potentiometer.

【Key Word】
Mini Excavator, Electric Joystick, Potentiometer, Electronic Control, A333

Related SDGs

1. Introduction

Mini excavators are mainly used for light-duty work, and while they are appreciated for their wide working range, they also need to be able to work in confined spaces in urban areas.

As shown in Fig. 1, there are two indicators of workability in confined spaces: the maximum bucket bottom height and the minimum distance between the bucket teeth and the blade (hereinafter referred to as the “minimum bucket tooth distance”). If the maximum bucket bottom height is low, the arm must be spread to maintain the bucket height when loading earth into a dump truck, resulting in a larger turning radius and reduced stability.

On the other hand, if the minimum bucket tooth distance is too large, asphalt chipping and debris collection operations, where soil and debris are scooped up against the blade, will be underperformed. Since increasing the maximum bucket bottom height also increases the minimum bucket tooth distance, the two are in a contradictory relationship, making it difficult to achieve both. The minimum bucket tooth distance can be easily shortened by extending the back-to-front length of the blade, but this will increase the overall length of the machine and shorten the length of the remaining loading space when the excavator is mounted on a dump truck,

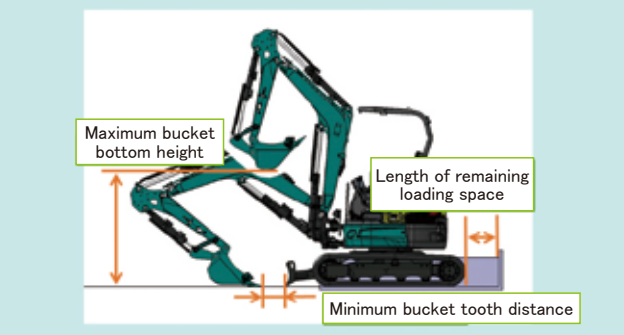

Fig. 1 Index of Mini Excavator Narrow-space Workability

resulting in another problem of reduced usability during transportation.

Existing machines had to balance these three requirements, making it difficult to design a machine that would outperform competitors' machines. Therefore, we have developed a new generation of equipment and attachment design technology that combines new equipment and attachment design and electronic control to significantly improve workability in confined spaces. This paper introduces some new technologies, mainly those related to electronic control.

2. Development concept and target values

2-1 Development concept

The design concept was to meet the three requirements at a high level while maintaining the same length of the remaining loading space and significantly improving the maximum bucket bottom height and the minimum bucket tooth distance.

By targeting the 3-ton mini excavator A333 (a derivative of the existing U-30-6α model), which is equipped with a previously developed electric joystick system, we also aimed to develop a system that takes into account the feasibility of mass production and to increase the market value of machines equipped with electric joysticks.

2-2 Target values

In order to develop a mini excavator in line with this concept, the development goals of the A333 were set as follows:

(1) Maximum bucket bottom height

The target value is 1,550 mm or more from the ground, compared to 1,489 mm for the conventional U-30-6α.

(2) Minimum bucket tooth distance

The target value is 150 mm or less from the ground, compared to 236 mm for the conventional U-30-6α.

(3) Length of the remaining loading space

The target value is 590 mm, the same as the conventional U-30-6α.

Fig. 2 Excess Length of Loading Space

3. Technical issues to be solved

3-1 Expansion of the range of the equipment and attachment's motion

To increase the maximum bucket bottom height, the arm length must be shortened relative to the boom length, but this would increase the bucket tooth distance. To compensate for this, extending the arm's range of motion on the closing side is effective. However, extending the movable range of the arm causes interference between the bucket and the boom cylinder, so technology to prevent this interference has been a challenge.

3-2 Bucket angle detection method

When detecting the position of equipment and attachment, mini excavators with conventional crane specifications and compact zero and tight tail swing excavators use potentiometers to detect the boom and arm angles, but there are no models that detect the bucket angle. Other companies' machines that are larger and more expensive than Kubota's use expensive sensors and devices to detect the bucket angle. To achieve similar performance with Kubota's machines, the bucket angle must be detected using the potentiometers used in conventional mini excavators. However, if a sensor is installed at the bucket pivot, where angle detection is easy, the sensor may be damaged during operation. Therefore, the challenge was to establish a bucket angle detection method where the sensor is installed at some distance from the bucket.

4. Developed technology

4-1 Interference prevention control

With conventional equipment and attachment design methods, there were limitations in avoiding interference between the bucket and boom cylinder caused by extending the arm's movable range on the closing side. Using electronic control, we have developed equipment and attachment control system that detects the bucket and arm angles and limits or allows the bucket and arm to move according to their angles.

Specifically, interference and non-interference areas are set for the movable range of both the bucket and arm, and when either the bucket or arm is in the interference area, the control limits the other's movement to the non-interference area.

The non-interference area of the bucket is defined as the movable range of the bucket where the bucket and the boom cylinder do not interfere with each other when the arm is in the closing end position. The non-interference area of the arm is defined as the movable range of the arm where the bucket and the boom cylinder do not interfere with each other when the bucket is at the angle closest to the boom cylinder. Then, within the movable range of either the arm or the bucket, the area that is not the non-interference area of the arm was defined as the arm's interference area, and the area that is not the non-interference area of the bucket was defined as the bucket's interference area (Fig. 3).

If the bucket angle is in the non-interference area, the arm's motion is not restricted, but if the bucket angle is in the interference area, the arm's closing motion is restricted to keep the arm angle within the non-interference area. Conversely, if the arm angle is in the non-interference area, the bucket's motion is not restricted, but if the arm angle is in the interference area, the bucket's closing motion is restricted to keep the bucket angle within the non-interference area. This prevents interference between the bucket and the boom cylinder while expanding the arm's movable range.

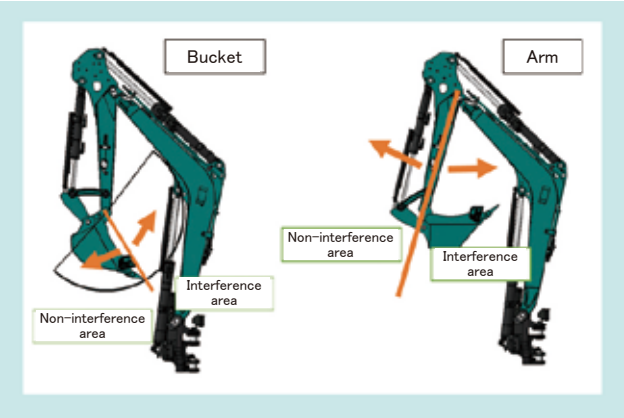

Fig. 3 Interference and Non-interference Areas

4-2 Bucket angle detection technology using a potentiometer

4.2.1 Problems with bucket angle detection technology

By using a potentiometer to detect the pivot angle of the bucket cylinder on the side away from the bucket (Fig. 4), bucket angle detection is achieved within an inexpensive and highly durable configuration. However, only the bucket cylinder swing angle can be obtained from the bucket cylinder pivot angle. Since there are two different bucket angles for the same bucket cylinder pivot angle, one for the closing side of the bucket and the other for the opening side, there is a problem that it is not possible to uniquely convert the angle detected by the potentiometer to the bucket angle.

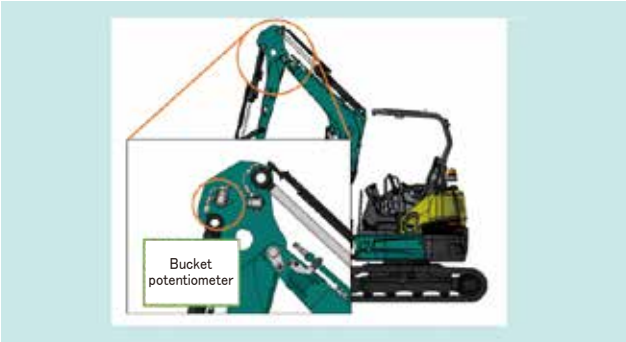

Fig. 4 Bucket Potentiometer Mounting Position

4.2.2 Bucket angle detection solution

There are two bucket angles for the same bucket cylinder pivot angle: the closing side angle (C in Fig. 5) and the opening side angle (A in Fig. 5). To determine the bucket angle, it is necessary to detect whether the bucket is on the closing or opening side in addition to the bucket potentiometer angle. Therefore, we focused on the fact that even with the same potentiometer angle, there is a difference in the direction in which the bucket potentiometer angle changes with respect to the direction of the bucket movement, depending on whether the bucket is on the closing or opening side.

The bucket has a closing and opening direction of movement. The bucket cylinder moves closer to the arm in the closing and opening end positions and away from the arm in the intermediate position (B in Figure 5). Thus, when the bucket is moved from one end position to the other, regardless of whether the bucket is about to close or open, the bucket cylinder starts from a position close to the arm, moves away from the arm until reaching the intermediate position, and then moves close to the arm again. In other words, if the bucket is on the closing side, the bucket cylinder moves closer to the arm when the bucket closes and moves away from the arm when the bucket opens. Conversely, if the bucket is on the opening side, the bucket cylinder moves away from the arm when the bucket closes and moves closer to the arm when the bucket opens.

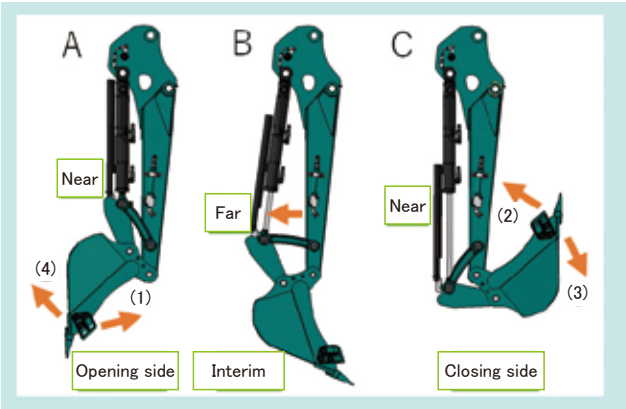

Fig. 5 Bucket Cylinder Position Relative to the Bucket Angle

This difference allows the bucket potentiometer to detect whether the bucket cylinder is moving toward or away from the arm as the bucket closes or opens, thus determining whether the bucket is on the closing or opening side (Table 1). Therefore, the bucket angle can be derived by combining this determination with the potentiometer angle.

The electric joystick system inputs the direction of operation to the control unit, which outputs electric current to the proportional solenoid valve to operate the equipment and attachment. Therefore, the electric joystick system allows the control unit itself to know the bucket's operating direction, making it possible to calculate the bucket angle without installing an additional pressure sensor.

Table. 1 Bucket Position Determination Table

Item	Operating direction	Bucket cylinder	Judgment
(1)	Closing operation	Moving away from the arm	Opening side
(2)	Closing operation	Moving closer to the arm	Closing side
(3)	Opening operation	Moving away from the arm	Closing side
(4)	Opening operation	Moving closer to the arm	Opening side

4-3 Technology to prevent bucket position misjudgment

The establishment of new bucket angle detection technology made it possible to calculate bucket angles with a low-cost, highly durable configuration. However, since there were cases where the bucket position was misjudged depending on the condition of the machine, it was necessary to equipment and attachment controls to prevent misjudgments.

4.3.1 Memorization of the bucket orientation

In the current configuration, since the bucket angle is calculated using the direction of the bucket movement and the direction of the angle change of the potentiometer, the bucket movement allows the bucket angle to be calculated. However, there was a problem that the bucket angle could not be calculated correctly immediately after turning on the key because the bucket was not in operation at startup.

To estimate the state of the bucket immediately after turning on the key, it was decided to store the information about whether the bucket is on the closing or opening side, which is the information previously used to determine the bucket angle. This allows the controller to retain information about whether the bucket is on the closing or opening side even after the controller has stopped operating when the key is turned off, so that the calculation can be performed correctly immediately after the key is turned on.

Initially, information was stored each time the result changed to determine whether the bucket was on the closing or opening side, but this led to exceeding the allowable number of writes, and misjudgments were caused by battery removal.

To solve this problem, it was decided that when the judgment result is written to the storage area, a flag indicating whether the writing was performed or not is also written to the storage area. On turning on the key, if the flag indicates that the writing has been done, the stored value is adopted, and if the writing has not been done, the stored value is not adopted and instead, the closing side, which contains the interference area of the interference prevention control, is always adopted (Fig. 6). This allows for re-determination of the bucket orientation and prevents the bucket from contacting the boom cylinder even when the battery is removed.

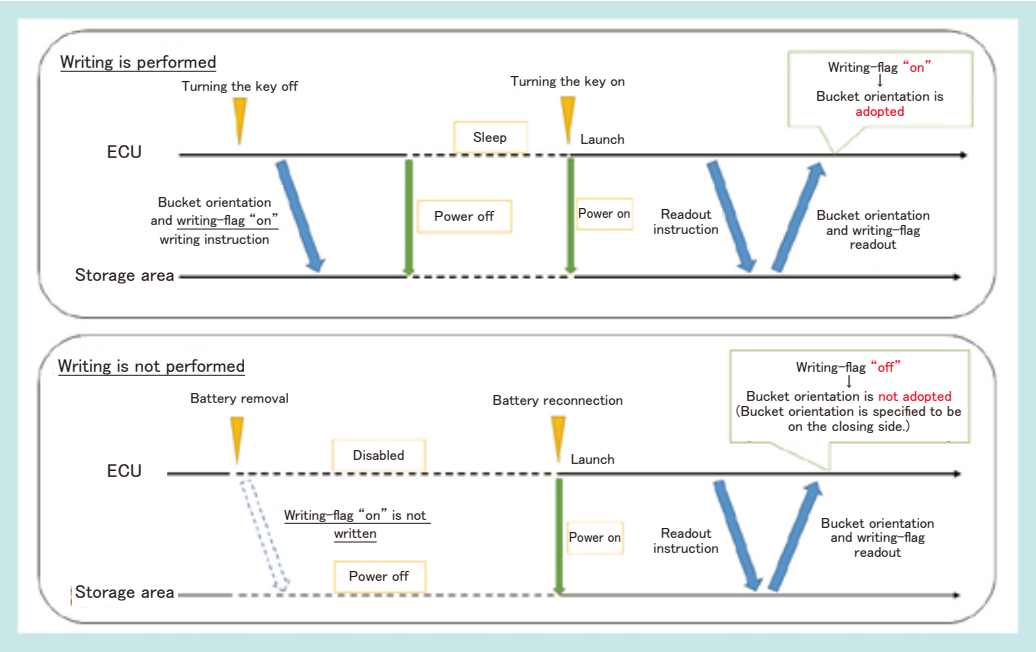

Fig. 6 Bucket Direction Storage Sequence

4.3.2 Judgment at startup

The interference prevention control prevents the arm and bucket from entering the interference area simultaneously during normal operation. However, if the equipment and attachment move due to external factors while the key is turned off, or if the key is turned off after the equipment and attachment are moved with the interference prevention control disabled in "special mode," the arm and bucket may enter the interference area simultaneously. If the arm and the bucket are in the interference area at the same time and both the arm and the bucket are in the closing end position, the bucket will not contact the boom cylinder. However, if the bucket begins to open from this posture, it will contact the boom cylinder (yellow colored area in Fig. 7).

During normal operation, the movement of the arm and the bucket is restricted only for closing. However, if the arm and bucket are in the interference area at the same time immediately after the key is turned on, the opening movement of the bucket is restricted, in addition to the closing movement of the arm and the bucket. This prevents the bucket from contacting the boom cylinder even in an irregular position.

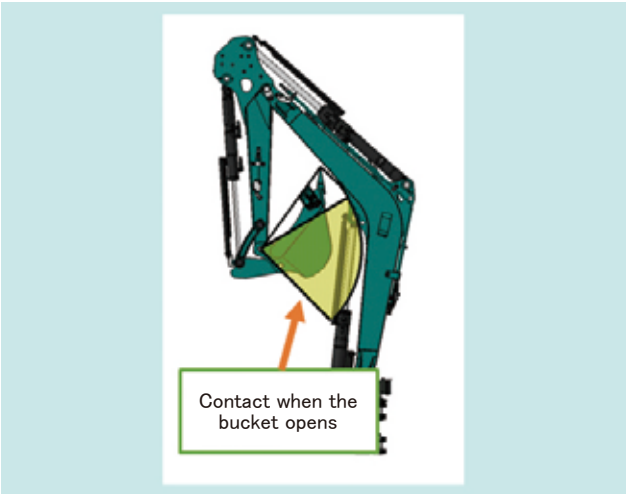

Fig. 7 Interference Posture at Startup

4.3.3 Setting the time for judgment

The potentiometer outputs voltage according to the equipment and attachment's angles, but the voltage fluctuates even when the equipment and attachment are not moving. Therefore, when determining the direction of the potentiometer's angle change, a fixed time (about several tens of milliseconds) is set to determine that the potentiometer change remains in the same direction during this time. Misjudgment can occur if the time for judgment is too short, and if it is too long, the calculated bucket angle will not match the actual bucket angle for a prolonged period. In either case, there is a possibility that the bucket and the boom cylinder will come into contact without the interference prevention control working. Therefore, the judgment time must be set appropriately.

On the other hand, there is backlash in the bucket movement, and the potentiometer may move by the amount of this backlash when other components, such as the boom and arm, are moved. The direction of the bucket movement is determined by whether the proportional solenoid valve in the hydraulic circuit is energized. Because energization starts at a slightly lower current than the current at which the bucket actually begins to move for the sake of a smooth start of movement, there is a condition in which the bucket does not move even though the proportional solenoid valve is energized. As a result, if the arm or boom is operated while the bucket is being operated at a minute level to the extent that the bucket do not actually move, the bucket may move by the amount of backlash opposite to the direction of bucket operation, causing a misjudgment of the direction of the bucket potentiometer angle change.

To solve this problem of misjudging the direction of the potentiometer's angle change, we focused on the fact that the bucket does not move or moves only slowly in response to minute bucket operations that cause misjudgment, and added a control to increase the judgment time longer than usual for such operations. Our view on the negative impact of extending the judgment time on interference prevention control is as follows. If the bucket is moving slowly, even if there is a false judgment, there is no problem with increasing the judgment time more than usual, because it takes time for the bucket to contact the boom cylinder. Accordingly, it is possible to improve the judgment accuracy during minute bucket operations. This approach simultaneously prevents misjudgment due to backlash and avoids contact between the bucket and the boom cylinder during minute bucket operations.

4-4 Development results

We have established a new-generation design method that meets the requirements of maximum bucket bottom height, minimum bucket tooth distance, and length of the remaining loading space at a high level by extending the movement range of the arm, providing interference prevention control, and using new bucket angle detection technology.

Table 2 shows the results of a comparison between the A333 equipped with the developed technology, a conventional model, and competitors' machines. The A333 has achieved goals that would have been unattainable with the conventional front-end design alone through the addition of electronic controls.

Table 2 Comparison of the A333 with the Conventional Model and Machines of Other Companies

Item	A333		Conventional machine U-30-6 α		3-t machine of company A		3-t machine of company B	
Maximum bucket bottom height Target: 1,550 mm or more from the ground	1,596 mm	Good	1,489 mm	Fair	1,440 mm	Poor	1,680 mm	Excellent
Minimum bucket tooth distance Target: 1,550 mm or less	120 mm	Good	236 mm	Fair	235 mm	Fair	130 mm	Good
Length of the remaining loading space Target: 590 mm or more	590 mm	Good	590 mm	Good	500 mm	Fair	400 mm	Poor

5. Conclusion

The technologies for preventing interference and detecting the bucket angle have enabled us to achieve a working range exceeding the target. In addition, the bucket angle detection technology and bucket position misjudgment prevention technology have made it possible to achieve the cost and quality that make mass production possible. The A333, which incorporates these technologies, has been well received by customers since its market launch in 2022.

In the future, we intend to improve our products' competitiveness by extending the electric joystick system, including the interference prevention technology developed here, to other models. We also intend to develop low-cost, high-value-added functions that match the characteristics of mini excavators, thereby improving productivity and helping to solve labor shortages.

Contribution to SDG targets

8.2 Increase of productivity through innovation
Extending the working range with a new electric joystick system

9.2 Strengthening of inclusive and sustainable industrial infrastructure
Improved workability in narrow spaces

Development of the Compact Track Loader SVL75-3 for North America

Construction Machinery Engineering Dept. for Loader

Compact Track Loaders are compact construction machines used in the North American market. They have good running ability on rough terrain, high maneuverability, and versatility. Kubota launched the 75-horsepower base model SVL75 in 2010, but in recent years, there have been no significant improvements. There have been increasing criticisms that it is inferior to competitors, particularly in terms of noise and vibration, maneuverability, and its outdated operating system. Therefore, in the SVL75-3, we implemented an integrated cab and a variable control fan to reduce noise. We also focused on power source security and heat balance, and added Auto-shift control for improved maneuverability. A 7-inch LCD touch panel and a wide-angle rear camera were introduced for the operating system. This article introduces these technological developments.

【Key Word】
Compact Track Loader, Integrated Cab, Auto-shift, LCD Touch Panel

Related SDGs

1. Introduction

Compact track loaders (CTLs) are compact construction machines used primarily in the North American market (Fig. 1) . Featuring spin turn, the ability to use a wide range of attachments, and the ability to run on rough terrain with crawler tracks, CTLs are used for various applications such as earthmoving, excavating, and grading in a variety of fields including construction, infrastructure development, and agriculture. The construction equipment market is growing steadily on the back of a strong economy and robust housing demand, with the CTL market being the largest at 89,000 units in 2022, accounting for 46% of the small construction equipment market. In addition, CTLs are highly regarded for their all-weather performance and rough terrain drivability and stability, and are expected to grow as replacements for skid steer loaders (SSLs) and small bulldozers[1] (Fig. 2) . In terms of the composition of demand by CTL class, the 2,300–2,600 pound rated operating capacity (ROC) class, which includes the SVL75-3, accounted for only 13% of the total CTL market in 2011. However, this class is now one of the most important markets, with competitors entering the market one after another and the class's share of the CTL market increasing every year. In 2022, this class surpassed the 2,000–2,300 pound class to become the second largest class[1] (Fig. 3) .

Fig. 1 SVL75-3

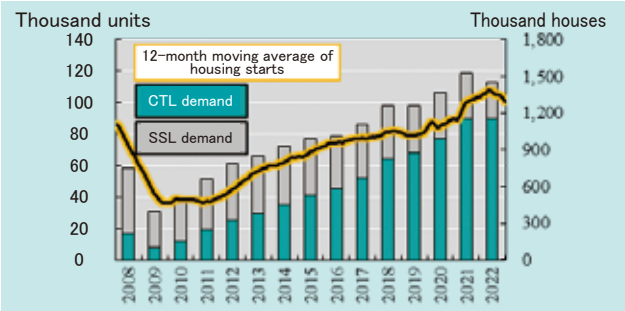

Fig. 2 Transition of the North American CTL Market

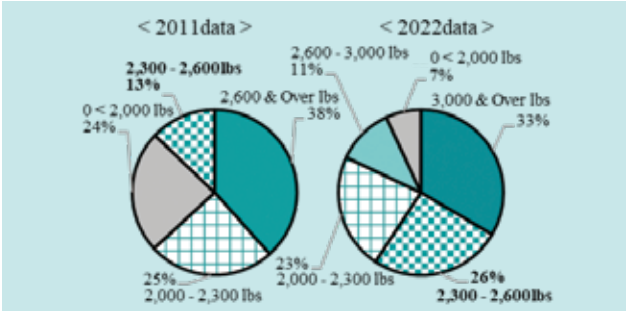

Fig. 3 Market Composition Segmented by CTL Class[1)]

2. Development concepts and target values

2-1 Development concepts

CTL operators spend most of their day in the cab, as CTLs are most often used for construction-related work. Therefore, CTL operators need a comfortable environment that helps reduce fatigue and improves their concentration during work. Therefore, high basic performance and technology that provides comfortable, stress-free operation are important to differentiate our machines from the competition. Accordingly, with the following three concepts, the SVL75-3 has been developed as a basic model for a next generation SVL series that strives for comfort and basic performance:

(1) Products with industry-leading operator comfort

(2) High-performance products that inherit the idea of prioritizing basic performance

(3) Products that strive for simplicity, with strength in easy operation, easy maintenance, and easy cleaning

In this report, the above concepts (1) through (3) are referenced throughout the following sections.

2-2 Target values

In order to realize the development concepts and create a product that outperforms the competition, the following targets were set for each concept:

For concept (1), the target was to reduce the noise level at the ear to industry-leading levels, with 5 dBA reduction from the noise of a conventional model.

For concept (2), the target was to improve work efficiency by 15% compared to an existing model.

For concept (3) (focusing on easy operation in this report), a 7-inch LCD color touch panel, the largest in the industry, was installed as standard, with the goal of creating a layout that would allow the operator to perform touch operations closely at hand without looking away from the work being done. A rearview camera was also installed as standard, with the goal of providing a layout that displays various meters and rearview camera images on a single monitor.

3. Technical issues to be solved

3-1 Technical challenges for noise reduction

For concept (1), we considered it necessary to add a stopper to regulate the lateral movement of the front window, change the material of the sliding roller, and convert the conventional cab to an integrated cab. However, since the ability to tilt the cab up for maintenance is an essential feature of the CTL, the challenge was to avoid interference between the tilt trajectory and surrounding parts, while designing the cab to be one piece extending to the floor. Another issue with the one-piece cab was to ensure the quality of the painting inside the cab and the ease of assembly. In addition, to reduce noise, it was necessary to switch to a variable fan system using a hydraulic motor, but this impairs direct rearward visibility due to the large space required for mounting the system, and it is also a challenge to solve the power transmission loss due to pressure loss.

3-2 Technical challenges to improve workability

For concept (2), it was essential to increase the vehicle speed, but there was concern that this would increase the engine load and generate more heat. Therefore, the challenge was to secure a stronger power source in line with the increased vehicle speed and to improve thermal performance. In addition, there was concern that increasing the speed of CTLs equipped with an auxiliary transmission (low speed mode and high speed mode) would compromise comfort. In particular, there was a need to suppress the shift shock and the vibration of the machine body caused by turning at high speed with the implement raised.

3-3 Technological challenges for easy operation

For concept (3), we aimed to differentiate the new machine from competitors' machines by placing the monitor around the control lever at the lower right in front of the operator, the same location as on existing machines with established reputations in the market, so that the operator can see the monitor without looking away from the work being done and perform touch operations closely at hand. The challenge, however, was to ensure that the enlarged monitor and operator would not interfere with the enlarged front window, and that the view of the monitor would not be obstructed by the control lever.

4. Developed technology

4-1 Technology development for enhanced comfort

4.1.1 Development to achieve an integrated cab

When the integrated cab was introduced, a large cutout was made in the front of the main frame to avoid interfering with the surrounding parts, since the trajectory of the cover near the operator's feet protrudes forward from the machine body when the cab is tilted (Fig. 4). Since stresses generated in this area when driving over bumps, making a pivot turn, and operating the bucket need to be maintained at the same level as the existing model, reinforcing ribs have been added to ensure strength.

The front of the cab has an apron-like structure that seals the gap with the frame, while the rear

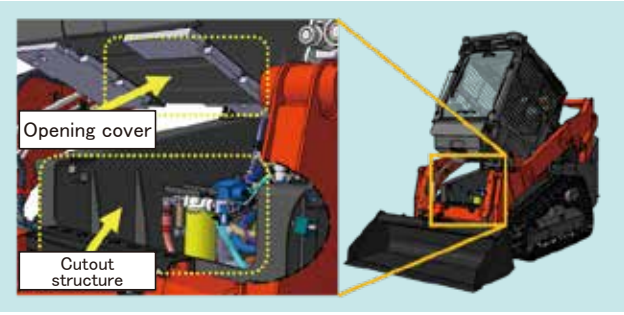

Fig. 4 Frame Structure of the SVL75-3

has a labyrinth structure that prevents debris from entering the hot section of the engine. In addition, to ensure the quality of the painting in areas overshadowed by the introduction of the one-piece cab and to facilitate the assembly of in-cab parts on the production line, the minimum necessary work openings were provided in the cab floor and were covered after painting and assembly.

4.1.2 Adoption of a variable hydraulic fan and fan power control technology

A cooling fan system that controls the fan speed to the minimum necessary according to the temperature of oil and grease was adopted, similar to the variable hydraulic fan used in the Kubota SSL series. This reduced ambient noise by nearly 10 dBA (Table 1).

As mentioned earlier, challenges included ensuring rearward visibility and reducing power transmission loss. The issue of rearward visibility was addressed by installing a rearview monitor as standard equipment (see Chapter 5 for details). The issue of power transmission loss was addressed by the introduction of fan power control, which senses the engine speed and temporarily reduces the fan speed to suppress power consumption when the engine speed drops due to load (Fig. 5). This allows the operator to work without compromising performance by securing horsepower for travel and implement operation even when the engine is heavily loaded, such as when digging, climbing hills, and repositioning the implement after soil removal. Specifically, the uphill speed during high-load work has been increased by approximately 20 %.

Table 1 Comparison of Effects with the Old Model

Model name	Conventional model SVL75-2	Developed model SVL75-3
Ambient noise	110 dBA	100 dBA
Hill climbing speed under heavy load	2.1 km/h	2.5 km/h (horsepower controlled)

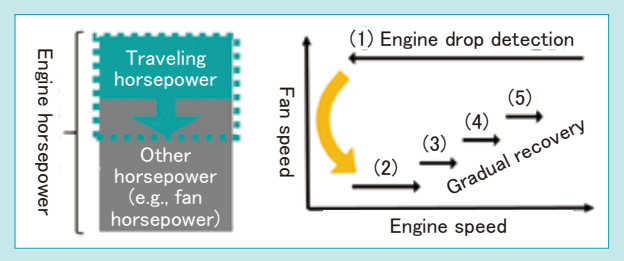

Fig. 5 Horsepower Control

4.1.3 Final improvement effect

With the above measures, we were able to reduce the noise level at the ear from 80 dBA in the conventional SVL75-2 to 74 dBA without sacrificing basic performance, achieving the target reduction of 5 dBA. This noise level is also superior to that of the competitors' machines (Table 2).

Table 2 Comparison of Noise Levels Near the Ear

Company	Kubota		Company A		Company B
Model name	SVL75-3	SVL75-2	A1	A2	B1
Noise level at the ear	74 dBA	80 dBA	84 dBA	80 dBA	78 dBA

4-2 Technology to improve basic performance

4.2.1 Auto-shift during turning

Auto-shift during turning is a function that automatically downshifts from high-speed mode to low-speed mode and restores the speed by sensing the operator's operating pattern with pilot pressure sensors and sensing the traveling load with traveling pressure sensors (Fig. 6). Pressure is constantly monitored by the traveling pilot pressure sensors and traveling pressure sensors to detect load increases during turning and automatically downshifts for increased turning torque. When the load decreases, the system automatically upshifts and smoothly returns to high-speed driving. A shift-shock reduction function has also been incorporated to temporarily reduce the traveling pilot pressure during shift changes, in order to reduce shocks caused by volume changes. The system also detects changes in the traveling pressure in response to changes in the vehicle's turning speed and changes the threshold for auto-shift according to the load. In addition, a control system has been developed to prevent the machine from wobbling back and forth when turning at high speed with the implement raised and unstable. This system fully tilts and rotates the HST pump's swash plate so it does not wobble during turning, optimizes the swash plate characteristics with respect to the pilot pressure variation range (Fig. 7), and temporarily reduces the engine speed during spin operations.

These measures have made it possible to perform stable turning operations and achieve stress-free, seamless operation without reducing the working speed due to excessive engine speed reduction during turning and without the need for cumbersome shifting.

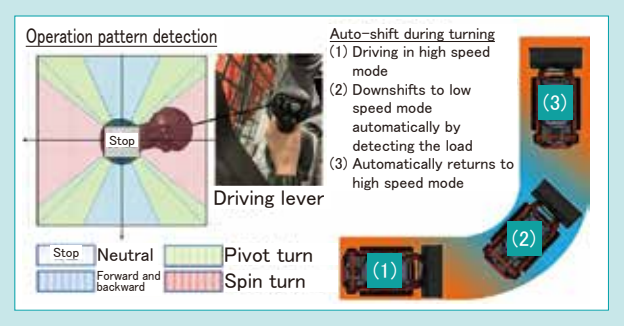

Fig. 6 Auto-Shift During Turning

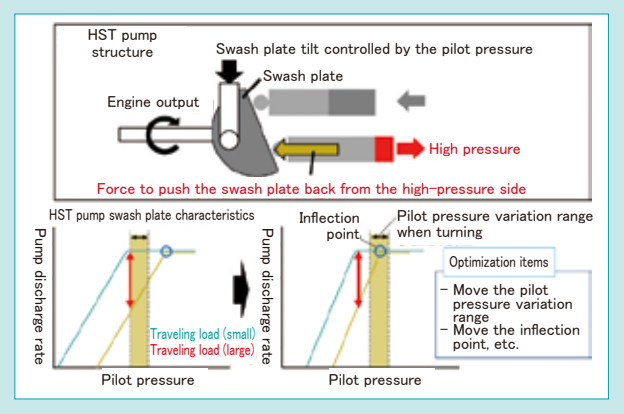

Fig. 7 Optimization of the Swash Plate Characteristics of the HST Pump and Pilot Control Range

4.2.2 Shift shock reduction control

To reduce shocks during shift switch operation, the engine speed is gradually reduced when shifting from high speed mode to low speed mode, and the engine speed is restored at the same time as shifting, thereby slowing the deceleration caused by shifting and reducing shocks (Fig. 8). Conversely, when shifting from low speed mode to high speed mode, the traveling pilot pressure is immediately reduced and then gradually restored, resulting in slower acceleration due to shifting and thereby reducing shocks. The combination of these controls provides both improved maneuverability and smooth shifting.

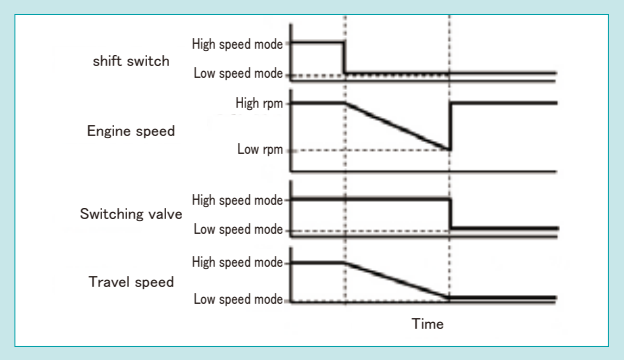

Fig. 8 Shift Shock Reduction Control

4.2.3 Improvement of cooling efficiency

While the vehicle speed was increased, it was necessary to address the worsening heat balance. While conventional machines have a fan directly connected to the engine, the developed design uses a variable hydraulic fan for horsepower control as mentioned above, with the fan duct and variable hydraulic fan mounted on top of the engine (Fig. 9).

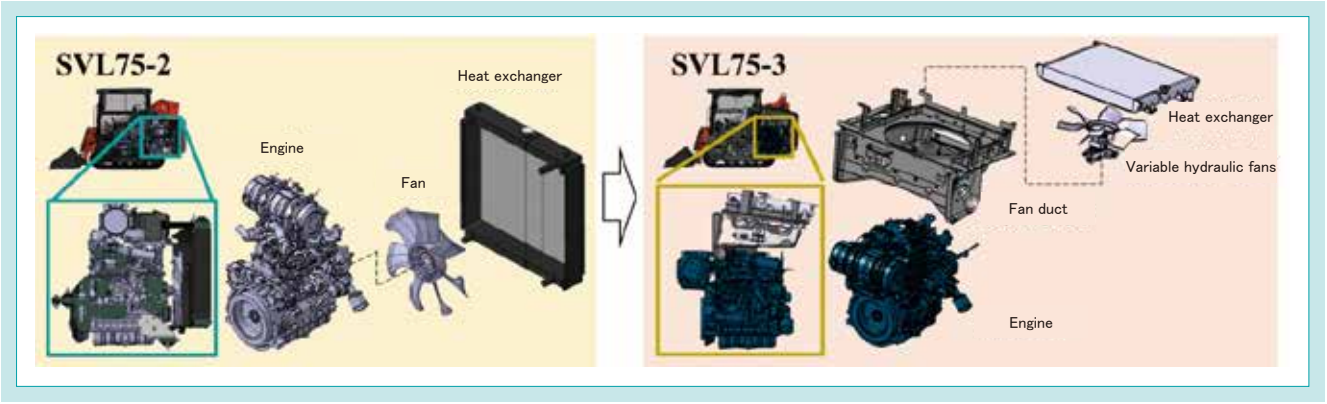

Fig. 9 Cooling Layout Change

In adopting this structure, the cooling airflow was changed from an outflow type to an intake type. This aims to send outside air, which is cooler than the engine compartment, directly to the heat exchanger, rather than the conventional method of blowing air warmed by passing through the engine compartment. In addition, by adjusting the fan angle and optimizing the shape and layout of the cooling system components using fluid analysis, we were able to smooth the airflow (Fig. 10) and reduce pressure loss. Comparative tests conducted prior to this development with a Kubota SSL showed improvements of 2°C to 3°C in coolant and hydraulic oil temperatures. In addition, dust ingress into the engine compartment was suppressed by using a fan duct that isolates the inlet to outlet route of outside air from the engine compartment.

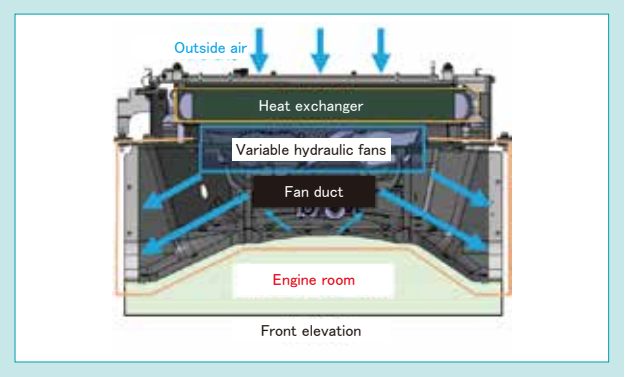

Fig. 10 Suction Fan

4.2.4 Final improvement effect

These measures enabled the SVL75-3 to achieve both a high load capacity and comfortable operation at housing construction sites, where frequent turnarounds and turning movements are required. The results of actual machine verification, which simulated an actual work site, show that the work efficiency was improved by 15% compared with the existing machine, achieving the target and surpassing the basic performance of other companies' machines (Fig. 11).

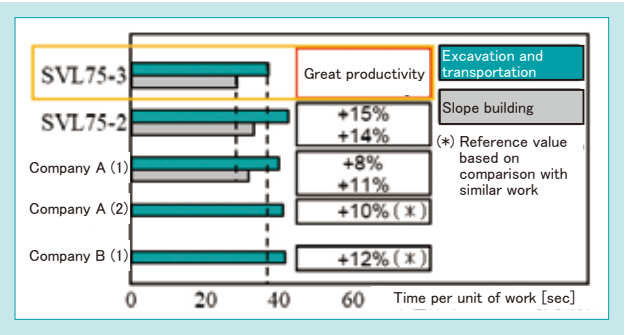

Fig. 11 Effect of Improved Work Efficiency

4-3 Technology for easy operation

4.3.1 Development of the industry's largest-size meter panel

The issues related to the placement of the meter panels were solved by the following means (Fig. 12). The large size of the panel required a compact design of the peripherals. First, we developed bezel-less thin meters (minimizing the monitor frame size) and moved the cab door forward by reducing the thickness of the work lights on the cab. This provides clearance between the opening/closing trajectory of the front window and the meter panel. The hydraulic hose coupling for the control lever was changed from the conventional quick release type to a threaded type, and by adjusting the hose layout, the position of the control lever could be shifted 20 mm down and 5 mm back to ensure meter visibility. These improvements have resulted in a layout that allows hand operation without looking away from the work being done.

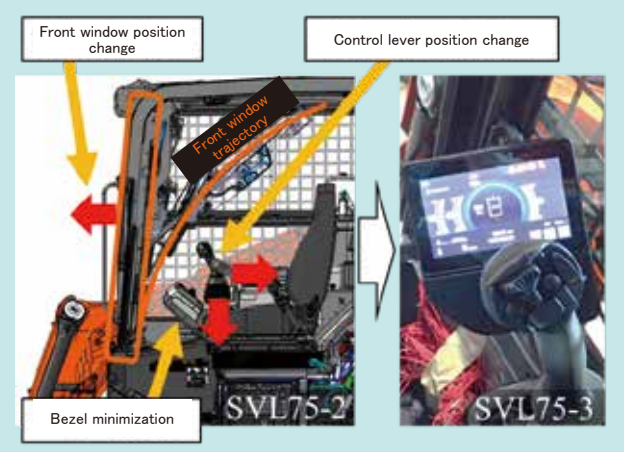

Fig. 12 Overview of Layout Adjustments and View of the Monitor After Adjustment

4.3.2 Development of the wide-angle rearview monitor

The layout was changed so that the rearview monitor screen is displayed on the same panel. Specifically, when the rearview monitor is activated, the indicator position on the screen is moved to the center, and the camera screen is displayed in the upper area, improving visibility while minimizing overlap with the driving lever. A camera with a wide viewing angle is employed, and a large monitor is positioned horizontally to reduce blind spots and ensure better rearward visibility. As shown in Fig. 13, the SVL75-3 can detect people who are positioned behind objects and cannot be seen directly by the operator.

These measures have greatly improved operability and visibility, making it possible to develop products with the advantage of easy operation.

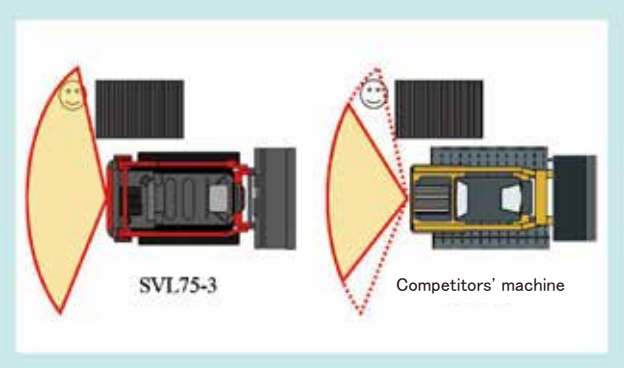

Fig. 13 Field of View Image Diagram

5. Conclusion

The SVL75-3 has achieved industry-leading comfort, basic performance that exceeds competitors' machines, and a design that pursues simplicity. In addition, the first production unit of this machine was subjected to a field monitoring test by users, resulting in verification of the concept. Through these activities, the SVL75-3 has become highly evaluated by users. The machine was launched in the North American market in May 2023, and sales have been steadily increasing. We started mass production of the product for Australia in November 2023, and plan to launch the product in the European market in 2025. The technologies developed for the SVL75-3, such as the integrated cab, LCD touch panel, and auto-shift during turning, can be used as core technologies for changes in subsequent models, contributing to the development of the construction equipment business in North America and elsewhere. Through these innovations, Kubota will continue to meet the needs of the market.

Contribution to SDG targets

9.2 Strengthening of inclusive and sustainable industrial infrastructure
Contributing to industrial development by improving basic performance and comfort

11.3 Enhancement of inclusive and sustainable settlement planning and management capacity
Contributing to infrastructure development by improving basic performance and operability

Reference
1) Association of Equipment Manufacturers (AEM)

Development of a Feeder Controller with a Focus on DX at Manufacturing Sites

Precision Equipment Engineering Dept.

Kubota's feeder business has secured a high share of the global market through cooperation with Kubota Brabender Technologie, which became a subsidiary of Kubota. In recent years, the need for continuous production has increased not only in the existing resin compound market, but also in new markets, making it essential to evolve with new markets in mind. Kubota developed a feeder controller that responds to new technologies such as DX, ahead of our competitors, and also responds to changes in the manufacturing site.

【Key Word】
Feeder Controller, DX, High Connectivity, Auto Tuning, Remote Maintenance

Related SDGs

1. Introduction

A gravimetric feeder (hereinafter referred to as “feeder”) is a device mainly used in the continuous production process of resin compounds to continuously feed powdery and granular materials at a flow rate indicated by the equipment downstream or upstream of this device (prescribed flow rate). This device has become indispensable on production lines, especially in large-scale continuous production processes, to ensure stable feed of raw materials. Its control methods include the loss-in-weight method and the integrated transport amount method. Both these methods control the feeding of raw materials at a constant flow rate by performing control calculations based on the output values from a load cell, which is a weight sensor. Figure 1 shows the system diagram of a typical loss-in-weight feeder. The basic control principle of the integrated transport amount method is the same as this, but it differs in that it controls the amount of passing raw materials on the belt, while the loss-in-weight method controls the rate of weight reduction.[1)]

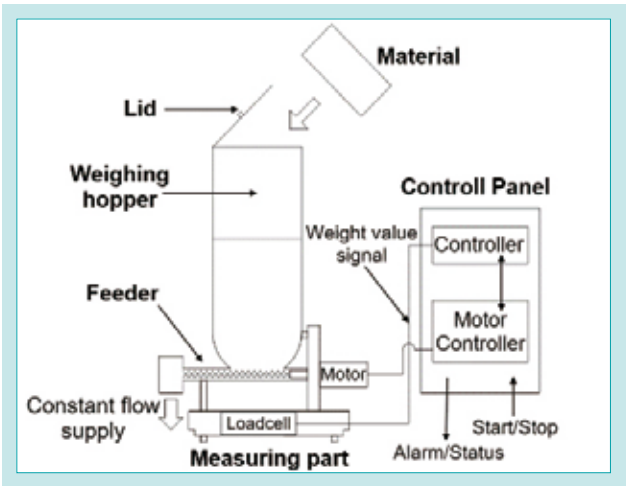

Fig. 1 System Diagram of the Loss-in-weight Feeder

2. Development concept and target value

2-1 Development concept

The concept is to develop a feeder controller that adapts to market changes while maintaining the high functionality that has been cultivated in the resin compound market, our main market. Specifically, the controller is expected to be easy to operate interactively without relying on skilled operators and to facilitate entry into new markets (pharmaceuticals, rechargeable batteries, recycling, and other growth areas).

There are two main technologies that are important to feeders. One is the handling technology of the raw materials (powder and pellets), as a mechanical aspect. The other is the feeder operation control technology (controller part), and the level of both technologies determines the market share. Kubota's existing controls are highly functional and reflect many past market requirements. However, the large number of feeder types, the daily increase in new raw materials, and the wide variety of powdery and granular materials resulted in many control parameters, requiring proficiency sufficient to maximize performance of the feeder. In addition, feeders are expected to enter not only the existing mainstream resin compound market, but also new markets such as pharmaceuticals, where the shift from batch production (producing a certain amount of product separately in batches) to continuous production is underway. Therefore, Kubota has responded by developing a new controller with high usability and expandability.

2-2 Development goals

The development goals were set as follows:

(1) Improved usability

The controller shall be able to perform initial set up at the time of feeder installation and adjust the control parameters interactively, reducing set up time by 50% or more compared to conventional controllers.

(2) Support for Industrial Ethernet and Fieldbus

The controller shall be able to support the following communication protocols, which are already widely used in overseas manufacturing sites:

- Modbus-RTU/Modbus-TCP
- Profibus-DP V1/Profinet
- CC-Link/CC-Link IE Field

(3) Controllers that can be remotely controlled

It should be possible to perform all operations from a remote PC over the Internet.

3. Technical issues to be solved

3-1 Facilitating the setting of various parameters for constant flow control

To make the controller easy to use for non-skilled operators while maintaining the high functionality of conventional controllers, it is necessary to have an interface that anyone can use. There are two possible reasons why the operation is considered difficult:

- There are many setting items to operate the feeder.
- The number of adjustments and the time required to determine the optimal parameter values depend on the operator's skill level.

3-2 Adding industrial field network functionality to a compact controller

The DX wave is now coming to the production lines of resin manufacturers, and a system is desired that not only digitizes analog data but also allows users to instantly obtain the data they need, regardless of time or location, as long as each device is connected to a network. To achieve this, it is necessary to provide a system that can be easily connected to a variety of peripheral devices, with the controller alone supporting communication protocols such as Industrial Ethernet and Fieldbus, which are widely used in overseas markets.

3-3 Developing a secure communication network and intuitive application

Since feeders are used in production lines, they need to minimize unexpected stoppages and downtime. To meet this need, a remote maintenance capability must be implemented, allowing service personnel to immediately investigate, diagnose, and repair problems from a remote location when they occur. In addition, it is essential to establish a communication network with a high level of security and an application that is easy for operators to use without discomfort.

4. Developed technology

4-1 Initial set up guidance function and PI control parameter auto-tuning function

4.1.1 Initial set up guidance function

Conventional controllers have responded to many types of feeders and raw materials, so nearly 500 parameters must be manually set up to operate the feeders (Figure 2). For this reason, if not operated by a skilled operator, the feeder cannot be made ready for use immediately. To solve this problem, we developed an interactive initial set up guidance function that makes it easy for non-skilled operators to set up.

To realize an interactive initial set up guidance function, we implemented a mechanism that allows all basic parameters required for operation to be set by retaining the standard setting data of various feeders in the controller beforehand and allowing the user to interactively select the model's name and device configuration. As a result, the feeder can be operated with only a ten-step interactive set up. The initial set up, which used to take more than two hours even for a skilled operator, can now be completed in about 10 minutes (Fig. 3). In addition, we separately developed a tool to create standard set up data for various feeders, preparing an environment in which data held inside this controller can be updated. This makes it possible to respond to new feeders as they are added.

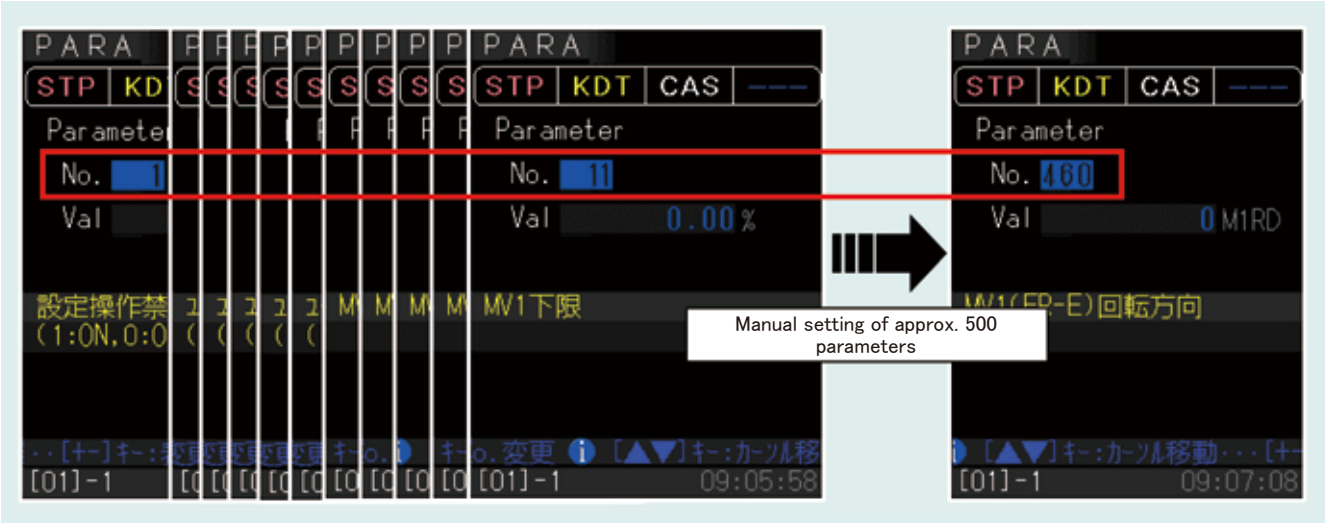

Fig. 2 Parameter Setting Screen of the Conventional Model

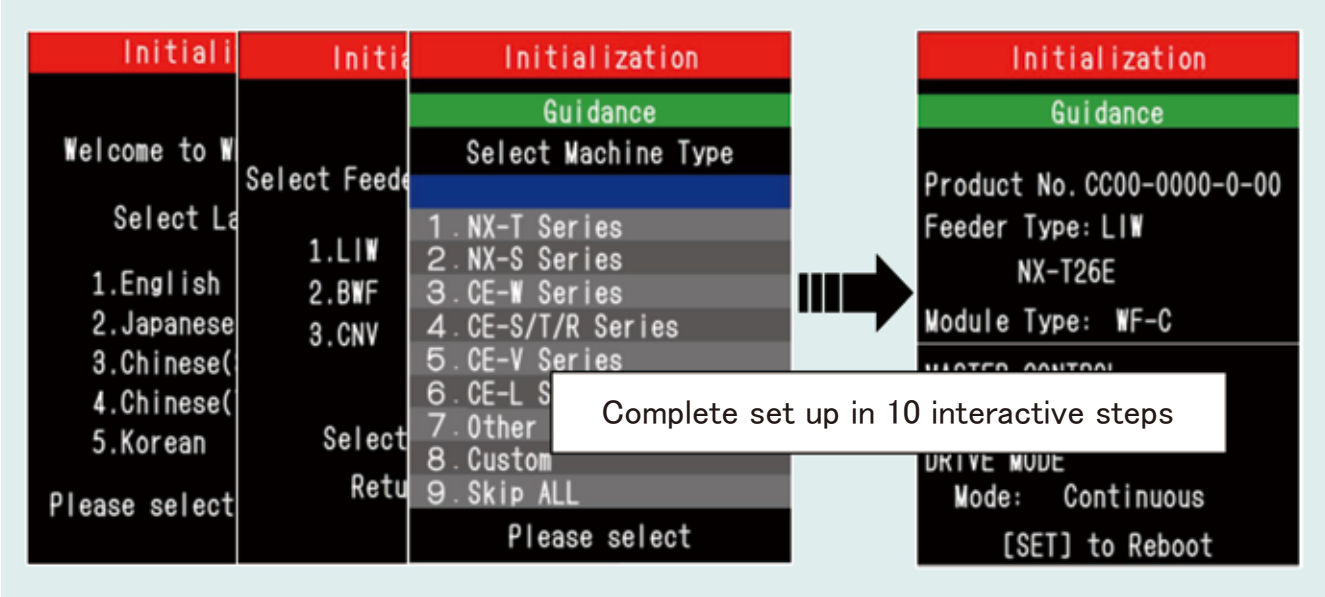

Fig. 3 Initial Setting Screen (Interactive)

4.1.2 PI control parameter auto-tuning function

Feeder flow rate control uses proportional integral (PI) control, where the P and I parameters must be adjusted after the initial set up described in the previous section to achieve sufficient accuracy, and the adjustment process requires time and skill. Specifically, the operator actually conducts raw material feeding and measures the flow rate waveform many times, and then determines each parameter value for optimal feeding accuracy based on empirical rules (Fig. 4). For this reason, the results would vary from operator to operator, and in some cases, the optimal parameters could not be derived.

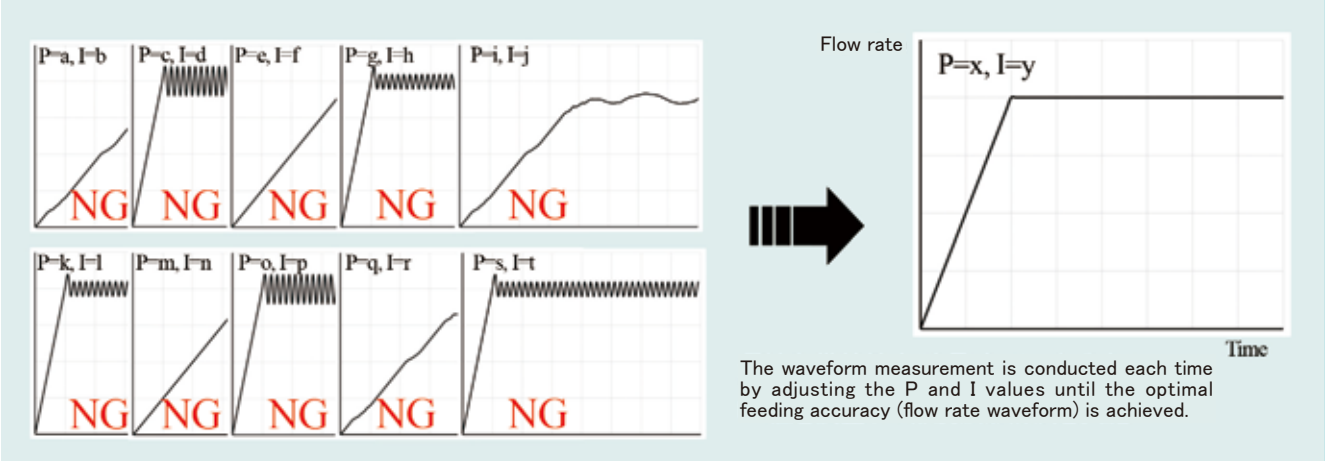

Fig. 4 PI Value Adjustment Based on the Flow Waveform

To eliminate this operator dependency, we developed an operation flow that allows anyone to obtain optimal parameter values in any environment, and an auto-tuning function that does this interactively. Figure 5 shows the operation flow. The P and I parameters are calculated using the Ziegler-Nichols step response method, where they can be calculated solely by measuring the waveforms from the stop state to reaching the prescribed flow rate. In addition, Kubota's proprietary technology is implemented to minimize raw material consumption and stabilize compaction (the compacted state of the powder) inside the feeder by performing two processes, i.e., low-speed and high-speed discharge of raw material, before waveform measurement (Fig. 6). This allows for higher measurement accuracy in subsequent processes and solves the problem of not being able to measure "the correct flow rate waveforms", which has been a major obstacle to the practical application of auto-tuning in the past. In addition, we implemented calculation logic that considers flowability of powder, and this controller excludes abnormal values from the calculation and ensures the accuracy of the calculated values by repeating the waveform measurement and arithmetic processing multiple times. As a result, the feeding accuracy of raw material comparable to manual adjustment by a skilled operator has been achieved. Figure 7 shows an example.

ATmax and ATmin in the figure are the results of the raw material feeding test using the P and I values (worst condition) that take into account the maximum standard deviation (average +3σ) of the calculated P and I values obtained by performing auto-tuning 20 times. The results obtained in the practical range (flow rate of 4 kg/h or more) are accurate to within 1%, which are comparable to manual adjustment. In addition, the adjustment process, which used to take 40 minutes or more for even a skilled operator, or several hours depending on conditions, can now be completed in about 10 minutes, regardless of skill level. This auto-tuning function is patent pending.

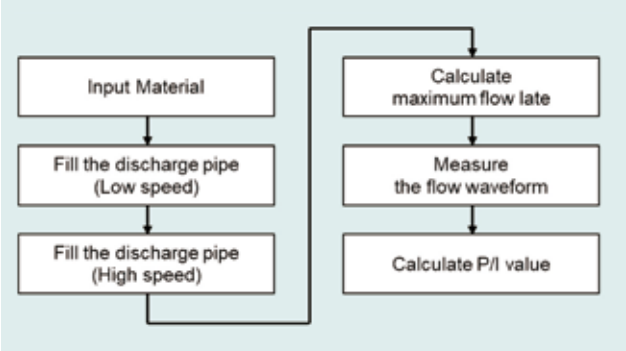

Fig. 5 Auto Tuning Flowchart

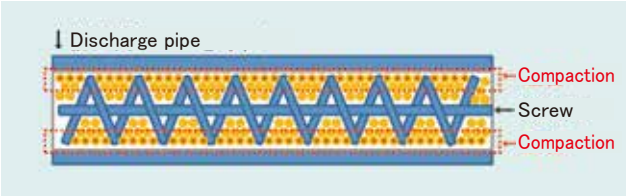

Fig. 6 Steady State Inside the Feeder

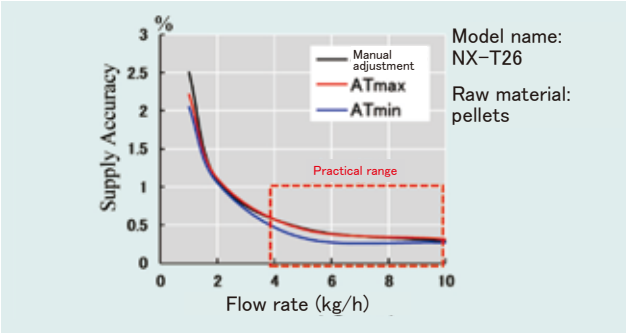

Fig. 7 Supply Accuracy Comparison Graph

4-2 Standard support for Modbus TCP/RTU and add-on functions with an optional board

Conventional controllers only supported proprietary serial communication, making it difficult to program on the connected device side. In addition, to support other communication protocols, it was necessary to install external equipment separately. To support global standard communication formats without increasing the size of the controller, in addition to supporting Modbus-TCP/RTU as standard, we developed an optional board that can be fitted with commercially available units that support other communication formats, creating a system that is easy for customers to implement (Fig. 8). The communication protocols supported by this controller, including optional items, are as follows:

- Modbus-TCP/RTU (standard support)
- CC-Link/CC-Link IE Field (optional)
- PROFINET/PROFIBUS (optional)

This makes it easy to connect to a wide range of devices without relying on external equipment and covers more than 50% of the communication protocols on the market.

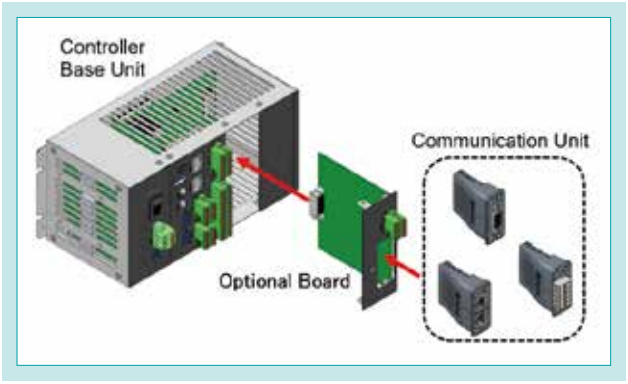

Fig. 8 Controller Base Unit and Optional Board

4-3 Standard support for VPN-connected devices and reproduction of operation terminals by application

4.3.1 Standard support for VPN-connected devices

For remote maintenance, the controller must be connected to the Internet. However, in the feeder market, compounding recipes is very sensitive information and are tightly controlled, requiring a high level of security for handling them over the network. To achieve such a highly secure connection, it is necessary to either install a dedicated wired line or establish a virtual private network (VPN) connection over the Internet. Since it would be impractical from a cost perspective to install the dedicated line, the VPN connection was adopted to provide sufficient security for the communication details of the application described in the next section. We decided to use off-the-shelf products for the VPN connection equipment.

Whereas conventional controllers required USB memory sticks for log data collection and parameter backup, more production sites are restricting the bringing in of recording media in recent years. Therefore, this controller also supports FTP communication, a protocol that allows file transfer over a network. This not only eliminates the need for USB memory sticks but also enables log data collection and parameter backup from remote locations via VPN.

4.3.2 Development of an application version of the operation terminal

We developed a Windows application that reproduces the same screen and key layout as the actual operation terminal so that service personnel who are familiar with it can operate it without any discomfort when performing remote maintenance (Fig. 9a).

In addition, we developed an Android application with self-sampling and graph display functions for customers (Fig. 9b). By installing this application on a commercially available Android device such as a tablet, the operator terminal can be made wireless. In addition to the above-mentioned remote maintenance, this application enables the controller operation and monitoring of the feeder from the vicinity of upstream and downstream equipment and from the office, thereby improving customer convenience.

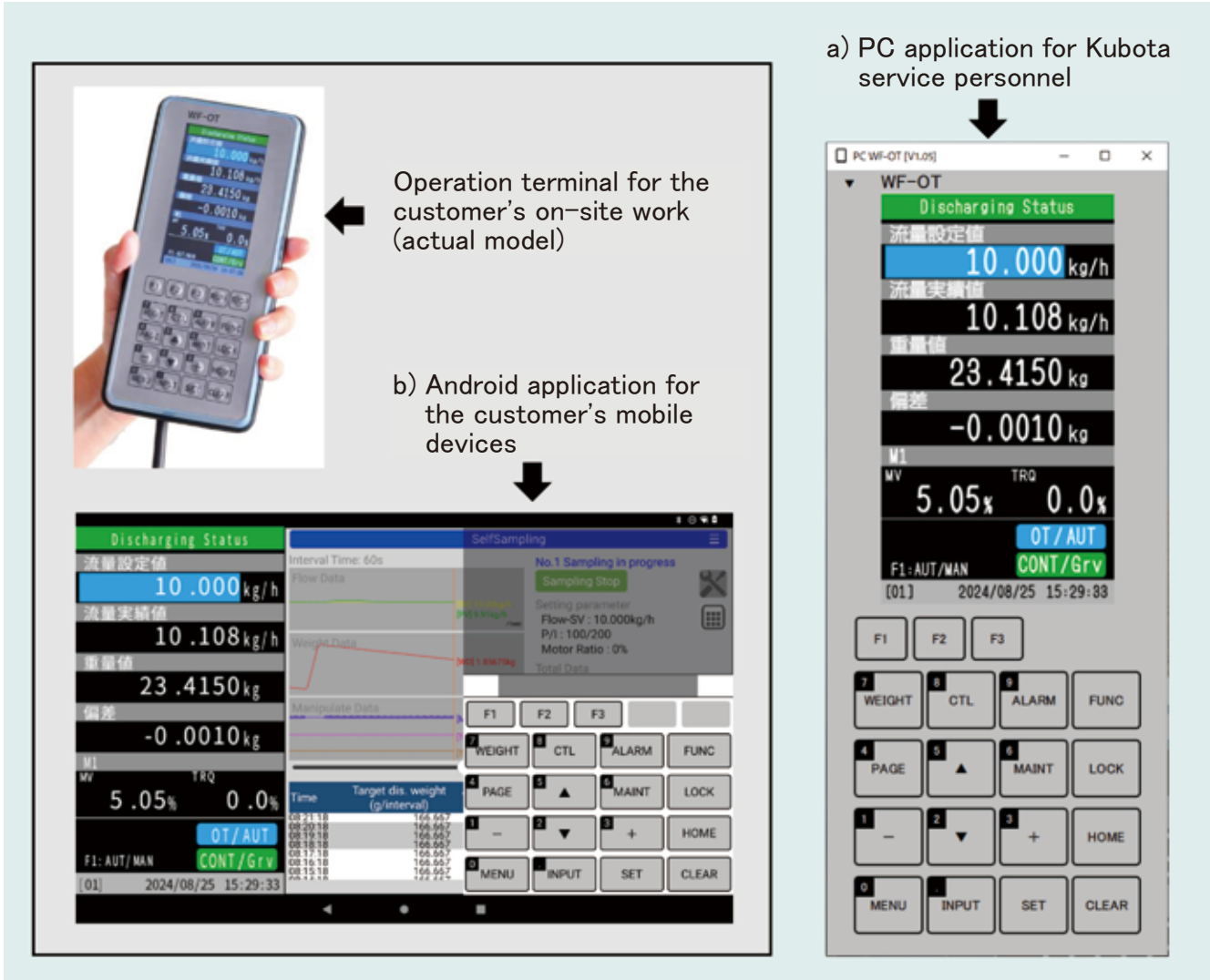

Fig. 9 Operation Terminal Application

5. Conclusion

By incorporating the guidance function for initial set up and adjustment of control parameters, we developed a new controller that can be easily set up and operated by non-skilled operators, while maintaining the high functionality of conventional models. In addition, by supporting various communication protocols and wireless connection devices, we can propose new services such as remote maintenance and remote monitoring to customers through this controller.

Going forward, we will embrace new technologies such as AI and machine learning and work to apply them to growth areas such as pharmaceuticals, rechargeable batteries, and recycling, thereby contributing to the realization of a sustainable society.

Contribution to SDG targets

7.3 Improvement of energy efficiency
15.2% reduction in controller power consumption compared to a conventional model

9.2 Strengthening of inclusive and sustainable industrial infrastructure
Developing an interface that can be operated and set up by non-skilled operators

12.4 Achieving waste management throughout the product life cycle
Using the auto-tuning function to avoid wasteful raw material consumption, thereby contributing to waste reduction

Reference

1) Nikkan Kogyo Shimbun: “Handbook of Weighing Instruments, 2nd Edition, 7.2.1 Plastic Raw Material Weighing and Blending Systems” (referenced on September 13, 2024)

Development of an Automatic Watering Control System Based on Wilt Detection

Technology Innovation R&D Dept. Ⅲ

In recent years, extreme weather events have become frequent, and climate change, such as rising temperatures, has become increasingly evident. As a result, the importance of greenhouse horticulture, which can control the environmental conditions, has grown significantly for ensuring a stable food supply. Additionally, due to factors like an aging population, the number of farmers is decreasing, leading to a demand for more efficient and labor-saving production methods. In response to this situation, Kubota launched its first in-house product for greenhouse horticulture, the automatic watering control system based on wilt detection (Hamirus), in October 2022. This system automates watering management for high-sugar tomatoes, contributing to labor savings in watering management and stable production. This article introduces the technology behind it.

【Key Word】
Greenhouse Horticulture, Automatic Watering System, Wilt Detection, Image Sensing

Related SDGs

1. Introduction

The production value of horticultural crops, namely vegetables, fruit trees, and flowers, accounted for nearly 40% of Japan's total agricultural output in 2022.[1)] Although vegetables make a small contribution to food self-sufficiency on a caloric basis, they are important crops for maintaining and promoting health and agriculture. To meet consumer demand for these horticultural crops, a stable year-round supply through greenhouse horticulture has become essential. Especially in recent years, with the frequent occurrence of extreme weather events and climate changes such as rising temperatures, greenhouse horticulture, which is able to control the environment inside the greenhouse, is becoming increasingly important in ensuring a stable food supply. In addition, the number of farmers is declining year by year due to an aging population and other factors, leading to demand for more efficient and labor-saving production methods. Kubota has been engaged in research and development of smart agriculture for greenhouse horticulture since 2016, and in October 2022, the company launched its first in-house product for greenhouse horticulture called Hamirus, an automatic watering control system based on wilt detection.

This system quantifies the wilting of tomato leaves based on images captured by a camera installed above the tomato colony, and automatically applies water when the quantified value falls below a certain threshold (Fig. 1). This feature automates watering control to grow high-sugar tomatoes, contributing to labor-saving watering control and stable production. This paper presents the technology developed for the automatic watering control system based on wilt detection.

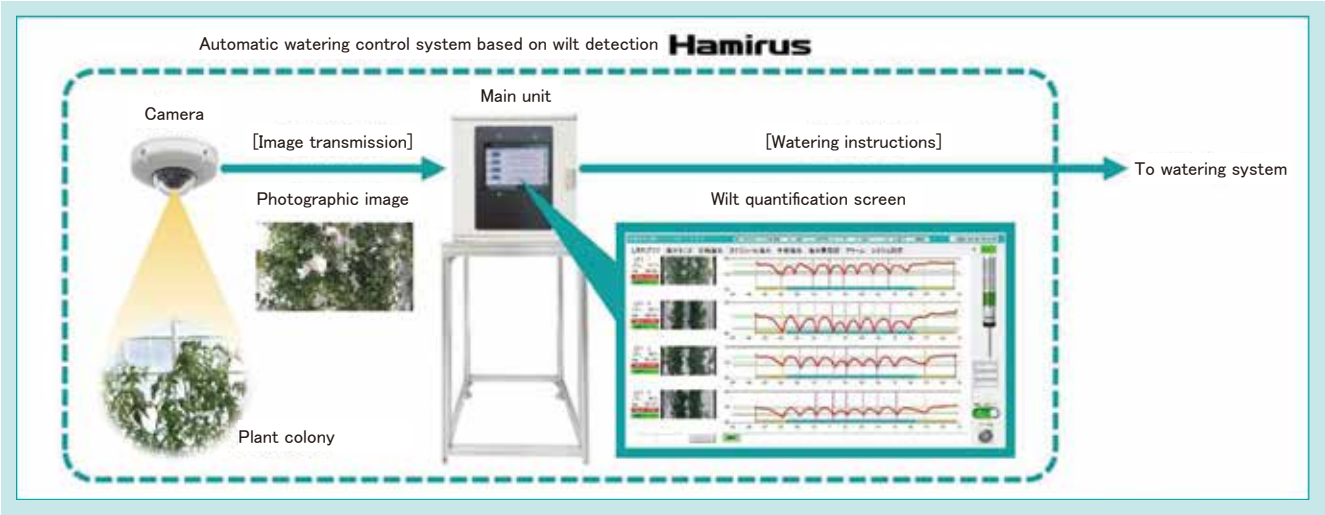

Fig. 1 Overview of the Automatic Watering Control System Based on Wilt Detection

2. Development concept and target values

2-1 Development concept

In high-sugar tomato cultivation, watering must be kept to the minimum necessary to prevent water from entering the fruit and to promote the accumulation of sugars and other components that help prevent water loss from the fruit. Leaf wilt is known to be an effective indicator of when to water. Here, wilt is defined as the loss of water in the plant due to the rate of transpiration exceeding the rate of water uptake. When wilting occurs, plant cells lose their firmness and shrink (Fig. 2).

In conventional high-sugar tomato production, experienced growers visually inspect for wilt and use years of experience and intuition to determine when to water. Therefore, in order to replicate the watering management of experienced growers, it is necessary to quantify leaf wilt and control watering based on the quantified results.

The cover materials used in greenhouses where the system is installed include scattering film, transparent film, and glass. The light environment inside the greenhouse varies depending on the cover material, and the system is required to provide stable watering control even in differing light environments.

Another issue is that during cultivation, the tomato plant posture changes as a result of crop management practices, such as vine lowering and leaf picking. Therefore, the system must be able to control watering as intended by the farmer, even as the plant posture changes.

Based on the above, the following development concepts were identified:

(1) Ability to control watering based on leaf wilt

(2) Ability to install the system regardless of the greenhouse cover material

(3) Ability to control watering in response to changes in the plant posture

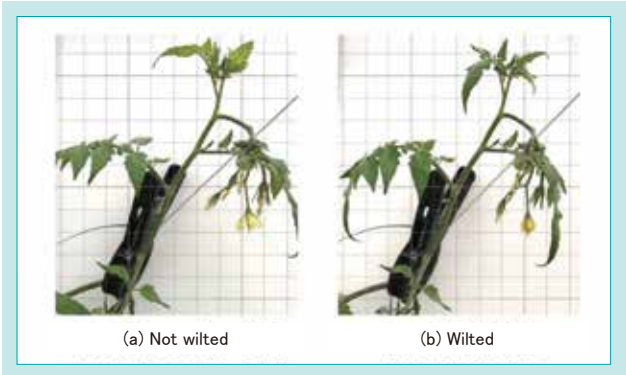

Fig. 2 Appearance of a Plant Before and After Wilting

2-2 Development goals

The goals for developing the system according to our concept are as follows:

(1) Establishment of wilt quantification technology
(2) Establishment of image sensing technology that is robust in differing light environments
(3) Establishment of a watering control algorithm that can adapt to changes in plant posture

3. Technical issues to be solved

3-1 Establishment of wilt quantification technology

To control watering based on leaf wilt, it was first necessary to quantify leaf wilt. Since experienced farmers visually inspect for leaf wilt, it was thought that image sensing technology could be used to quantify leaf wilt. At the time of development, there were previous studies[2] of wilt quantification using image sensing technology. Because wilt is quantified as a relative value, it was necessary to consider how to set a reference value in order to apply this approach to watering control. Therefore, the challenge was to develop a practical technique to quantify wilt.

3-2 Establishment of image sensing technology that is robust in differing light environments

If the cover material of the greenhouse is a scattering film, direct sunlight will be scattered by the cover material and enter the greenhouse. As a result, the lighting in the greenhouse will be relatively even. In such a light environment, white or black clipping is less likely to occur in captured images. Here, white clipping refers to a condition in which the bright areas of an image have lost their tonal gradation and are pure white, while black clipping refers to a condition in which the shadow areas of an image have lost their tonal gradation. In both cases, information about the subject is lost, so images without white or black clipping are suitable for image sensing.

On the other hand, if the cover material of the greenhouse is transparent film or glass, direct sunlight will enter the greenhouse without being scattered by the cover material. Therefore, the greenhouse will have both sunny and shady areas. In such a light environment, white and black clipping is likely to occur in the captured images and is an obstacle to stable image sensing.

High dynamic range (HDR) photography is an effective way to reduce white and black clipping. However, even with HDR photography, white and black clipping still occurs, so the challenge was to develop image sensing technology that is robust in differing light environments.

3-3 Development of a watering control algorithm that can adapt to changes in plant posture

During the growing period of tomatoes, crop management, such as vine lowering and leaf picking, is carried out. In commercial tomato production, it is common to use training systems in which some of the branches are attached to strings or posts to shape the plant. Vine lowering refers to the process of lowering the height of the plant when the height has reached the upper limit of the strings or posts and reshaping the plant (Fig. 3). Leaf picking refers to the process of thinning leaves to improve sunlight exposure and air circulation and removing leaves that do not contribute to photosynthesis. Therefore, vine lowering and leaf picking change the appearance of the tomato plant.

Because it is difficult to eliminate the effects of such changes in plant posture, the challenge for the wilt quantification technology was to develop a watering control algorithm that could prevent unnecessary watering even when the plant appearance changes.

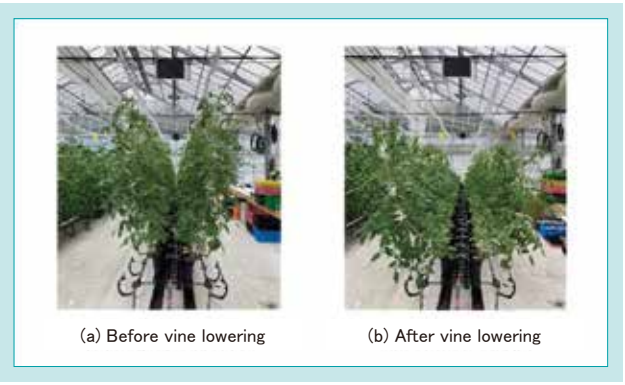

Fig. 3 Appearance of Plants Before and After Lowering

4. Developed technology

4-1 Wilt quantification technology

Figure 4 shows a flowchart of the developed wilt quantification technology. For wilt quantification, images taken at one-minute intervals by a fixed-point camera installed above the tomato colony are used. For each time-sequence image, white balance adjustment is performed first, followed by detection of the plant areas, including the leaves. The coverage is then calculated using the following formula:

Coverage = (Number of pixels in the plant area) / (Number of pixels in the total area)

Plant leaves shrink when they wilt. Therefore, the coverage decreases as wilt occurs. This system uses this characteristic to quantify plant wilting.

Next, noise reduction is applied to the time-series data of coverage, and finally, the wilt rate is calculated using the following equation:

Wilt rate = (Coverage at each time in the sequence) / (Reference coverage)

Here, the reference coverage is the coverage when there is no plant wilt. The wilt rate can be used to quantify the relative degree of wilt that has occurred. The wilt rate is an index that decreases from 100% as the plant wilts.

Figure 5 shows a graph quantifying the daily wilt of high-sugar tomatoes using this wilt quantification technology. The red line in the figure represents the coverage (wilt rate) at each time. The yellowish green line in the figure represents the reference coverage. The reference coverage is automatically set based on the coverage observed during the reference coverage calculation period, which is set as morning hours when no plant wilting occurs. By resetting the reference coverage each morning, wilting can be quantified appropriately even if the coverage changes as the plant grows.

This system has an automatic watering control mode, where watering is done based on wilting, and a scheduled watering control mode, where watering is done at preset times. During the reference coverage calculation period, watering is done in scheduled watering control mode, and after the reference coverage is set, watering is done in automatic watering control mode.

The green line in the figure represents the wilt rate threshold, and automatic watering takes place when the wilt rate falls below this threshold. The pink vertical lines in the figure indicate the timing of automatic watering, showing that the wilt rate recovered with watering. The above results indicate that we have been able to develop a practical wilt quantification technology that can actually be applied to watering control.

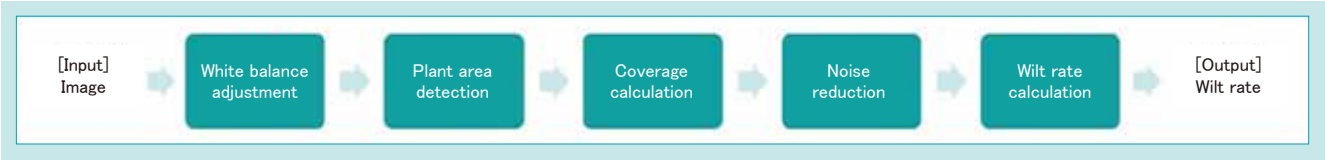

Fig. 4 Flowchart of Wilt Quantification

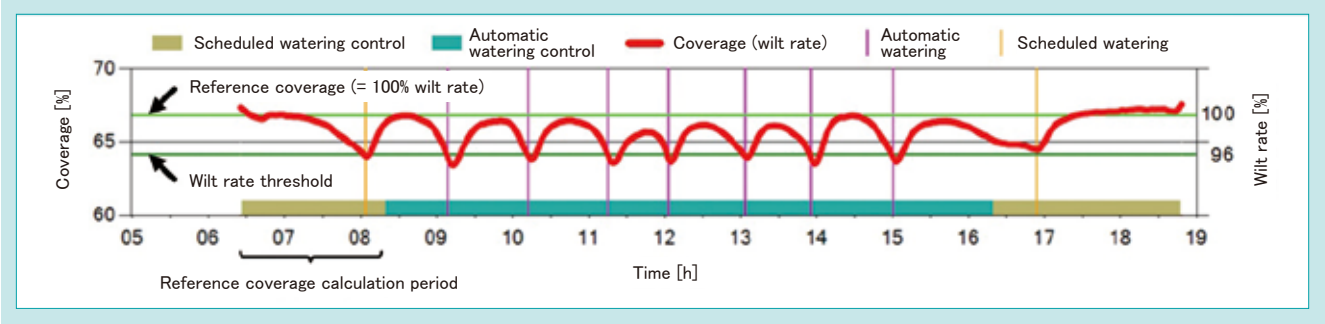

Fig. 5 Graph of Wilt Quantification

4-2 Image sensing technology that is robust in differing light environments

When the cover material of a greenhouse is transparent film or glass, white or black clipping is likely to occur in the captured images. In wilt quantification, image processing for plant area detection is most affected by this clipping.

A color extraction method using the HSV color space is commonly used for plant area detection. The HSV color space consists of three components: hue, saturation, and value. Hue represents the type of color in the range of 0 to 360°, saturation represents the vividness of color in the range of 0 to 100%, and value represents the lightness of color in the range of 0 to 100%. When detecting plant areas, it is necessary to set the range of these three features so that plant areas can be detected properly.

However, when white or black clipping occurs, the saturation is reduced and the hue becomes unstable. This makes it difficult to detect plant areas where white or black clipping has occurred. Figure 6(a) shows an example of a captured image in which white clipping has occurred. There is a white clipping in the upper left corner of the image where the plant is exposed to direct sunlight. Figure 6(b) shows the result of plant area detection with the color extraction method using the HSV color space. The red-colored areas represent the detected plant areas, showing that the plant areas where white clipping occurred could not be detected. Such omissions in plant area detection could cause the system to incorrectly water even though the plant is not wilted. Countermeasures were needed because unnecessary watering leads to physiological disorders such as root rot.

We therefore examined methods using deep learning as a solution. Since deep learning automatically finds features through learning, we expected to be able to create a detector that combines color information with various features such as shape and texture.

The model created is a semantic segmentation task model that performs classification for each pixel; for each pixel in the input image, the model performs binary classification to determine whether the pixel is a plant area or not. Figure 6(c) shows the results of detecting plant areas using a deep learning method, showing that the system could detect all the plant areas where white clipping occurred. Quantitatively, we found that the F value, which measures detection performance (the closer to 1, the better), improved to 0.984 for the method using deep learning, compared to 0.831 for the color extraction method using the HSV color space. These measures have allowed us to develop image sensing technology that is robust in differing light environments.

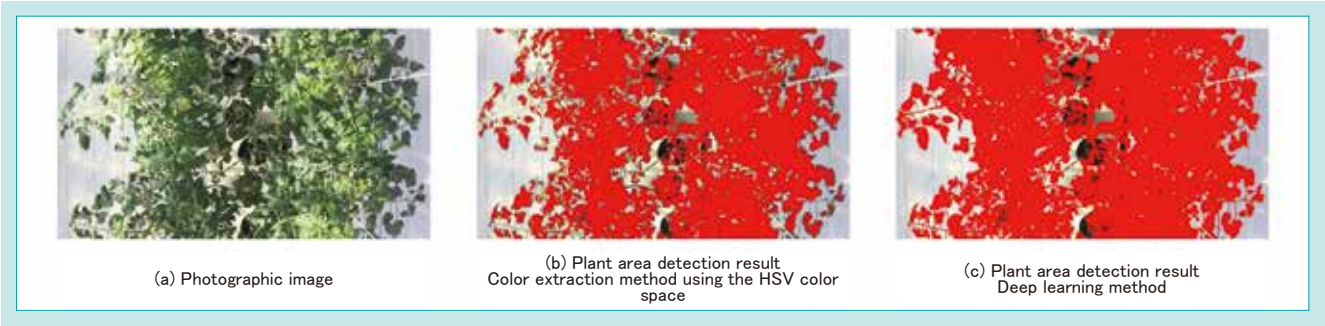

Fig. 6 Comparison of the Plant Region Detection Results

4-3 Automatic watering control algorithm that adapts to changes in plant posture

The plant coverage changes as vine lowering and leaf picking are done during the tomato's growing period. Figure 7 shows how the photographic images changed before and after vine lowering. In this example, tomato vines on the left side of the image have been lowered, resulting in reduced plant coverage in the area where the vines have been lowered. Since this decrease in coverage is not due to wilting, if the wilt rate is calculated under the same conditions as before, it will remain extremely low, resulting in unnecessary repetitive watering.

Therefore, we developed an automatic watering control algorithm that adapts to such changes in plant posture. Figure 8 shows an example of automatic watering control based on the developed algorithm. When a sudden decrease in coverage occurs, such as due to vine lowering, and the wilt rate falls below a threshold value, automatic watering is first performed. The developed algorithm determines whether this sudden decrease in coverage is due to a change in plant posture based on the coverage during "N" minutes after automatic watering. If the coverage remains below the wilt rate threshold for more than a certain number of times within N minutes, the sudden decrease in coverage is considered to be due to a change in plant posture. Otherwise, the sudden decline in coverage is judged to be due to wilting. If the sudden change is found to be due to a change in plant posture, the reference coverage is reset using the coverage observed during the N minutes. Using this algorithm to reset the reference coverage helps prevent unnecessary repetitive watering and allows watering control based on plant wilting, even after the plant posture changes.

In this section, we have introduced an algorithm that is adapted to the case where the coverage decreases due to changes in plant posture. However, the system is also equipped with an algorithm that automatically resets the reference coverage when the coverage increases due to changes in plant posture. The development of these algorithms has made it possible to automatically control watering in a stable manner, even when the plant posture changes.

Fig. 7 Comparison of Images Taken Before and After Lowering

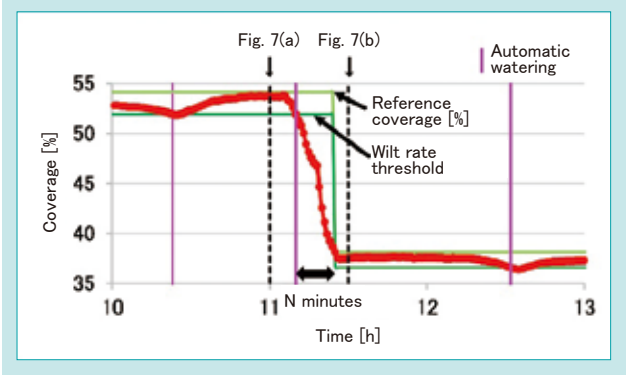

Fig. 8 Example of the Automatic Watering Control Adapted to Changes in Plant Coverage Due to Lowering

4-4 Examples of system implementation

The following sections will present examples of how this automatic watering control system, based on wilt detection, can save labor and increase crop yield. In each case, a comparison is made between automatic watering based on wilt detection and scheduled automatic watering.

4.4.1 Example of labor saving

The stacked bar graph in Fig. 9 compares the work time for watering control. The vertical axis shows the work time per month, the green bars represent the time needed to check tomato leaves for wilting, and the gray bars represent the time needed to set up automatic watering.

The scheduled watering system takes time to set up automatic watering because the number of waterings and the amount of watering need to be adjusted depending on the day's weather conditions. On the other hand, the wilt detection system automatically waters plants at the stage when they begin to wilt (i.e., when they need water), so there is no need to change the settings based on the weather. This greatly reduces the time required to set up the system. Overall, the system has reduced the work time for watering control by 46%, proving that it saves labor.

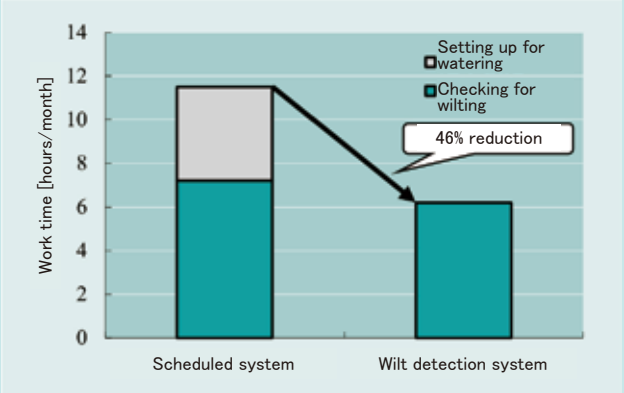

Fig. 9 Comparison of the Working Time for Watering Management

4.4.2 Example of yield increase

The stacked bar graph in Fig. 10 compares the yield of high-sugar tomatoes. Each colored bar shows the yield during a different period. This test compared the yield when watering was controlled under conditions that resulted in equivalent sugar content. To see how the different watering methods affected the sugar content and yield of fruit, watering control by each method was conducted for at least two months prior to harvest.

Compared to the scheduled system, the wilt detection system resulted in an 8% increase in yield. The increased yield may be explained as follows: In the scheduled system, excessive wilting of the plant due to sudden sunny periods or other factors can cause damage to the plant, but the wilt detection system can prevent this by watering according to wilt.

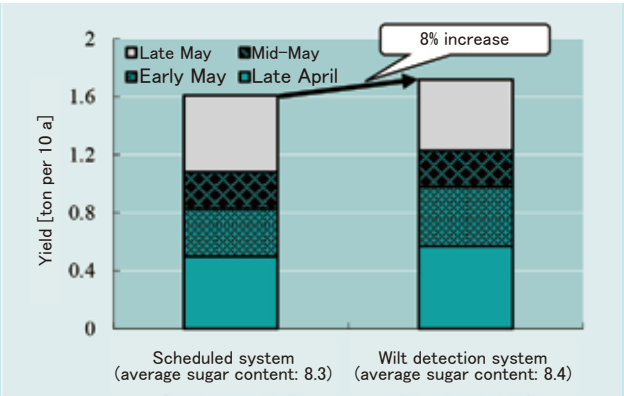

Fig. 10 Comparison of the Yield

5. Conclusion

Kubota developed and launched in October 2022 its first in-house smart agricultural system for greenhouse horticulture called Hamirus, an automatic watering control system based on wilt detection. By replacing the eyes, experience, and intuition of experienced farmers with image sensing technology and automatic watering control algorithms, anyone can now easily control watering to grow high-sugar tomatoes. In the future, we will work to solve farmers' watering control challenges by expanding the range of crop types, varieties, and cropping practices to which this system can be applied, as well as by expanding the system's capabilities.

Based on the technology and experience gained through this development, we will also work to develop technologies to automate crop management tasks other than watering control, thereby contributing to the realization of sustainable greenhouse horticulture.

Contribution to SDG targets

2.4 Realization of sustainable and robust agriculture
8% yield increase compared to scheduled watering

8.2 Increase of productivity through innovation
46% reduction in work time compared to scheduled watering

9.5 Promotion of science, technology, and innovation
Promotion of development of smart agriculture technology using image sensing technology

Reference

1) Ministry of Agriculture, Forestry and Fisheries: "Agricultural Income Statistics" https://www.maff.go.jp/j/tokei/kouhyou/nougyou_sansyutu/ (referenced on September 30, 2024)
2) Hiroshige Nishina, Kotaro Takayama, and Kenji Hatou: "Liquid Supply Control Device" Japanese Patent No. 4820966 (issued on November 24, 2011)

Development of Inspection Technology for the Outer Surface of Pipes

Pipe Systems Manufacturing Engineering Dept. ／ Keiyo Plant
Pipe Systems Quality Assuranse Dept.

Because of visual sensory inspection for ductile iron pipe, we have the risks of inspection judgement variation by the inspectors and the overlooking of defects. To solve these problems, we have developed automatic inspection technology using image analysis by AI. With this technological development, we have achieved reliability improvements in inspection and labor saving for inspectors. In addition to the production line of iron pipe, we are going to promote technology expansion to the production line of synthetic pipe.

【Key Word】
Ductile Iron Pipe, AI (Artificial Intelligence), Image Analysis, Automatic Inspection

Related SDGs

1. Introduction

1-1 Project overview

In Japan's waterworks industry, shipments of water supply materials and equipment have been declining year by year due to a decline in revenue from water charges resulting from a declining population. In addition, the business environment is difficult not only in manufacturing, but also in construction due to a decline in the number of skilled workers.

Meanwhile, to continue providing safe and reliable water to people, iron pipes (Fig. 1) and plastic pipes are important water supply materials/equipment that support the water infrastructure, and Kubota has a responsibility to continue supplying highly reliable products. Therefore, in iron pipe production lines, we are working to develop technologies that improve the reliability of inspection and save labor.

Fig. 1 Example of Water Supply Materials and Equipment

1-2 Challenges addressed

For many years, iron pipe production lines have relied on people for adjustments and visual inspection. Although all products are visually inspected, the sensory nature of visual inspection introduces inspection quality risks such as variation in pass/fail decisions and missed defects. In addition, it takes time to train inspectors with appropriate judgment skills, which, combined with future decline in the workforce, will make it difficult to retain inspectors. Therefore, there is an urgent need to automate inspections based on objective data.

On the other hand, automated inspection technology must have an inspection accuracy equal to or better than that of human inspectors. In the past, we considered automating inspection using surface shape measurement but could not achieve sufficient inspection accuracy due to obstacles such as scratches and dirt caused by product transport in the line. Therefore, as an inspection method that replicates the inspector's eyes, we have developed an automatic inspection technology that correctly detects defects using AI-based image analysis.

2. Development concept and goals

2-1 Development concept

An automatic inspection system using AI-based image analysis, which has the same or better judging accuracy as visual inspection, was introduced to the production line at the Keiyo Plant (production processes shown in Fig. 2). This was combined with visual inspection for double-checking to prevent defective pipes from being passed onto the next process. The following three development concepts were identified:

(1) Fully automated in-line inspection

The inspection system should be capable of automatically inspecting the outer surface of all iron pipes produced on the target line. To do this, the system must be designed in such a way that it can be installed on an existing line and be able to inspect (photograph) the entire outer surface of the pipes.

(2) Pass/fail judgment including identification and recording of defects

There are different types of defects, such as cracks, dents, and pores, each with different causes. With an eye toward expanding the system to quality improvement activities based on inspection results, it should not only perform simple pass/fail judgments but also enable the identification and recording of defect types and locations.

(3) Automatic stop in case of equipment failure (fail-safe)

Obtaining proper inspection images and maintaining proper communication between control devices, such as PCs, is essential to a normal inspection. Therefore, to ensure that inspections are performed normally, the equipment's operating status is automatically monitored, and if an equipment abnormality occurs, the inspection system automatically stops the inspection and notifies the operator.

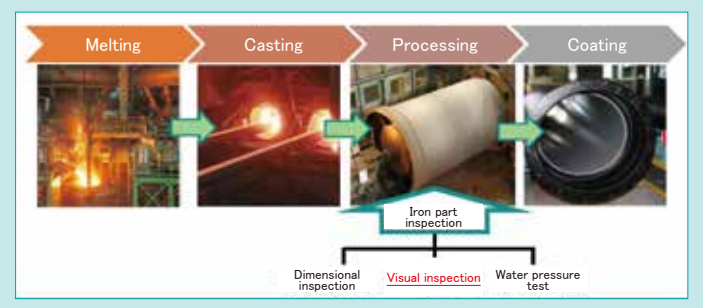

Fig. 2 Production Process of Ductile Iron Pipe

2-2 Development goals

(1) Zero leakage of defective pipes to the next process, i.e., the coating line
(2) Ability to correctly determine the type of defect
(3) No overlooking of equipment anomalies
- Ability to determine if appropriate inspection images are being captured
- Ability to detect communication anomalies between devices

3. Developed technology

3-1 Inspection image photographic technology

3.1.1 Challenges in photographic technology

(1) Use a camera to capture images of the entire inspection area of the outer surface of a cylindrical iron pipe without omission.
(2) Clearly photograph the difference between the defective part and the normal part.

3.1.2 Photographic technology solutions

To overcome the technical challenges, appropriate imaging equipment was selected, equipment placement was studied, and imaging conditions were set.

First, a camera with a pixel count corresponding to the smallest defect size was selected. In order to obtain images of the entire inspection area of the outer surface of the iron pipe without omission and with minimal variation in brightness, we devised a configuration in which a photographing device with a light-shielding cover moves over the iron pipe as the iron pipe rotates.

To clearly capture the features of cracks and other defects, the lighting was positioned away from the center axis of the camera to illuminate from an oblique direction (Fig. 3). In addition, appropriate imaging conditions, such as exposure time, were set to obtain blur-free images even when the iron pipe and camera moved at high speed.

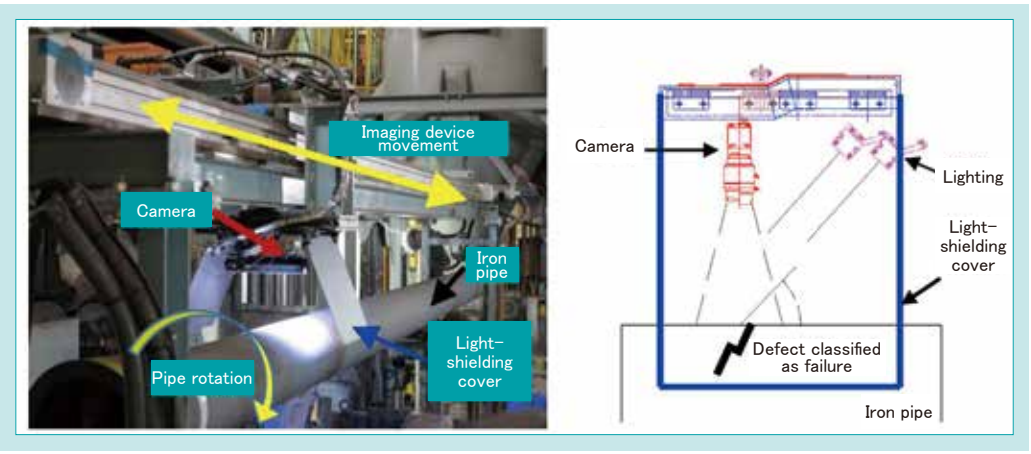

Fig. 3 Appearance of Inspection Equipment and Configuration of the Imaging Device

3-2 Pass/fail judgment technology

3.2.1 Challenges in pass/fail judgment technology

(1) Classify defects with different shapes and characteristics.

(2) Ensure proper judgment accuracy.

3.2.2 Solutions for the pass/fail judgment technology

Supervised learning, which learns the characteristics of each defect, was used to classify defects with AI. The learning method is shown below:

(1) By making the system learn the images of all types of defects separately, the system was made to recognize differences in the characteristics of defects.

(2) Since the shapes of defective cast products such as ductile iron pipes vary, multiple images of different shapes for the same defect type were selected and used for learning.

(3) To properly learn the size and other characteristics of each defect, the location where the defect occurred was specified (annotated) for each image (Fig. 4).

To ensure proper judgment accuracy, the judgment method was based on comparing each learned defect with the inspection image and outputting an agreement rate, based on which a pass/fail threshold was set for each defect to ensure reasonable accuracy of judgments.

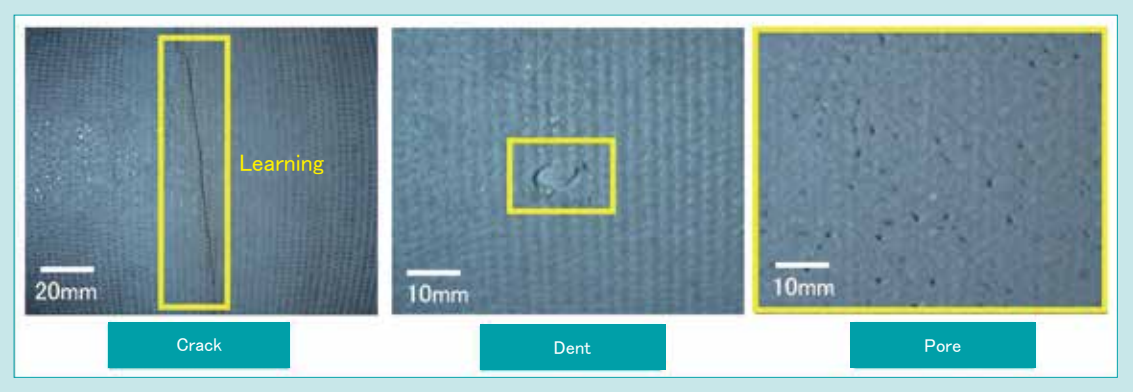

Fig. 4 Sample of AI Learning with Images of Defects

3-3 Automatic equipment stop technology

3.3.1 Challenges in automatic equipment shutdown technology

(1) Confirm that the camera has worked properly and that captured inspection images are suitable for pass/fail judgment.

(2) Confirm that the AI has successfully made a pass/fail judgment and that the production line control equipment has received the judgment result.

3.3.2 Solutions for automatic equipment stop technology

The system was designed to analyze the brightness and other characteristics of the obtained inspection images in parallel with the pass/fail judgment operation to determine whether the images were taken under normal conditions (Fig. 5). If an anomaly occurs, the system issues an on-the-spot anomaly signal, stops the inspection equipment, and notifies the operator of the anomaly.

Similarly, the communication status between the PC that uses AI to make the pass/fail judgment and the PLC that controls the production line is monitored, and an anomaly signal is sent if the judgment result is not received. By constantly monitoring the equipment condition during inspection, the occurrence of anomalies is detected immediately, preventing incompletely inspected iron pipes from being passed on to downstream processes.

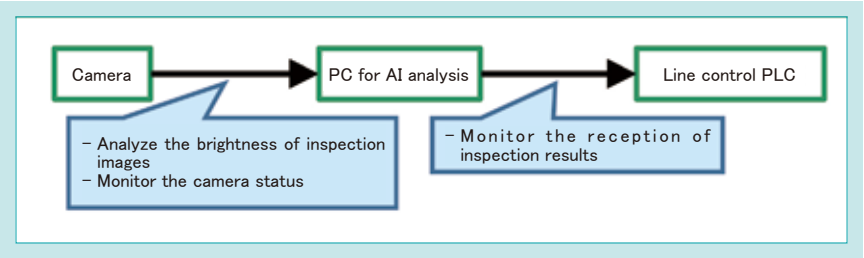

Fig. 5 Operation Flow of Inspection

4. Development results

Automatic visual inspection equipment incorporating the developed technologies was installed on the production line at the Keiyo Plant, and evaluation tests using a total of 5,000 iron pipes were conducted on the equipment over several separate days.

The results are as follows:

(1) The AI system was able to detect all defects, and no defective pipes were passed onto the next process, i.e., the coating process.

(2) The types of defects detected were correctly classified.

(3) Equipment anomalies (inability to take proper inspection images or communication anomalies between devices) were correctly detected, preventing uninspected pipes from being passed on to the next process.

In the two years since the automatic visual inspection system was introduced, there have been no major problems.

5. Conclusion

We have developed technology for judging defects on pipe outer surfaces and enabled automatic inspection using certain judgment criteria based on objective data, eliminating the need for human intervention.

In the future, we will use this judgment technology for iron pipe production lines at other plants and for other products, such as synthetic pipes, in order to make inspections in the pipe system business more reliable.

Contribution to SDG targets

6.1 Increased availability of safe and affordable drinking water
Providing reliable water supply materials and equipment

9.1 Development of high quality, sustainable, and resilient infrastructure
Contributing to building resilient pipelines by providing water supply materials and equipment

Development of a Large Diameter Electro Fusion Socket

Kubota ChemiX Co., Ltd.

Steel pipes, which were used as piping materials in many factories built during the period of economic growth, are suffering corrosion problems due to aging. Kubota Chemix (hereinafter referred to as "KC") is promoting market development by proposing plastic pipes as an alternative to these metal pipes.

We use injection molding to continuously produce polyethylene EF fittings of φ200 or less. However, for sizes of φ250 or more, we have developed equipment and manufacturing techniques specifically for original pipe-type EF fittings, which have heating wires embedded in short pipes, and are able to produce many models in small quantities.

【Key Word】
Pressure Pipeline, Lathe Processing, Applicability, Electro Fusion Socket

Related SDGs

1. Introduction

Kubota Chemix is expanding its business of polyethylene pipes, which have been increasingly adopted for water distribution applications, to the plant and civil engineering markets, including piping for cooling water and various types of drainage in factories and for small hydroelectric power plants, thereby increasing the demand for polyethylene pipes as an alternative to metal pipes. As part of the product lineup expansion, we are promoting the development of straight and bent pipes with a single socket (hereinafter referred to as “single-socket pipes”), which excel in applicability (Fig. 1) .

Fig. 1 Pipe and Bend with a Single Socket (φ250)

2. Development concept and goals

2-1 Development concept

Kubota Chemix offers single-socket pipes in different sizes from 50 to 200 mm in diameter, and their sockets are made using an injection molding machine (Fig. 2) and a winding machine (Fig. 3) in combination.

The newly developed fitting is made using a lathe with a special blade placed against a rotating raw pipe to embed an electric heating wire on the inner pipe surface. The special blade cuts through the inner surface of the raw pipe with the cutting edge to insert the heating wire, and then the opened area is pressed to hold the heating wire in place while the blade advances (Fig. 4). This processing method can be applied to various sizes of raw pipe, making it

suitable for small-lot production.

The fittings are structured so that they can be fused separately on the right and left sides, and one end of the pipe is joined to a socket to form a single-socket pipe. The single-socket structure has the advantage of halving the amount of pipe surface cutting and cleaning work required at the time of electro-fusion welding at the construction site.

Fig. 2 Injection Molding Machine

Fig. 3 Winding Machine

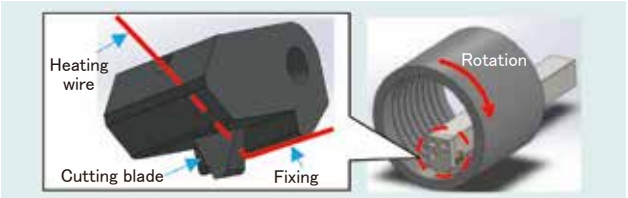

Fig. 4 Schematic of Heating Wire Installation

2-2 Development goals

The performance requirements for the socket are to meet: (1) the standard test (JP K 013) established by the Japan Polyethylene Pipe System Association, and (2) the marginal performance test specified as an in-house standard.

3. Developed technology

3-1 Challenges in prototype performance testing

The energy output from the controller used for electro-fusion welding can change because of errors in temperature measurement and output voltage tolerance. As a result, it was found that the conventional fitting shape could not meet the performance requirements because molten resin popped out from the gap between the pipe and the socket end surface (Fig. 5). The challenge was to solve this problem and achieve the aforementioned goals.

Fig. 5 Leaked Resin

3-2 Solution

To solve the above problem, we focus on the outer shape of the socket and created a groove that can collect extra molten resin (Fig. 6). As a result, the ejection of molten resin was eliminated (Fig. 7). This shape causes a highly complex mold structure for conventional injection molding fittings, but the socket of the newly designed fitting can accommodate this shape relatively easily by using the cutting mechanism of equipment dedicated to electro-fusion fittings.

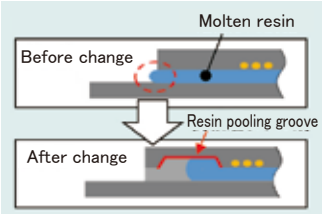

Fig. 6 Schematic of the Shape Change

Fig. 7 Evaluation Results

4. Conclusion

We have developed fittings of 250 and 300 mm in diameter, which have been highly evaluated for their applicability at actual construction sites (Fig. 8) . We will keep expanding the size range and develop products that meet what our users need.

Fig. 8 Plumbing Conditions

Contribution to SDG targets

8.2 Increased productivity through innovation
Saving construction time by adopting pipe with a single-socket

9.1 Development of high-quality, sustainable, and resilient infrastructure
Contributing to the achievement of leak-proof, resilient pipelines

Development of an Automatic High-pressure Cleaning System for the Gravity Belt Thickener

Water Circulation Engineering Design Dept. ／ Environmental Business Planning and Sales Dept.
Water and Environment R&D Dept. Ⅱ ／ Environmental System Control Dept.

The “Kubota Gravity Belt Thickener” for wastewater treatment plants is low-cost, low-power, and easy to manage, and it has been widely adopted in domestic wastewater treatment plants, significantly contributing to energy savings and labor reduction. However, certain substances contained in some of the treatment targets can cause clogging on the stainless steel belt, leading to a decrease in concentration performance. To reduce the frequency of this clogging and minimize maintenance efforts, we have developed an automatic high-pressure cleaning device.

【Key Word】
Wastewater Sludge, Gravity Belt Thickener, Stainless Steel Belt, Clogging, High-pressure Cleaning

Related SDGs

1. Introduction

Mechanical thickeners at wastewater treatment plants are installed at the front of the sludge treatment flow to thicken the sludge produced by the water treatment process from a concentration of about 0.5%–1.0% to about 4%–5%. They are important devices whose performance greatly affects sludge treatment in the subsequent stages (Fig. 1) .

The gravity belt thickener, a mechanical thickener, performs the following functions. A flocculant is added to sludge and stirred in a flocculator to create flocculated sludge, making it easier to separate water. The flocculated sludge is fed onto an endless belt, which is driven by a belt drive to transport the sludge to the discharge section. During this process, water is separated by gravity, resulting in the separation of the flocculated sludge into thickened sludge and filtrate. The belt undergoes continuous cleaning to maintain its thickening capability (see Fig. 2) .

Kubota’s gravity belt thickeners are the only wastewater sludge thickeners in Japan to use stainless steel belts (Fig. 3) , and are available in nine models (SNM-01X to SNM-15X) with sludge throughputs ranging from 10 to 150 m^3/h. Their stable thickening performance, energy efficiency, and excellent maintainability have been highly evaluated by many customers, and more than 280 units have been delivered to sewage treatment plants across the country.

Although gravity belt thickeners at many treatment plants can keep stable thickening performance for a long time, wastewater sludge contains various substances, and depending on the sludge characteristics, some substances that cannot be removed by continuous cleaning may adhere to and accumulate on the stainless steel belt. As a result, the belt may become clogged, which can lead to a reduction in thickening performance even after only a few months of operation (Fig. 4) .

If the stainless steel belt becomes clogged, the maintenance manager can stop the thickening operation and perform high-pressure cleaning using a high-pressure cleaner, or chemical cleaning using acid or alkali, to clear the clog and restore the thickening performance. However, high-pressure washing and chemical cleaning are manual operations, which are a burden on maintenance.

Therefore, there was a need for an automatic high-pressure cleaning system that can significantly reduce the time and effort required for maintenance and can also maintain thickening performance over a long period.

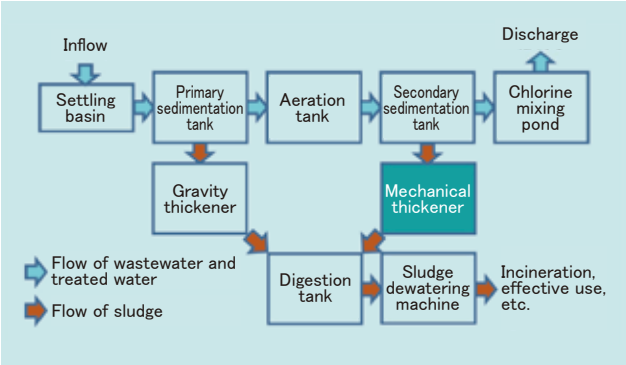

Fig. 1 Typical Flow of a Wastewater Treatment Plant

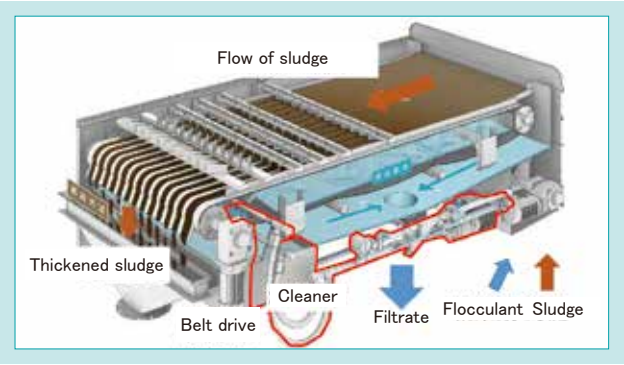

Fig. 2 Schematic Diagram of the Gravity Belt Thickener

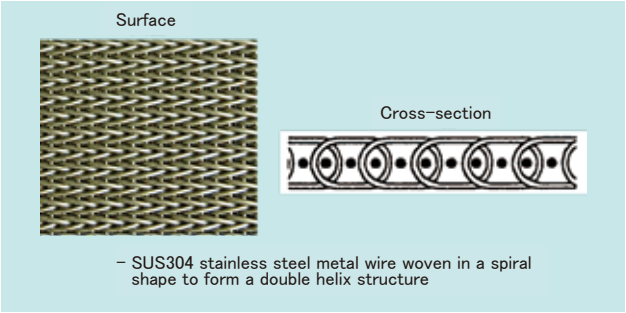

Fig. 3 Structure of the Stainless Steel Belt

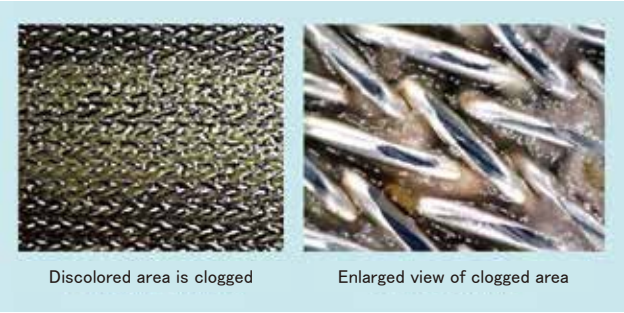

Fig. 4 Example of Clogging in the Stainless Steel Belt

2. Development concept and target values

2-1 Development concept

Since high-pressure cleaning is more frequent than chemical cleaning, automating high-pressure cleaning is a very effective way to reduce maintenance. Therefore, the development concept was to create a cleaning system that would automate manual high-pressure cleaning, stabilize thickening performance, and reduce maintenance and management efforts.

2-2 Target values

In order to realize the above concept, the following development goals were set based on a survey of manual high-pressure cleaning performed at actual sewage treatment plants, as well as the results of interviews with customers:

(1) Cleaning effectiveness: Equivalent to or better than manual high-pressure cleaning

(2) Cleaning frequency: Once a week and one hour each time for model SNM-12X at a sludge throughput of 120 m^3/h

(3) Power: A 5.5 kW high-pressure cleaning water pump (equivalent to the existing washing water pump)

(4) Maintainability: High-pressure nozzle blockage detection, automatic operation (zero man-hours except for inspection), and a chemical cleaning frequency of no more than twice per year

(5) Other: A structure that can be retrofitted to previously delivered machines

3. Technical issues to be solved

3-1 Determination of the washing impact force

In order to achieve cleaning effectiveness equal to or better than that of manual high-pressure cleaning performed when belt clogging occurs in a sewage treatment plant, it is necessary to study the washing impact force of high-pressure cleaners and determine the sufficient washing impact force. The washing impact force of cleaning water ejected from the cleaning nozzle can be calculated using the following formula, but the result should be confirmed by actual measurement.

Washing impact force [N/m] = 0.745 × Flow rate [L/min] × (Pressure [MPa])$^{1/2}$ ÷ Jet width [m]

Jet width [m] = Jet height [mm] × tan(Jet angle ÷ 2) × 2

The stronger the washing impact force, the higher the cleaning performance. However, since excessive cleaning force has caused deformation of stainless steel belts in the past, a washing impact force that does not deform the belt should be used.

For reference, the washing impact force for continuous cleaning is about 10 N/m.

3-2 Divided belt cleaning

Kubota's gravity belt thickeners have a belt width of 0.5 m to 3.0 m, depending on the model. A large flow rate is required to clean the entire belt width at once under conditions that meet the required washing impact force. Since pump power is proportional to flow rate and pressure, a 5.5 kW high-pressure cleaning pump is not powerful enough for even the smallest belt width of 0.5 m. Therefore, it is necessary to develop a mechanism that allows the belt to be cleaned in a divided manner.

3-3 Foreign material removal

During high pressure cleaning, the sludge feed is stopped and the stainless steel belt is activated. During this process, foreign matter such as residue remaining in the thickener may somehow fall onto the belt and be transported. Due to concerns that high-pressure cleaning without foreign material removal may adversely affect the stainless steel belt, manual high-pressure cleaning is performed with personnel visually inspecting for and removing foreign material. Even with automatic high-pressure cleaning, foreign matter on the stainless steel belt must be removed beforehand to prevent adverse effects on the stainless steel belt.

3-4 Detection of high-pressure cleaning nozzle blockage

Since there are only a small number of high-pressure cleaning nozzles, if even one becomes blocked, the effect will be significant, and the clogging of the stainless steel belt will worsen. Therefore, a device that detects and issues a warning when high-pressure cleaning nozzles are blocked is required.

4. Developed technology

4-1 The washing impact force, divided belt cleaning, and foreign material removal technology

Manual high-pressure cleaning at wastewater treatment plants A and B was studied (Fig. 5 and Table 1).

The results of the study were used to determine the washing impact force and the divided belt cleaning method, which led to the development of the foreign material removal technology.

Fig. 5 Manual High-pressure Cleaning Work

Table 1 Investigation Results of Manual High-pressure Cleaning Operations

		Treatment plant A	Treatment plant B
Model name		SNM-15X	SNM-12X
Cleaning water flow		13 L/min	13.8 L/min
Cleaning water pressure		5.2 MPa	10 MPa
Pump power		2.2 kW	3.7 kW
Cleaning position	Carrier side	Near the feed chute	Upper part of the drive roller
	Return side	Near the drive roller	None
Cleaning height		0.2 m	0.2 m
Washing impact force		420 N/m	600 N/m
Cleaning method		Stop the belt and move the nozzle over an area of about 3 m in width and 1 m in length for about 15 minutes to clean. After cleaning, run the belt and repeat the cleaning process.	Run the belt at 5 m/min and move the nozzle over a width of about 0.3 m to perform one lap of cleaning. Since the overall width is approximately 3 m, the belt will be divided into 10 sections for cleaning. If foreign material is carried on the belt, blow it off by tilting the nozzle tip at an angle.
Work time per job – (Cleaning time as an internal count)		7 h – (approx. 360 min (both directions))	1 h – (approx. 20 min (one direction))
Cleaning frequency		2 times/year	1 time/week
Man-hours for work		28 man-hours/year	104 man-hours/year

4.1.1 Determination of the washing impact force

At treatment plant B, high-pressure cleaning is performed once a week at a washing impact force of 600 N/m, and no damage to the stainless steel belt from high-pressure cleaning has been reported.

With this in mind, we applied high-pressure water to a stainless steel belt in a small testing machine, gradually increased the washing impact force to a maximum of 700 N/m, and ran the belt for 2,400 laps to confirm that there was no elongation or deformation of the belt. Assuming a high-pressure cleaning frequency of once a week, the number of laps in high-pressure cleaning over the six-year life of the belt is determined as 1 lap/week × 52 weeks/year × 6 years = 312 laps. This results in a margin ratio of 2,400 ÷ 312 = 7.7.

Based on the above, the washing impact force of 600 N/m was adopted as in treatment plant B.

4.1.2 Determination of the divided belt cleaning method

Since the cleaning time per job was shorter at treatment plant B than at treatment plant A, we adopted a method of dividing the stainless steel belt into sections in the width direction while running the belt, with reference to the cleaning method at treatment plant B.

Since the stainless steel belt at plant B was only washed from one direction on the carrier side (the surface on which the sludge rides), we considered that washing from one direction would be sufficient to achieve the same cleaning effect.

To clean the belt in sections divided in the width direction, a device is required to move the cleaning nozzle in the width direction of the stainless steel belt. A width-direction reciprocating device, which has been used in other sludge treatment equipment (screw press dewaterer), was adopted (Fig. 6).

The cleaning mechanism uses a combination of a chain-driven reciprocating device, high-pressure rubber hose, and hose support. The drive unit allows the nozzle to move freely through the chain, and the high-pressure rubber hose follows the movement of the nozzle.

In addition, a plunger pump with a proven track record was used for the high-pressure cleaning water pump.

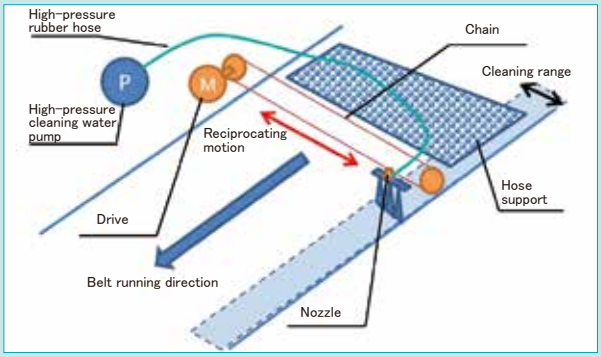

Fig. 6 Schematic Diagram of the Automatic High-pressure Cleaning Device

4.1.3 Development of the foreign material removal technology

In the small testing machine, foreign material was placed on the stainless steel belt and high-pressure water was vertically applied to see if it had any effect on the belt. Cotton, string, and scrap metal were used to simulate foreign material such as debris contained in sewage sludge.

The test results showed that the string and scrap metal could be blown away by the force of the high-pressure water, but the cotton was pushed into the stainless steel belt. Cotton pressed into the belt could be removed by pinching with fingers, but not by high-pressure water applied vertically (Fig. 7).

In the manual high-pressure cleaning at treatment plant B, the nozzle tip of the high-pressure cleaner is tilted at an angle to blow away foreign material, and we used this practice as a reference for designing our device. By attaching an additional nozzle capable of cleaning at a wider angle than the high-pressure cleaning nozzle and applying high-pressure water at an angle to the stainless steel belt, we verified that cotton could be removed on the upstream side of the high-pressure water hitting the belt vertically (Fig. 8).

Fig. 7 Cotton Trapped in the Stainless Steel Belt

Fig. 8 Foreign Object Removal Nozzle

4-2 Detection of high-pressure cleaning nozzle blockage

We considered whether the blockage of the high-pressure cleaning nozzle could be detected from the characteristics of the high-pressure cleaning water pump by the low-flow warning of a contact flow meter. A volumetric plunger pump is used for the high-pressure cleaning water pump, and a spring pressure regulator is used in its discharge section. When the cleaning nozzle is clogged, excess cleaning water flows to the surplus water side because of the spring action of the regulator. This causes the flow rate of the high-pressure water to decrease, allowing detection of low flow.

We replaced the nozzle with a plug to simulate nozzle blockage, and measured the high-pressure water flow rate and the nozzle section pressure. When one nozzle was blocked, the high-pressure water flow rate decreased from 48.4 L/min to 45.1 L/min, indicating that the flow rate can be used to detect nozzle blockage. Since the pressure at the nozzle section is 6.25 MPa when all nozzles are blocked, we chose a maximum working pressure of 7.0 MPa or less for hoses and piping (Fig. 9).

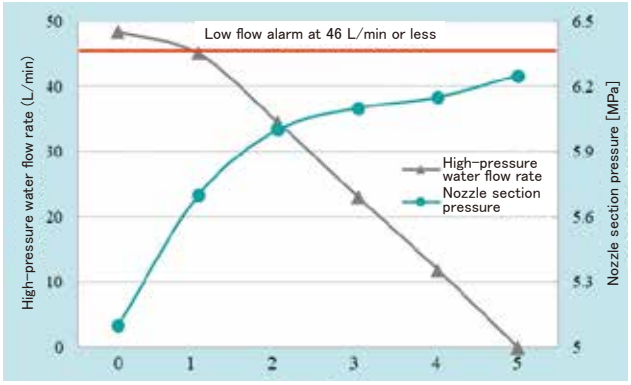

Fig. 9 Relationship Between Nozzle Blockage, High-pressure Water Flow Rate, and Nozzle Pressure

4-3 Confirmation of the cleaning effectiveness and long-term stability using an actual machine

The prototype system developed was attached to an existing actual machine at treatment plant B, and tests were conducted on the machine for one year and three months (Figs. 10 and 11).

The sludge thickener at treatment plant B was operating for about 7,000 to 8,000 hours per year (approximately 290 to 330 days). During the period of the actual machine testing, manual high-pressure cleaning was performed once every two weeks and chemical cleaning was performed five times per year. On the other hand, the test machine did not undergo manual high-pressure cleaning but rather underwent automatic high-pressure cleaning at a frequency of once a week.

We conducted water passage tests on a thickener with an automatic high-pressure cleaning system (the test machine) and on a thickener without the system (the reference machine) to confirm the cleaning effectiveness of the system.

The test was conducted over three different periods to investigate the following: (1) automatic high-pressure cleaning performance after clogging, (2) short-term stability, and (3) long-term stability. A comparison of the results obtained from the test machine and the reference machine has confirmed the satisfactory cleaning effects and long-term stability of the system, as described below.

Fig. 10 State of High-pressure Cleaning

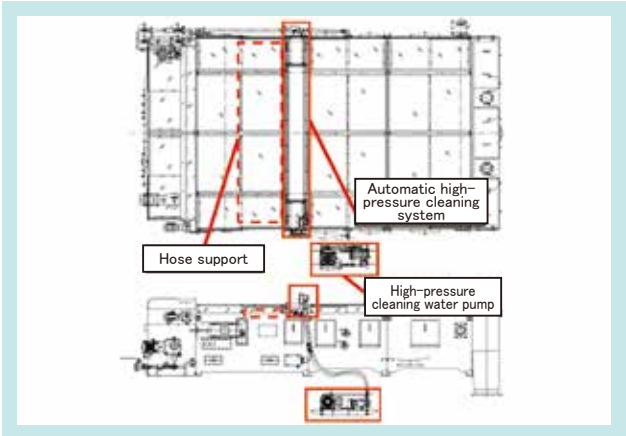

Fig. 11 Gravity Belt Thickener Equipped with the Automatic High-pressure Cleaning Device

4.3.1 The water passage test method

Kubota conducts water passage tests to evaluate the clogging status of stainless steel belts and has established the following standard procedure and criteria for judging clogging.

The standard procedure is to store approximately 0.9 L of water in a test device placed on the belt, allow the water to flow down through the belt, and measure the time it takes for the specified amount of water to flow down (Fig. 12). The mean of three measurements at each location is calculated, and the mean values obtained at 12 locations across the entire belt are further averaged.

The criteria for judging clogging are as follows. When the stainless steel belt is new or has been thoroughly cleaned with chemicals, the optimal water passage time is 4.0 seconds or less. If the water passage time exceeds 5.0 seconds, the belt is considered to be clogged.

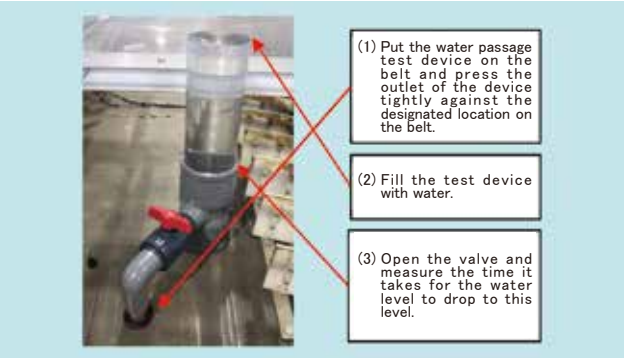

Fig. 12 Water Flow Testing Device

4.3.2 Verification of the cleaning effectiveness

The time when chemical cleaning was performed was set to 0 hours, and the subsequent relationship between the thickening operation time and the water passage time was compared between the test and reference machines over two distinct test periods.

During test period (1), an automatic high-pressure cleaning system was installed to initiate an actual machine test 600 hours after the chemical cleaning process (Fig. 13). The belt in the test machine exhibited a water passage time that exceeded 5.0 seconds at 600 hours, indicating a state of clogging. However, automatic high-pressure cleaning reduced the water passage time to about 4.1 seconds, indicating that the clogging had been removed. Thereafter, the water passage time was kept below 5.0 seconds by the subsequent automatic high-pressure cleaning.

On the other hand, the reference machine showed no clogging, with a water passage time of less than 5.0 seconds, but the water passage time gradually increased.

During test period (2), automatic high-pressure cleaning was started after chemical cleaning. The water passage time was less than 4.0 seconds for both the test and reference machines, which continued to perform well without clogging (Fig. 14).

These results show that the automatic high-pressure cleaning system is as effective as or more effective than manual high-pressure cleaning.

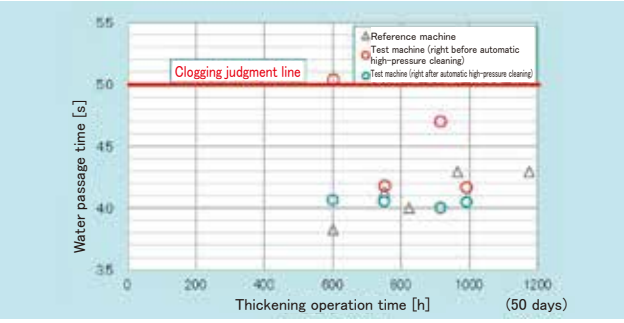

Fig. 13 Transition of Water Flow Times (Test Period ①)

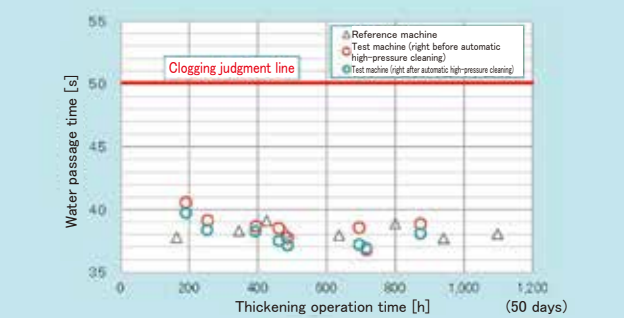

Fig. 14 Transition of Water Flow Times (Test Period ②)

4.3.3 Confirmation of long-term stability

During test period (3), the long-term stability of the test machine without chemical cleaning was verified. During this period, the reference machine underwent chemical cleaning three times (Fig. 15).

The test machine remained in good condition with no clogging in the stainless steel belt for approximately 4,500 hours (about 190 days). These results confirm that the introduction of the automatic high-pressure cleaning system can reduce chemical cleaning from five times per year to two times per year at treatment plant B.

During this period, the test machine was operated semi-automatically by its maintenance manager. To visually check for any abnormalities when starting up, the operator switched on the startup button when performing high-pressure cleaning; after startup, the control system operated automatically to complete the cleaning process. Consequently, there were no major problems during the test period and the stainless steel belt did not clog for an extended period, which was highly appreciated by the maintenance manager. Since it has been confirmed that visual checks during startup are not required, the full-fledged machine to be manufactured will achieve fully automatic operation of high-pressure cleaning by adding the process of automatic high-pressure cleaning at the end of the thickening operation or at a time set by a timer.

The maintenance manager responsible for the automatic high-pressure cleaning system is required to perform 0 man-hours for cleaning and only about one hour of inspection work (strainer cleaning, visual inspection, water leakage checks, etc.) once every six months. Consequently, the implementation of this system can achieve a significant reduction in man-hours for high-pressure cleaning work (Table 2).

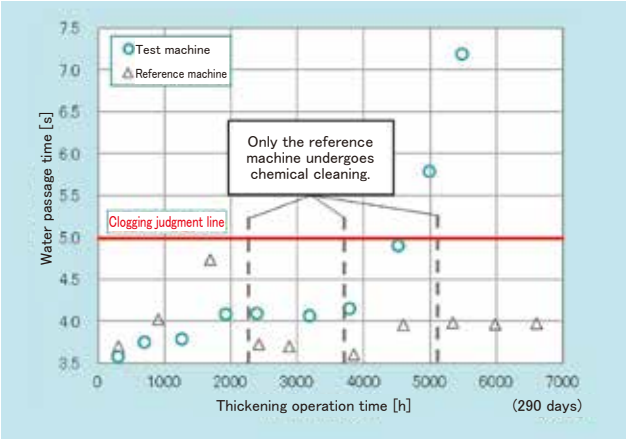

Fig. 15 Transition of Water Flow Times (Test Period ③)

Table 2 Comparison of Specifications and Maintenance Efforts between Test Equipment and Reference Equipment

		Reference machine	Test machine
Specifications	Cleaning water flow	13.8 L/min	50 L/min
	Cleaning water pressure	10 MPa	5 MPa
	Cleaning height	0.200 m	0.109 m
	Washing impact force	600 N/m	600 N/m
	High-pressure cleaning frequency	1 time every 2 weeks	1 time/week
Maintenance man-hours	High-pressure cleaning	52 man-hours/year	2 man-hours/year
	Chemical cleaning	160 man-hours/year	64 man-hours/year

Basis for calculating man-hours for high-pressure cleaning

Reference machine: 1 hour/time × 2 persons × 365 days/year ÷ 14 days/time = 52 man-hours/year

Test machine: 1 hour/time × 1 person × 2 times/year = 2 man-hours/year

Basis for calculating man-hours for chemical cleaning

Reference machine: 8 hours/time × 4 persons × 5 times/year = 160 man-hours/year

Reference machine: 8 hours/time × 4 persons × 2 times/year = 64 man-hours/year

5. Conclusion

A highly reliable automatic high-pressure cleaning system has been developed by adopting a reciprocating cleaning mechanism with a proven track record of use and by designing a simple structure. This system, which can be retrofitted to existing thickeners, can be confidently recommended to customers experiencing problems with clogging in stainless steel belts.

At treatment plant B, where an actual machine was tested, the system received high marks from the maintenance manager and was adopted for use.

We will continue to closely monitor the needs of our customers and contribute to the stable operation of wastewater treatment plants, which are essential infrastructure for daily life.

Contribution to SDG targets

6.2 Increased availability of sewage and sanitation facilities
Contributing to low-cost wastewater treatment

8.2 Increased productivity through innovation
Contributing to the reduction of man-hours required for wastewater treatment plant maintenance from 212 man-hours/year to 66 man-hours/year

9.4 Infrastructure improvement by introducing environmentally friendly technologies
Contributing to the maintenance of stable thickening performance in wastewater treatment

Development of Inspection Rationalization Technology Using MR Devices

KUBOTA Environmental Engineering Corporation
DX Planning & Promotion Dept.

Drainage pumping stations, which play a role in preventing flood damage, are becoming increasingly old after 40 years of use since their installation. Therefore, facility maintenance is becoming increasingly important. Meanwhile, the inspection workers at drainage pumping stations are aging, leading to a decrease in the number of skilled workers and issues with passing on know-how to unskilled workers. As a solution, the Ministry of Land, Infrastructure, Transport, and Tourism's Kanto Regional Development Bureau introduced "inspection rationalization technology" in April 2024 to improve the efficiency of inspection and maintenance. The Kubota Group has developed "inspection rationalization technology" using MR devices to further pursue the work efficiency required and pass on the know-how of inspection workers.

【Key Word】
MR Devices, Machine Maintenance, Server Management, Point Cloud Data

Related SDGs

1. Introduction

Due to recent climate change, the annual frequency of heavy rainfall events is increasing. The frequency of localized heavy rainfall events with hourly precipitation exceeding 50 mm is about 1.5 times higher than around 1980.[1)] To prevent flood damage due to heavy rainfalls, 534 drainage pump stations have been installed across Japan. However, it is estimated that by 2030, more than half of these stations will be over 40 years old, which is the recommended time for equipment replacement.[2)] Although the importance of inspection work in facility maintenance is growing, there is a shortage of workers due to the aging of the inspection workforce and related knowledge transfer issues.

Accordingly, the Kanto Regional Development Bureau of the Ministry of Land, Infrastructure, Transport, and Tourism (MLIT) introduced the Inspection Rationalization Technology Initiative in April 2024 to improve the efficiency of inspection and maintenance. In the traditional inspection process, the contractor would record inspection results in the field and enter the data into a PC after returning to the office. Then the electronic data was transmitted to the purchaser. On the other hand, the purchaser had to input the received data again into the purchaser's server, and the whole process was time-consuming for both the contractor and the purchaser. Inspection rationalization technology reduces the workload of both the contractor and the purchaser by linking their servers. Thereby, the inspection data entered by the contractor using a smart device in the field is directly transferred into the purchaser's server, streamlining the inspection process (Fig. 1) .

The Kubota Group has developed an inspection rationalization technology using a head-mounted mixed reality (MR) device (Fig. 2) manufactured by another company. These MR devices further improve the operability of inspection work while leading to achieve sustainable development of the inspection business by transferring the know-how of skilled workers.

This paper presents the features of this technology and the impact of its implementation.

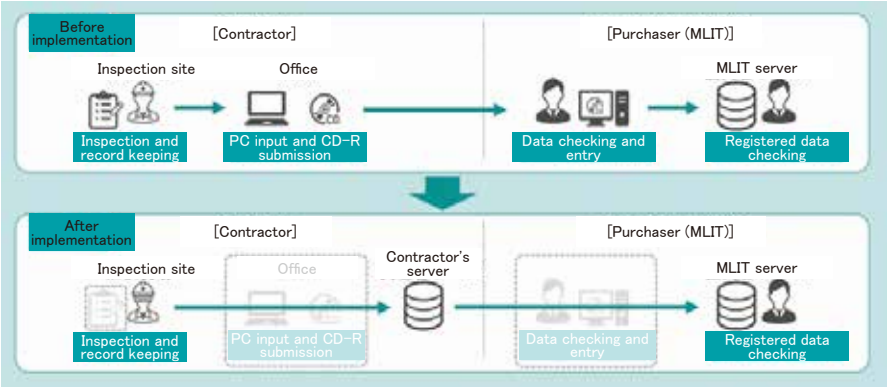

Fig. 1 Overview of Inspection Rationalization Technology

Fig. 2 Head-Mounted MR Device
(Photo: Microsoft HoloLens 2*)

* HoloLens 2 is a trademark or registered trademark of Microsoft Corporation in the United States and other countries.

2. Development concept and target values

2-1 Development concept

Traditionally, the storage medium for inspection work has been paper, and the only technology to streamline inspection has been the use of tablet terminals. While tablets are more convenient than paper, they can be cumbersome to hold while working and can malfunction if they are knocked or dropped.

Therefore, the concept for the development of the MR device was to ensure the same or better operability and safety as tablet terminals in inspection work using the MR device as a storage medium and to enable unskilled workers to perform the same level of inspection work as skilled workers.

2-2 Development goals

The following goals were set based on the above development concept:

(1) Operability and safety

The device should have the same or better operability and safety as a tablet terminal or other smart device.

(2) Working hours

Non-skilled workers should be able to perform inspections in the same amount of time as skilled workers.

3. Technical issues to be solved

3-1 Visualization of inspection points and establishment of an input method

(1) Typically, there are more than 200 inspection points in a drainage pumping station, and it takes a lot of skill to identify all of them. Workers must be able to accurately identify the inspection points.

(2) Inspection recording at visualized inspection points must be completed with the MR device without requiring a separate smart device for input.

3-2 Standardization of inspection work and enhancement of assist functions

(1) For unskilled workers to perform the same level of work as skilled workers, there is a need for a function that assists workers by standardizing and visualizing the work of skilled workers.

(2) The system should be able to assist unskilled personnel in case of a breakdown or another problem occurring during inspection.

4. Developed technology

4-1 Utilization of 3D point cloud data and MR technology

4.1.1 Visualization of inspection points by using 3D point cloud data

To visualize the vast number of inspection points at a drainage pumping station, the entire station was first scanned in three dimensions and converted to 3D point cloud data (Fig. 3).

Next, the inspection points were clarified by placing flags on the virtual point cloud data (Fig. 4).

Finally, by aligning the coordinates of this virtual point cloud data with those of the actual drainage pumping station and projecting the data into the field of view of the worker wearing the MR device, flags indicating the inspection points were visualized in the real space. This allowed the inspection points to be accurately identified (Fig. 5).

Fig. 3 3D Point Cloud Data of Drainage Pumping Station

Fig. 4 Flag Inspection Points Overlaid on 3D Point Cloud Data

Fig. 5 Inspection Points Visible to Workers

4.1.2 Realization of spatial input by the MR device

To enable operators to record inspection results at visualized inspection points, an input method using the spatial recognition of the MR device was established. Specifically, the method is to display a table of inspection records in space by the operator touching inspection point flags displayed on the MR device, and to allow spatial input by touching a record field (Fig. 6).

The establishment of this method has improved operability, compared to tablet terminals, by reducing the risk of failure and eliminating input problems caused by wet or dirty hands. In addition, the ability to perform hands-free inspections has improved safety when going up and down ladders and stairs or performing other tasks (Fig. 7).

Fig. 6 Spatial Input of Inspection Log

Fig. 7 Conditions While Climbing and Descending a Ladder During Inspection

4-2 Enhanced inspection assist functions

4.2.1 Inspection procedure assistance

To enable unskilled workers to perform the same level of efficient inspection work as skilled workers, we studied the inspection procedures of skilled workers.

Based on these results, we made it possible to visually distinguish the next inspection points by changing the color of the flags so that they could be inspected, similar to a skilled worker.

(Fig. 8).

This allowed unskilled workers to work in sequence following the color of the flags, eliminating confusion about the inspection sequence and omissions, and enabling them to perform inspection work as efficiently as skilled workers in the same amount of time.

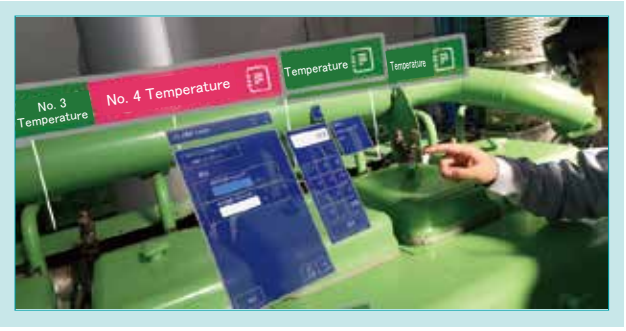

Fig. 8 Assistance Display for the Inspection Sequence

4.2.2 Remote assist functions

A system that uses an MR device to provide remote technician support was developed to assist non-skilled workers who are unsure how to respond to a breakdown or other problem at an inspection site. A technician in a remote location can view real-time images of the work site captured by a field worker using the MR device and can display the materials needed on the worker's MR device based on the situation. This enables the technician to provide accurate instructions to improve worker support (Fig. 9).

Fig. 9 Remote Assist Function

5. Conclusion

This technology was developed as an inspection rationalization technology, which was ordered by MLIT. It was examined that the annual inspection time of 729 hours was reduced by 274.5 hours, approximately a 37% reduction (Table 1). We expect that the newly developed inspection support technology using the head-mounted MR device can be used not only for inspections of public and private water control facilities nationwide, but also at construction and manufacturing sites. We will continue to contribute to the improvement of business efficiency and the transfer of know-how in variety of areas using this technology.

Table 1 Time Reduction Effect of Inspection Rationalization Technology

Item	Unit	Inspection and record keeping	Documentation	Reporting and registration	Total
Before implementation	Hours	432	288	9	729
After implementation	Hours	405	45	4.5	454.5
Effect of implementation	Hours	−27	−243	−4.5	−247.5

Contribution to SDG targets

4.4 Improvement of the technical and vocational skills of youths and adults
Contributing to the training of young and unskilled workers for inspections

8.2 Increased productivity through innovation
Approximately 37% time savings compared to traditional inspections

9.1 Development of high-quality, sustainable, and resilient infrastructure
Contributing to the maintenance of drainage pumping station facilities

Reference
1) Japan Meteorological Agency: “Climate Change Monitoring Report 2023”
https://www.data.jma.go.jp/cpdinfo/monitor/2023/pdf/ccmr2023_all.pdf, p. 59 (referenced on September 9, 2024)
2) The River Machinery and Equipment Subcommittee, the River Committee of the Infrastructure Development Council, the Ministry of Land, Infrastructure, Transport and Tourism: Document 3 for the 1st meeting “Current Status and Issues in River Machinery and Equipment”
https://www.mlit.go.jp/policy/shingikai/content/001396613.pdf, p. 1 (referenced on September 9, 2024)

Development of the MBR Operating System with a TMP Prediction Model

Water and Environment R&D Dept. Ⅱ
Kubota Membrane USA Corporation

Membrane Bio-Reactor (MBR) is a wastewater treatment process which features superior effluent quality and a small footprint. Although it is a technology used for wastewater reuse due to its high solid-liquid separation performance, the reduction of energy and costs related to membrane scouring power is a challenge needing further discussion. In addition to hardware improvements, such as high integration of membrane modules and units, Kubota has developed a membrane scouring airflow control. This paper introduces our approach to membrane scouring airflow control using an automatically updated machine learning model that diagnoses membrane conditions. This developed system uses edge AI and can be easily introduced into existing systems, achieving more than 20% reduction in membrane scouring airflow compared to conventional models, with stable operating performance.

【Key Word】
MBR, Energy Saving, Machine Learning, TMP Prediction, Edge AI

Related SDGs

1. Introduction

The membrane bioreactor (MBR) is a wastewater treatment technology that combines biological treatment and membrane filtration. This technology, which is unique in that it saves space and produces clear, treated water suitable for reuse, is used in industrial wastewater and sewage treatment plants both in Japan and overseas.

The global market for membrane equipment for MBRs is approximately 56 billion yen (actual figure for 2021). With stricter wastewater regulations and increasing demand for wastewater reuse, the market is expected to continue expanding at a rate of 6%–7% per year (including replacement of existing facilities), exceeding 100 billion yen by 2030.[1)]

Despite their high solid-liquid separation performance and space-saving capability, MBRs suffer from clogging (fouling) due to the accumulation of dirt on the membrane surface after continuous filtration operation. As the trans-membrane pressure (TMP) increases due to progressive fouling, the power needed for filtration increases and, in severe cases, the necessary filtration capacity is lost. Therefore, for antifouling and cleaning, physical cleaning is always performed by air blowing from a membrane scouring blower, and chemical cleaning with sodium hypochlorite or acid is performed after the TMP has risen. Compared to the conventional activated sludge process, the required power and cost of membrane scouring are significant. Improving the cleaning efficiency and reducing the operating costs have long been issues for further deployment of MBRs.

On the other hand, fouling is more likely to occur under conditions that are more demanding for membrane filtration, such as operating at higher fluxes (permeate flux for the membrane area) or higher contaminant concentrations than originally designed. Due to the increased membrane scouring airflow required to prevent sludge from adhering to the membranes, there are cases

where the TMP increases rapidly if membrane filtration is continued with insufficient airflow. Fouling control and cleaning also require technical elements that provide resistance to inflow fluctuations and stable operational control.

Although there have been improvements in hardware technology, such as higher integration of membrane equipment, active control of the membrane scouring airflow, which accounts for a large portion of the power and cost, is limited, and in many cases, the equipment is operated at a constant airflow with some tolerance. The recent need to reduce greenhouse gas (GHG) emissions from wastewater treatment processes also requires smart operation control technology to achieve further energy savings. Therefore, this project focused on the development of MBR operation control technology that appropriately controls the membrane scouring airflow while maintaining stable operation.

2. Development concept and target values

2-1 Development concept

This development project was based on Kubota's previous work in developing a long-term TMP prediction model. In developing long-term TMP prediction technology, we have found that a machine learning model can accurately predict the TMP five to seven days in advance. This enables operational support, such as predicting the timing of chemical cleaning and more accurate ordering of chemicals and scheduling of personnel.

The machine learning model technology cultivated here will be used to realize robust automatic MBR control, which will involve: (1) high treatment stability in response to fluctuations in the quality and quantity of influent raw water, and (2) automation and labor reduction in MBR operation management that does not require human judgment or adjustment. This operation control system also employs edge AI to facilitate its installation in existing MBR plants (Fig. 1). An edge PC equipped with a machine learning program is connected to a programmable logic controller (PLC) via Ethernet to read sensor values and write membrane scouring airflow control values.

The system takes into account sensor characteristics used in the MBR, filtration operating cycles, and data fluctuation patterns, and collects data every 10 seconds, performs model inference (diagnosis and prediction), and calculates membrane scouring airflow control values every 10 minutes, with the ability to update the model every 24 hours.

The system minimizes modifications to existing PLCs and leverages large amounts of historical data that would be difficult to process by PLC calculations alone, making it an easy-to-market product.

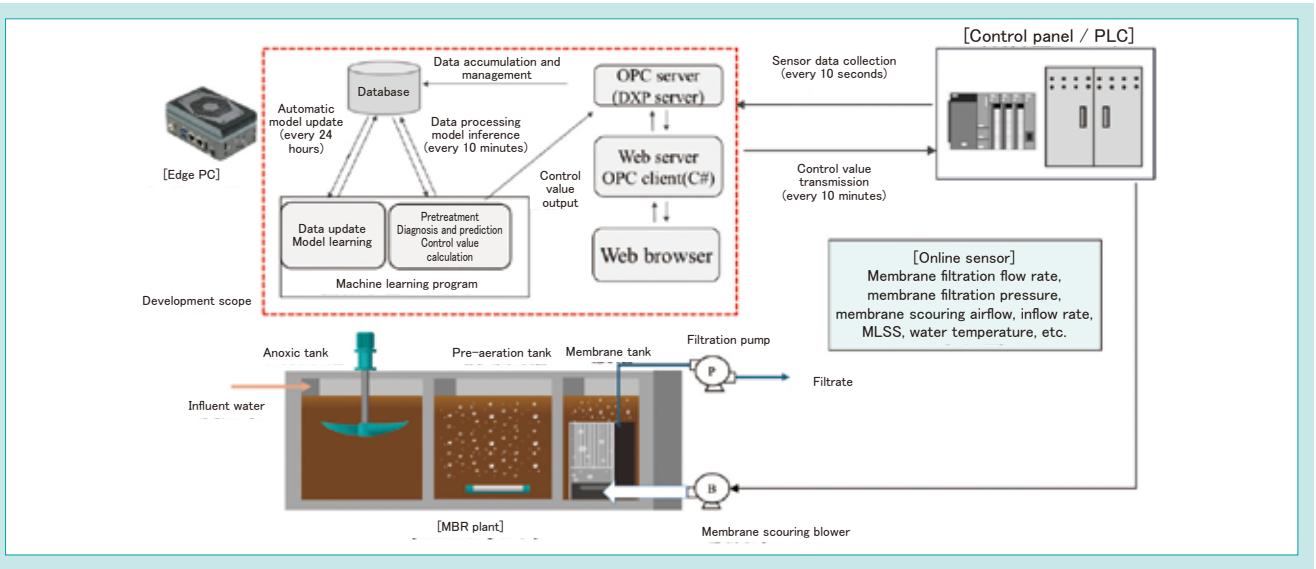

Fig. 1 Configuration of the MBR Operating System with a TMP Prediction Model

2-2 Target values

The airflow reduction effect varies depending on various plant operating conditions such as mixed liquor suspended solids (MLSS) and flux. In the present case, based on the rated airflow of conventional machines, we established the following target values for the reduction of membrane scouring airflow and the reduction of power consumption per volume of water treated under (1) standard flow conditions (section 4.2.1), and (2) high-load flow conditions (sections 4.2.2 and 4.3):

(1) For average daily flux of 0.6 m/d: 20% reduction in membrane scouring airflow

(2) For average daily flux of 0.87 m/d: 15% reduction in power consumption per treated water volume

The indexes of scouring airflow per membrane area (SAD_m) and scouring airflow per membrane filtrate flow (SAD_p) are for reference only, as they are affected by the layout conditions of the membrane modules and units in the experimental machine.

3. Technical issues to be solved

Kubota has developed the following technologies to control the membrane scouring airflow: (1) feedback control that increases or decreases the airflow based on the ⊿TMP of the past few hours as a threshold for judgment,[2] (2) energy-saving MBR control with a TMP prediction function,[3] and (3) rule-based control that calculates the membrane scouring airflow using a regression equation based on the MLSS concentration and flux (Table 1). These efforts still face issues such as control responsiveness and the ability to respond to influent water quality and quantity and the resulting sludge characteristics. Our goal is to integrate the advantages of conventional control technologies to develop a membrane scouring airflow control system based on an automatically updated diagnostic model that can follow changes in influent raw water and sludge properties.

Table 1 Features and Problems of Conventional Membrane Scouring Airflow Control

	Features	Problems
(1) Feedback control	Exploration of the minimum required airflow based on pressure behavior Feedback control that explores the optimal airflow by increasing or decreasing the target airflow value by comparing ⊿TMP to the threshold value for judging whether to increase or decrease the airflow, where ⊿TMP is the difference between the reference TMP value calculated every few hours and the current TMP value of the membrane.	Delayed control response to differential pressure increases
(2) Predictive control	Preventive control with a TMP prediction model PI control to increase or decrease the membrane scouring airflow according to a comparison between the TMP value predicted by the machine learning model and the target TMP curve, and the amount of difference between them. Based on the predictions, it is possible to increase the airflow to prevent the membrane fouling from progressing.	Model degradation
(3) Rule-based control	Responsiveness of the control value calculation The membrane scouring airflow is calculated from a multiple regression equation specified by MLSS and flux using experimentally obtained parameters. Control operations are highly responsive even when the flow conditions fluctuate.	Unable to follow changes in the sludge properties

4. Developed technology

4-1 Membrane scouring airflow control logic

The basic policy of membrane scouring airflow control is as follows: (1) conventional feedback control to explore the minimum required airflow is performed (2) based on the diagnostic results of the membrane condition diagnostic model, and (3) this is combined with rule-based determination of the range of airflow control. The control range of the membrane scouring airflow is defined based on a rule-based regression equation to ensure responsiveness and safety against the fluctuation of flow conditions, and the minimum required airflow is explored in a complementary manner by increasing or decreasing the airflow according to the classification results of the machine learning model.

4.1.1 Exploration of the minimum required airflow through feedback control

The minimum required airflow is defined as the minimum membrane scouring airflow required to prevent adhesion and deposition of solids on the membrane surface. It is assumed that an airflow less than the minimum required will result in a decrease in the membrane scouring capacity and a rapid increase in the TMP due to significant adhesion and deposition of sludge on the membrane surface.

Feedback control has been used to explore the minimum required airflow by increasing or decreasing the airflow based on a threshold-based judgment of the most recent rise or rate of rise in the TMP (Fig. 2).

However, the conventional method has a problem of response delay, which results, for example, in an increase of airflow after an increase of the TMP. To solve this problem, a machine learning model using a large amount of data is processed by a PC to diagnose the membrane condition (rising TMP atmosphere), which includes predicting the future TMP in addition to determining the current and recent differential pressure changes. The membrane condition diagnostic model (supervised-learning multi-level classification model) classifies the membrane condition into three levels labeled [+], [N], and [-], and the results are reflected in operations to increase or decrease the membrane scouring airflow to find the minimum required airflow. Here, [+] is to increase airflow, [N] is to maintain airflow, and [-] is to decrease airflow.

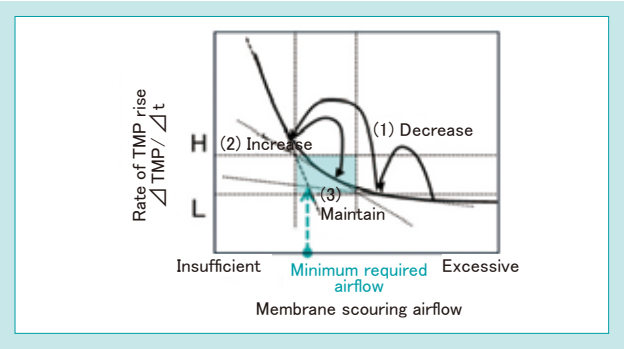

Fig. 2 The Concept of Exploring the Minimum Required Airflow Using Feedback Control

4.1.2 Membrane condition diagnostic model

Table 2 shows the conditions for building a machine learning model to diagnose the membrane condition. The labels [+], [N], and [-], which are the objective variables, are based on the threshold conditions for the rate of change of the TMP (dTMP/dt) or the rate of change of membrane filtration resistance R (dR/dt) when the TMP curve is categorized into the stable phase, the early phase of differential pressure rise, and the late phase of differential pressure rise. The labels are defined through further application and combination of the rate of change over multiple time ranges (recent, long-term trend, and future prediction) (Fig. 3). The features consist of membrane filtration pressure, membrane filtration flow rate, membrane scouring airflow, and water temperature as essential items, which are close to the minimum set as continuous sensor data measured in an MBR plant. Sensor data that can improve model accuracy, such as the MLSS and influent water flow, are optional variables in model building conditions.

In addition, to prevent model degradation, the just-in-time (JIT) concept is used to optimize the model through automatic updating. In the JIT model, data with high similarity to the features in the most recent operation are selected from the existing database as training data (Fig. 4). After setting multiple candidates for model construction conditions consisting of combinations of classifiers and features (X), and optimizing the hyper-parameters, accuracy of evaluation data that are different from the training data are compared, and the model with the highest accuracy is adopted.

Table 2 Overview of Machine Learning Model Construction Conditions

Objective variable (y)	Labels ([+], [N], [−]): They are categorized according to the threshold conditions of the TMP or the rate of change of membrane filtration resistance (dR/dt) for various time ranges (including future prediction). $\frac{dR}{dt} = \frac{\Delta \frac{TMP}{\mu J}}{\Delta t}$
Candidate features (X)	[Essential] Membrane filtration pressure, membrane filtration flow rate, membrane scouring airflow, and water temperature [Optional] Influent water flow, MLSS, DO, viscosity, COD, etc. * Pre-processed sensor values

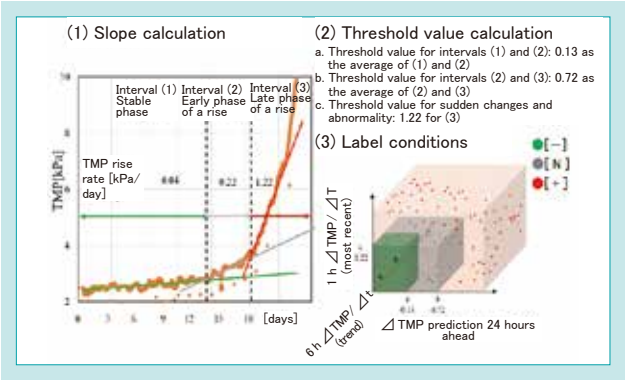

Fig. 3 Setting Method of the Label Condition

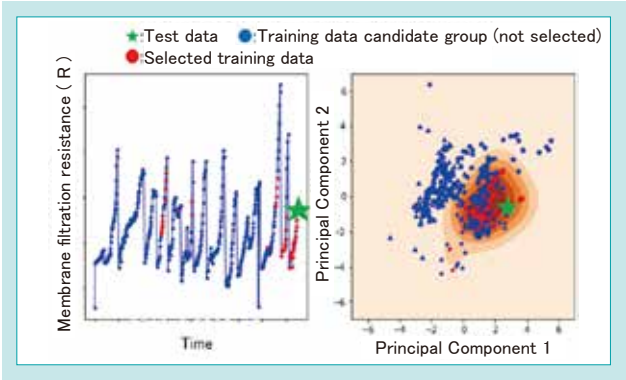

Fig. 4 Training Data Selection by the Just-in-time Method

4.1.3 Rule-based determination of the airflow control range

In conventional rule-based control, the inflection point of the TMP change rate is calculated by changing the MLSS, flux, and airflow conditions as a preliminary experiment, and the airflow at the inflection point is set as the minimum airflow required to obtain the regression equation (1) specified by the MLSS and flux.

$$Q_a = \left(1 + (FL - FL_b) \times K_{a,Fl}\right) \times \left(1 + (ML - ML_b) \times K_{a,Ml} \div 1000\right) \times Q_{a,b} \quad (1)$$

FL: flux FL_b: reference flux $K_{a,Fl}$: flux factor

ML: MLSS ML_b: reference MLSS $K_{a,Ml}$: MLSS factor

The minimum required airflow expressed by the regression equation obtained in the preliminary experiment is an approximation and will always change depending on the membrane surface conditions and sludge properties. Given the accuracy of the MLSS sensor, there is a deviation (room for adjustment) from the true minimum required airflow. On the other hand, airflow control values can be calculated immediately based on measured values, as opposed to searching for optimal values based on relative airflow increases or decreases using a diagnostic model.

With this in mind, we decided to determine a recommended range of airflow control based on the values calculated from the regression equation, and to increase or decrease airflow within that range based on the results of the diagnostic model.

4-2 Examples of application of developed technologies

We evaluated the performance of the developed control system at test plants installed in actual sewage treatment plants in Japan and overseas. The test plants consisted of an approximately 80 m^3 AO-MBR consisting of an anoxic tank and an oxic tank as common equipment, and a number of membrane tanks downstream. The effectiveness of reducing the membrane cleaning airflow was evaluated for each membrane tank by comparing the developed system to a reference system (design standard constant airflow operation or a conventional airflow control system). From both a stable operation and quality standpoint, the quality objectives were set to achieve a chemical cleaning interval equivalent to that of the reference system and to cause no significant membrane surface contamination. We then checked the operating interval between chemical cleanings and confirmed the amount of sludge adhesion by weighing or visually inspecting the membrane module. In this verification, we used two types of membrane units sold by Kubota, i.e., the standard flat plate type (RW series) and the high-flux-compatible, high-integration cartridge type (SP series), and collected data for various flux and MLSS ranges.

4.2.1 Constant flow rate operation (RW series)

In a test plant installed in Japan, comparative tests were conducted using an RW100 membrane unit (a membrane area of 145 m^2 and a rated airflow of 0.7 m^3/min) and actual sewage under constant flow rate conditions (an MLSS concentration of 9,500 mg/L and an average daily flux of 0.6 m/d) to compare the developed technology with a reference system that was based on conventional constant airflow operation (Fig. 5). In these tests, instead of specifying a control range through a regression equation, 70% to 100 % of the rated airflow was set as the airflow control range of the developed system.

Regarding the control behavior in the test, the developed system operated at the lower limit of airflow during the stable period of TMP, and the airflow increased as the TMP increased. The membrane cleaning airflow of the developed system during the one-month operation period from March to April 2022 was 0.54 m^3/min (22.9% reduction from the rated airflow, with SADm = 0.22 $m^3/(m^2 \cdot hr)$ and SADp = 8.9 m^3/m^3), achieving the airflow reduction target of 20%.

The number of operating days before the TMP began to rise was 15.5 days for the reference system and 16 days for the developed system, with no significant differences. At the end of the test, the membrane module was lifted and visually inspected for sludge adhesion. Although some sludge adhesion was observed at the bottom of the membrane module, the degree of adhesion was similar between the reference and developed systems, confirming that the airflow reduction was appropriately achieved.

4.2.2 High-load variable flow rate operation (SP series)

At the Kubota Water and Environment R&D Center USA, we conduct tests using the SP270 membrane unit (a membrane area of 270 m^2 and a rated airflow of 0.9 m^3/min) and actual sewage under high load fluctuation flow conditions with an MLSS concentration of 12,000 mg/L and a daily average flux of 0.87 m/d (hourly maximum of 1.2 m/d) to compare the developed technology to the reference system with rule-based control (Fig. 6). Due to the high-flux condition of these tests, rule-based control would result in operating at or above the rated airflow. Filtration was stopped for one to two hours during the day (while the membrane cleaning blower continued to operate), and automatic chemical cleaning consisting of low-concentration chemical cleaning for maintenance and high-concentration chemical cleaning for recovery was performed. The airflow control range of the developed system was set between -20% and +5% of the rule-based control range.

After one month of operation from July to August 2022, no significant membrane surface contamination was observed in either the reference or developed system, and no differences were found in the membrane module weight measurements. The average number of days of operation until automatic chemical cleaning was 5.2 days for the reference system and 7.8 days for the developed control system. In addition to achieving stable operation, the developed system reduced the membrane scouring airflow to 0.88 m^3/min, compared to 1.02 m^3/min in the reference system with rule-based control, confirming the effectiveness of the airflow reduction (13.4% reduction relative to the reference system, with SADm=0.20 $m^3/(m^2/hr)$ and SADp=5.4 m^3/m^3).

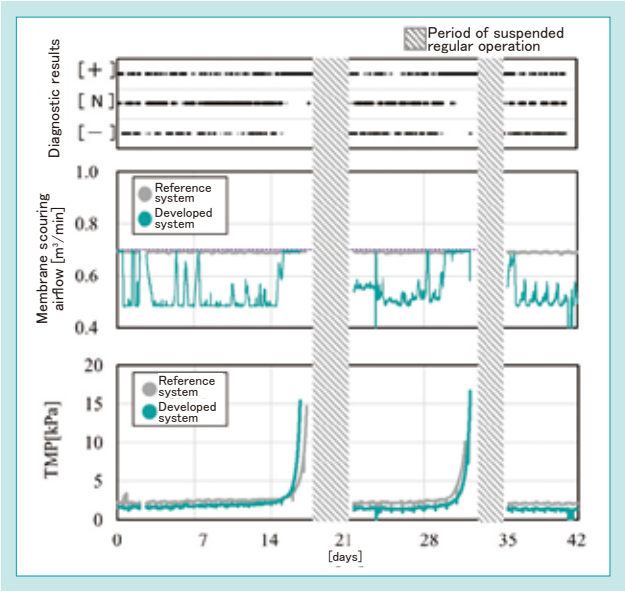

Fig. 5 TMP, MBR Airflow and Diagnosis in Constant Flux Operation

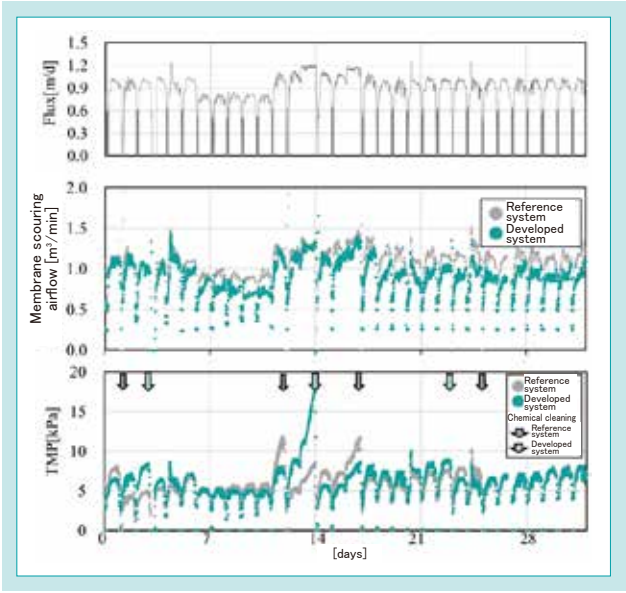

Fig. 6 TMP, MBR Airflow and Flux in High Loading and Variable Flow Rate Operation

4-3 Contribution to energy-saving operation

Based on the test results with the developed membrane scouring airflow control (section 4.2.2) and the conditions for estimating the energy consumption per volume of treated water given in Table 3, the results of the calculation are shown in Fig. 7.

The power consumption per volume of treated water was reduced by 17.5% to 0.242 kWh/m^3 with the developed system compared to 0.293 kWh/m^3 with the conventional MBR, confirming energy savings exceeding the target of 15%. It was also confirmed that the developed technology is applicable to high-flux, variable flow conditions.

This newly developed product is expected to strengthen the appeal of MBR introduction in overseas sewage markets where MBR introduction is being actively considered. In addition, the sale of this product as an after-sales service for existing equipment will enable us to provide customers with increased energy savings. This is expected to help strengthen and expand our after-sales service business.

Table 3 Conditions for the Calculation of Energy

Item	Remarks	
Processing method	Initial sedimentation + Circulating membrane bio-reactor method	
Equipment subject to power calculation	Initial sedimentation scraper, fine screen, anoxic tank agitator, nitrifying solution circulation pump, excess sludge pump, blower (membrane scouring and supplemental aeration)	
Water volume conditions	Maximum daily water volume: 10,000 m^3/d	
Water quality conditions [mg/L]	Reaction tank effluent: BOD=120, SS=100, and T-N=31.5 Treated water: BOD=1, SS=1 or less, and T-N=10	
Flux and membrane units	Conventional: 0.6 m/d, 28 units of SP600 Demonstration: 0.87 m/d, 20 units of SP600	
Blower power calculation conditions	Membrane scouring airflow	Rated: 2 m^3/min per unit Demonstration: 1.96 m^3/min per unit
	Supplemental aeration airflow	Calculated from the theoretically required amount of oxygen, which is calculated from the water quality and quantity conditions (corresponding to insufficiency in the membrane scouring airflow)
	Blower adiabatic efficiency	65%
	Water depth	5.0 m

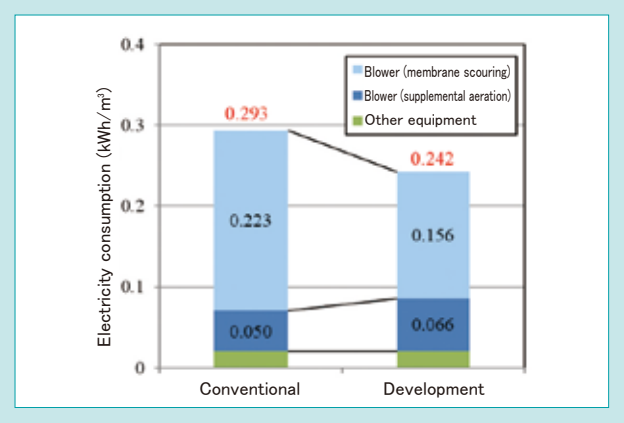

Fig. 7 Results of the Calculation of Energy

5. Conclusion

We developed a membrane condition diagnostic model for membrane scouring airflow control and constructed a control system in the form of edge AI. We conducted tests at test plants in Japan and overseas to compare the developed system with the conventional constant airflow control or rule-based control and confirmed that it is possible to reduce the membrane scouring airflow while maintaining stable operation. Although actual airflow reduction results varied due to limitations such as influent load conditions and the existing blower's performance, we confirmed that airflow reductions of 20% to 35% compared to the conventional system were possible under various conditions (RW/SP membrane unit types, MLSS ranging from 8,000 to 12,000 mg/L, and flux ranging from 0.4 to 0.87 m/d).

We are currently conducting a pilot installation at an in-plant wastewater treatment facility in Europe to promote the use of MBRs and optimize existing systems. We are also working to introduce the developed system to sewage treatment plants in North America. Going forward, we will work to improve the model accuracy by establishing new sensing technologies and develop an interactive user experience feature between the AI and operators in order to enable smart control of the entire MBR process, not just controlling the membrane scouring airflow. This will help address the challenges facing water environment projects, such as the global need to reduce GHG emissions and the shortage of technical personnel for water infrastructure.

Contribution to SDG targets

6.3 Water quality improvement through recycling of untreated wastewater
Contributing to appropriate wastewater treatment through the development of control technology applicable to MBRs

7.3 Improvement of energy efficiency
Development of control technology for proper MBR operation to help save energy in wastewater treatment

9.4 Infrastructure improvement by introducing environmentally friendly technologies
Development of smart control technology to help stabilize wastewater treatment operations

Reference
1) Fuji Keizai: "Current Status and Future Outlook of Water Resources Related Markets" 2021 Edition, 2021
2) Mikiharu Tokushima: "Development of Energy-saving MBR Technology" Membrane, 37 (5), 2012
3) "Development of Smart MBR (SCRUM) to Help Save Energy" Kubota Technical Report, No. 51, 2018

Introduction of Kubota Research and Development Europe (KRDE)

Kubota Research and Development Europe S.A.S.

Related SDGs

1. Introduction

After the launch of the M7 tractor in the factory of Kubota Farm Machinery Europe (KFM) in 2015, Kubota established an engineering department in Europe to support the development and maintenance of the M7 tractors. Farm Machinery Engineering Europe (FMEE) first started its operation in 2016 in the premises of Kubota Europe, then Kubota Research and Development Europe SAS (KRDE) was established in 2020, as a subsidiary of Kubota Holdings Europe, after the completion of the new European research and development site in Crépy-en-Valois, France (Fig. 1).

KRDE's main scope is the development of the M7 range for all Kubota markets worldwide, but also the development and integration of the Precision Farming features (ISOBUS, TIM...), and the development of an OEM front loader range for the M-series tractors sold in the European market. KRDE also supports the local development of specific sales features for the European market on M6 tractors.

The local engineers and technicians, representing 90% of KRDE's total workforce, are operating in Project Management, Engineering, Validation and Systems Controls in a brand new R&D Site utilizing state of the art equipment for the design and the evaluation of the tractors, such as CAD, virtual reality rooms, assembly workshop, test benches, test courses...

KRDE works in close cooperation with the Tractor Engineering Department II to ensure that M7 keeps both the Kubota tractors attributes and a common family look and feel with the M6 tractors. Additionally, a close cooperation with the Kverneland Group Mechatronics team supports the goal of developing agricultural tractors that are highly automated, easily customizable, connected, and strongly interfaced with the implements.

Summary of KRDE

- Name: Kubota Research and Development Europe S.A.S.
- Establishment: July 2020
- Employees: 100 full-time staff, of which 10 expats
- Total site area: 30 hectares
- Total building area: 10700 m²
- Location : 80 Rue du Bois de Tillet, 60800 Crépy-en-Valois, France

Fig. 1 KRDE Main Office

2. Overview of KRDE's Test Center

KRDE's major physical asset is the Test Center, which consists of 3 main facilities: Test Benches, Test Tracks and Agricultural Field. Additionally, the site is equipped with a fuel station, washing areas and garages to store tractors and agricultural implements.

The activity of the Test Center is mainly for internal KRDE purposes, to support the M7 development activities. However, KRDE also offers to the other Kubota Group entities the possibility to perform their testing activities in the Test Center.

Overview

- Agricultural Field area: 10 hectares
- Test tracks: 43000m² including a 1.8km long track
- Test Bench building area: 2480 m²

2-1 Test Benches

KRDE has 9 benches to perform mechanical, performance tests or environmental tests.

Mechanical benches: 3-point hitch, 4-poster, tilt angle, multi-axis simulation table (MAST), platform for mechanical components test, and dynamometrics wheels.

Performance benches: PTO bench, 5-axis driveline bench.

Environment: Cold cell.

Some of them are more precisely described in the next part.

2-2 Test Tracks

The test track area consists of a 1,6 km long and 12 m wide main flat track having an "8" shape. On one side, 4 slopes (6%, 12%, 18%, 36%) for dynamic or static tests are present.

In the center, a perfectly flat surface is used as the homologation area, to perform steering and braking tests. A portion of the inner track can be covered with water to execute wet braking tests.

Along the straight line of the main track are located 2 rough road tracks to measure whole-body vibrations according to ISO 5008.

Finally, a circle rough road test (Merry Go round) can be used for small tractors and turf machinery (Fig. 2).

Fig. 2 KRDE Test Track

2-3 Agricultural Field

The 10-hectare agricultural field is used for actual operations with the tractors and agricultural implements (Fig. 3). A dedicated area with sand, soil and piles of stones is used for front loader operations.

The field test activities can also be performed in the surrounding of KRDE, through a partnership with local farmers.

Fig. 3 M7 Tractor Operating in KRDE's Field

3. Details of 3 Test Benches

KRDE has invested in cutting edge testing technologies to ensure product's durability and comfort. The test benches are also a driver of the development efficiency, through their repeatability, accurate reproduction of the real usage of the machines, and their ability to work on single components or sub-assemblies instead of a complete machine.

3-1 Driveline Bench

The 5-axis driveline bench is dedicated to tractors (Fig. 4). It is equipped with 5 dynos (4 for the wheels' hubs and 1 for the PTO) that have been designed to Kubota's specification with a very low inertia in order to reproduce perfectly the wheels' torques measured in real conditions. The bench also has a climatic conditioning (temperature control, air flow and solar simulation).

The driveline bench can be used not only for endurance tests on powertrains, but also for the development and characterization of the transmission controls, or to check the performances of the cooling systems of the engine or in the cabin.

By accurately reproducing the measures collected on the test track or in the field, the driveline bench ensures a better repeatability of the tests during all the development steps.

Fig. 4 5-axis Driveline Bench

3-2 Multi-axis Simulation Table

The Multi-Axis Simulation Table (MAST), unique in Kubota, is capable of performing vibratory tests on machines or sub-assemblies up to 2 tons (Fig.5). The table is capable of moving in the 3 degrees (x,y,z) of freedom.

For the tractor development, the MAST is used to test components or sub-assemblies independently by reproducing accurately the excitation measured on the complete tractor, either in real conditions or on the 4-poster bench.

The MAST provides to the R&D engineers early results on their design in terms of vibrations and endurance. Associated with a Fatigue Simulation Software, the reliability of the assemblies can be evaluated for their all life-time to optimize the products' quality and cost.

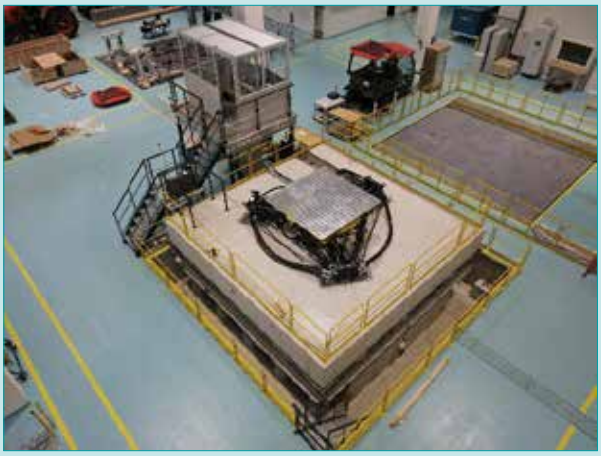

Fig. 5 MAST: Multi-axis Simulation Table

3-3 Mechanical Components Test Platform

The Mechanical Components Test (MCT) platform is used to perform mechanical strength and structural endurance tests. The primary goal of this bench is to perform FOPS (Falling Object Protection Structure) and ROPS (Roll Over Protection Structure) tests for the internal pre-homologation of our cabins.

The MCT platform is also used on complete machine bodies. The results are used by the R&D engineers in KRDE and the Analysis Center in KGIT (Kubota Global Institute of Technology) to develop accurate models of the structures, to improve the simulation and achieve the right design at the first time, to prevent from later test failures or molds modification cost.

As for the Driveline and MAST benches, the MCT platform is a key driver for KRDE's validation process efficiency by bridging the actual measurements on physical tractors parts and more robust simulation results.

Fig. 6 MCT Platform

4. Conclusion

As one of the 6 Global Sites of Kubota's R&D System, KRDE is acting both globally, as the engineering base for the M7 tractor, and locally to support the European Business Units for Tractors and Implements.

KRDE cooperates with the Engineering teams in Japan and Europe to develop innovative features.

To maximize the benefits of the cutting edge equipment, KRDE offers test services to the other Kubota entities.

Contribution to SDG Targets

8.2 Improvement in productivity through innovation
Accelerate development of precision farming and automation features

8.5 Achieving productive employment and rewarding work
Contribute to employee's satisfaction and loyalty

9.5 Promoting scientific research and innovation
Develop efficient development processes

17.16 Building Global Partnerships
Cooperate with Japanese and European bases, develop global test services for all Kubota machinery and regions.

Diagnostic Functions of a Centrifugal Dewatering Machine to Realize Condition-based Maintenance and Stable Operation

1. Introduction

Sewage sludge treatment has become a major issue as the amount of sewage sludge is increasing with the spread of sewage systems, and centrifugal dewatering machines (Fig. 1) , which are important pieces of equipment for sludge reduction, are required to operate stably. Centrifugal dewatering machines, which are high-speed rotating devices, are generally subject to periodic factory maintenance based on time. Since their maintenance costs are relatively high, there is a strong need to move to condition-based maintenance, which reflects the actual state of deterioration, in order to make effective use of limited budgets.

We have developed diagnostic functions of centrifugal dewatering machines based on operational data. This capability aims to achieve condition-based maintenance and stable operation by using diagnostics based on daily operating data.

Fig. 1 Centrifugal Dewatering Machine

2. Product overview

Figure 2 shows the diagnostic procedure for a centrifugal dewatering machine. Vibration sensors are attached to the main body of the dewatering machine to collect operating data, measurements are taken by instrumentation installed in the control panel, and the data is analyzed for each major part using a proprietary diagnostic algorithm. Diagnostic results are displayed for each machine part, showing the current level of soundness and predicting when repairs will be necessary. Five levels of soundness are defined according to the Ministry of Land, Infrastructure, Transport and Tourism's Guidelines for the Stock Management Implementation in Sewerage Projects (2015 Edition).

Diagnostic results are stored on a cloud server that users can access from their PCs to view the results. Trend management based on daily operating data (time series data) and soundness assessment enables condition-based repair and maintenance.

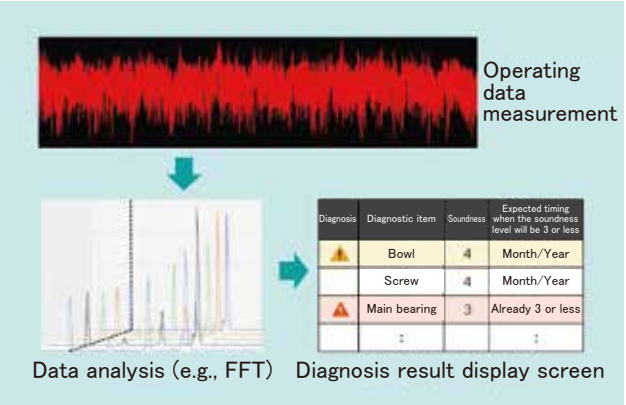

Fig. 2 Diagnostic Procedure for the Centrifugal Dewatering Machine

3. Conclusion

This diagnostic functions is included in the KUBOTA Smart Infrastructure System (KSIS), our proprietary water environment ICT solution system. As financial difficulties and labor shortages become more apparent due to the declining population, we believe that expectations for condition-based maintenance, which enables both effective use of budgets and stable operation of facilities, will continue to grow. We will continue to develop technologies and meet these expectations while contributing to the realization of a comfortable and sustainable society.

Contact information
Address: 2-1-3 Kyobashi, Chuo-ku, Tokyo, 104-8307
Company name: Water Circulation Engineering Sales Department, Kubota Corporation
Phone: 03-3245-3337

Polyethylene Pipe for High Pressure Fire Extinguishing Equipment

1. Introduction

Kubota ChemiX manufactures and sells polyethylene pipes and fittings for water distribution and building plumbing applications. In recent years, the company has been using these products to expand the market for fire extinguishing and sprinkler applications.

We have added high-pressure polyethylene pipes for fire extinguishing equipment to our product lineup (Fig. 1) installed in high-rise buildings (condominiums and office buildings), underground shopping malls, and so on. These pipes are suitable for applications with a maximum working pressure of 1.6 MPa. While steel pipes are mainly used to connect water pipes, they are expected to be replaced by polyethylene pipes, which do not pose corrosion problems.

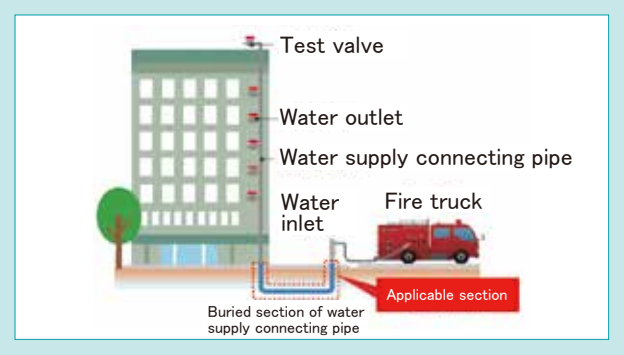

Fig. 1 Applicable Fire Extinguishing Equipment

2. Product overview

High-pressure polyethylene pipes for fire extinguishing equipment have the following features:

[Excellent corrosion and acid resistance]

They maintain excellent corrosion resistance even in acidic soils and coastal areas prone to salt damage. No corrosion protection is required when burying pipes, and the frequency of replacement is reduced, contributing to lower life cycle costs.

[High seismic performance]

The flexible and elastic properties of the material and the electro-fusion fittings that systematically integrate pipes and joints allow the pipes to follow ground displacement during earthquakes without losing their conduit function.

[Head loss comparable to metal pipes]

It is possible to secure a friction head loss equivalent to that of hard polyvinyl chloride-coated steel pipes for firefighting (STPG370-VS), which are mainly used at present.

Fig. 2 Product Lineup

3. Conclusion

As a leading manufacturer of plastic pipes and fittings, Kubota ChemiX is committed to extending the technology it has developed in water piping to other applications and further improving its product lineup to help ensure a safe and secure life for citizens.

Contact information

Address: 2-1-3 Kyobashi, Chuo-ku, Tokyo, 104-8307

Company name: Equipment Sales Department, Kubota ChemiX Co., Ltd.

Phone: 03-3245-3085

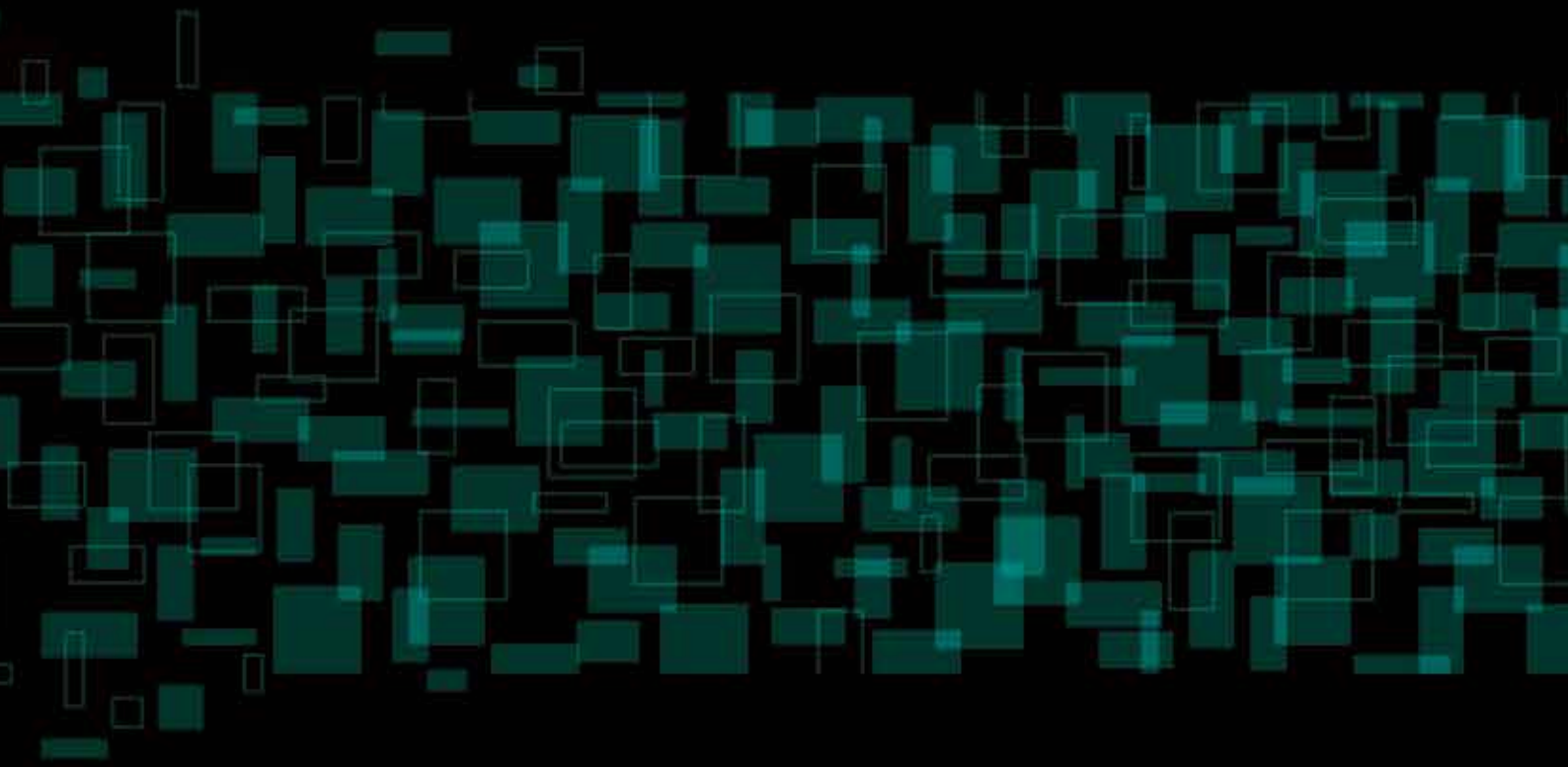

株式会社クボタ

www.kubota.co.jp